The Dissertation Committee for James Daniel Stiehl Certifies that this is the approved version of the following dissertation:

Model Catalyst Studies of the CO Oxidation Reaction on Titania Supported Gold Nanoclusters

Committee:

Charles B. Mullins, Supervisor

John G. Ekerdt

Gyeong S. Hwang

Greg O. Sitz

Thomas M. Truskett

Model Catalyst Studies of the CO Oxidation Reaction on Titania Supported Gold Nanoclusters

by

James Daniel Stiehl, B.S.

Dissertation

Presented to the Faculty of the Graduate School of

The University of Texas at Austin

in Partial Fulfillment

of the Requirements

for the Degree of

Doctor of Philosophy

The University of Texas at Austin

December 2004

Dedication

To Ronna

Acknowledgements

I would like to thank Dr. Buddie Mullins for giving me the opportunity to work in his lab. Buddie has been a great mentor and teacher, but most importantly I feel like he has been an excellent friend. I appreciate all the advice and help that he has given me over the past several years. He has definitely helped me become a better scientist and for that I will always be grateful. Working in Buddie's lab also gave me the opportunity to foster some friendships that I will remember fondly. I am specifically grateful for the chance that I had to interact with Randy Meyer, Tae Kim, and Sean McClure. Not only were these individuals labmates, they also became good friends who were there to help me whenever things got rough in the lab. The laughs that we constantly shared in the lab while "taking breaks" definitely helped relieve much stress.

I would also like to thank my friends outside of the lab for the part they played in making my graduate school experience memorable. I would like to thank Mohammed Al-Juaied for all the time that he spent with me teaching me about his life and culture in Saudi Arabia and for helping me with my Arabic studies. It was always a calming experience talking to Mohammed and a welcome distraction from the lab when things weren't going well. I wish Mohammed the best of luck in Saudi Arabia and hopefully, we will cross paths again some day. I would like to thank Jason O'Brien for being at

work everyday to keep me amused with at least one entertaining email per day. We have had many interesting discussions and I feel like I learned a great deal from him.

Most importantly, I would like to thank all of my family for all the love and support that they have given me throughout my graduate school career. I definitely could not have done this without them. I would especially like to thank my wife Ronna for putting up with me for the past five years. I know that at times I was a very difficult person to put up with and I am truly grateful for the love and support that Ronna gave me. She has truly been my muse and my reason for getting up every morning. Ronna, you share equally in this accomplishment and I definitely could not have done it without you. I would also like to thank my mom and Amy, my sister, for their support and their interest in what I do in the lab. I would like to thank Fred, my dad, for everything that he has done to help me get to this point. The breaks that I was able to share with him watching the Astros play baseball have truly been some of the most enjoyable moments of the last five years. Finally, I would also like to thank Ron and Glenna Osborn for all the help that they have given Ronna and me while I have been in school. They have been truly amazing in their love and support and I am very, very grateful.

Model Catalyst Studies of the CO Oxidation Reaction on Titania Supported Gold Nanoclusters

Publication No._____

James Daniel Stiehl, Ph.D.

The University of Texas at Austin, 2004

Supervisor: Charles B. Mullins

The chemical nature of gold has been determined to be much richer than previously thought. Recent discoveries that properly prepared gold catalysts (i.e. gold particle diameters in 2 – 5 nm size range) can catalyze the CO oxidation reaction at low temperature have spurned a renewed interest in the chemistry of gold. Despite the extensive research that has been performed regarding CO oxidation on Au based catalysts, many issues still remain unresolved. The origin of the particle size dependence of the reaction is not well understood. Also, details concerning the reaction mechanism, specifically identification of the active oxygen species, remain unresolved. In the following studies, ultra high vacuum, molecular beam, surface science techniques are used to study the CO oxidation reaction on titania supported gold nanoclusters (Au/TiO_2).

Using a radio frequency generated plasma-jet, it is possible to simultaneously populate the Au/TiO_2 samples with atomically adsorbed and molecularly chemisorbed oxygen species, allowing for the opportunity to investigate the reactivity of each respective species. The reaction of CO with atomically adsorbed oxygen has been

studied over a range of temperatures from 65 – 250 K as a function of gold coverage and oxygen coverage. The reaction is observed to be a strong function of both of the sample temperature and the oxygen coverage. The reaction is also relatively independent of the gold coverage on the sample, in contrast to findings for the reaction employing gas-phase reactants under moderate pressures.

The formation and reactivity of molecularly chemisorbed oxygen on the samples following exposure to the plasma-jet was also investigated. Evidence is presented showing that some molecularly chemisorbed oxygen is formed as a result of recombination of impinging atoms on the model catalyst surface. Evidence is also presented showing that adsorption of an oxygen atom on the sample influences the chemisorption of molecular species from the gas phase. Finally, evidence is presented showing that the molecularly chemisorbed oxygen species can participate in the CO oxidation reaction at 77 K. This finding reveals a reaction channel for CO oxidation on Au/TiO_2 model catalysts that does not require the dissociation of oxygen.

Table of Contents

List of Figures

Chapter 1: Introduction

Fascination for element number 79 on the periodic table, Au ([Xe]$4f^{14}5d^{10}6s^{1}$), has persisted for millennia. Since antiquity, gold has been revered as a precious metal and has found widespread use in jewelry, decorations, and money. One needs only to look at the history of mankind to see how important a role gold has played in society. Gold is mentioned in ancient religious texts like the Bible and the Torah, it plays an important role in ancient Greek traditions (e.g. Archimides is said to have come up with his principle of buoyancy while thinking about how to determine the purity of gold, and Homer's Iliad repeatedly speaks of gold treasures recovered as war booty), and it is credited with bringing about the demise of cultures like the Incas of South America. During the Middle Ages, gold was regarded as such an important metal by alchemists that one of their central goals was transforming other base metals into gold. Gold was, and still is, highly valued because of its appearance. The reputation that gold has received is due in part to its inherent stability. Bulk gold will not readily react with molecules such as oxygen[1-5] or hydrogen[1,6,7] and therefore, it is incredibly stable and resistant.

Many of the properties of bulk gold are, interestingly, related to the merger of two scientific concepts that at one time were thought to lie on opposite ends of the physics spectrum.[8] Much of gold's chemistry and appearance is dictated by relativistic effects.[8-15] The nucleus of a Au atom is sufficiently large to accelerate electrons to speeds at which relativistic effects become important. The increase in the mass of the s orbital electrons, and to a lesser extent the p orbital electrons, as a result of their relativistic speeds, causes a contraction of these orbitals. This contraction results in enhanced screening of the nuclear charge causing an expansion of the d and f orbitals. This relativistic contraction

is responsible for making Au the most electronegative metal, thus providing an explanation for its low chemical activity.[8] Also, the expansion of the 5d orbitals results in an energy difference between the Fermi level in bulk gold (~2.3 eV) where transitions in the visible range of the electromagnetic spectrum can occurr.[9,15] This is what gives bulk gold its unique yellow color. Not only can the appearance of bulk gold be explained by invoking relativistic effects, but they also provide an explanation to bulk gold's incredible lack of chemical activity.

Until recently, it was widely acknowledged that gold is a relatively inert material, which is not suited for use as a catalyst.[6] However, in 1987, Haruta reported that suitably prepared gold catalysts were surprisingly active for CO oxidation below room temperature.[16] Haruta discovered that gold particles in the 2 - 5 nm size range supported on metal oxide supports could catalyze the CO oxidation reaction at a temperature of –70 ^{o}C. Prior to Haruta's discovery, there were some indications that gold could be active as a catalyst. As early as 1925, there was evidence that gold could catalyze the oxidation of CO. In 1925, Bone and Andrew presented results suggesting oxidation of CO on a gold gauze sample at a temperature of 300 ^{o}C.[17] In the 1970's, Bond and Sermon reported on the hydrogenation of alkenes and alkynes at T < 473 K on Au supported on SiO_2,[18] while Parravano and coworkers showed that Au/MgO and Au/Al_2O_3 were active for some oxygen and hydrogen transfer reactions.[19,20] Another interesting result from the 1970's was the discovery by Huber et al. that single gold atoms could catalyze the oxidation of CO at a temperature of ~30 K.[21] Despite these early experiments on Au, Haruta's discovery of the catalytic activity of nanometer scale gold clusters is typically credited with spurning the renaissance of the study of gold-based chemistry.

Following the discovery of gold's unique catalytic ability, a renewed interest in gold chemistry developed and many research groups initiated studies aimed at

understanding Haruta's observations. This renewed interest has spanned the fields of classical catalysis,[13,22,23] surface science,[24-30] theoretical chemistry[6,28,31-35] and even gas-phase cluster studies.[36-38] These studies have all resulted in a great wealth of information, which has helped advance the understanding of gold chemistry. CO oxidation, and its elementary steps, has been the reaction of choice for most groups due to its inherent simplicity and also its technological importance. Issues such as support effects, particle size effects and the deciphering of the reaction mechanism on the catalysts have all been investigated. Classical catalysis and surface science studies have allowed for the experimental investigation of the activity of gold-based catalysts. While theoretical investigations of the chemical activity of gold and gold catalysts have been useful in trying to decipher details about the reaction mechanism for CO oxidation. Density functional theory (DFT) provides a way to investigate the energetics of adsorption of reactant species, like CO and O_2, and also to study the electronic properties of gold surfaces and small supported or unsupported gold clusters, which are known to behave differently than bulk gold. The energetics of reaction pathways can also be evaluated to determine their feasibility. Gas-phase gold cluster studies have also been very useful and interesting in that they provide a way to investigate the intrinsic activity of small gold clusters. In this way, support effects can be avoided. However, these studies have been performed on clusters that are smaller (2 to 20 atom clusters) than the typical size of particles on active gold catalysts (hundreds of atoms), and therefore comparison with "real" catalytic materials is not straightforward. Despite this potential problem, these studies have revealed much about the nature of nanoscale gold.

As is the case for many fundamental studies of catalytic activity, the field of surface science has played a major role in the quest for deciphering the details of gold-based chemistry. Surface science studies have historically focused on reactions on well-

defined single crystals under ultra high vacuum conditions. However, as bulk gold does not display the properties that were observed by Haruta and coworkers, studies on gold single crystals, although beneficial, were not fully suited for a study of the catalytic properties of supported nanometer gold particles. To study the properties of gold catalyst and employ standard surface science techniques, model catalyst samples have been used.[24-26,39] Model catalyst samples consist of planar metal oxide surfaces onto which metal particles can be deposited through various means (e.g. vapor deposition, colloidal deposition). These samples mimic "real" porous catalysts more closely than do their single crystal counterparts in the sense that there is a dispersion of catalytically active metal on a support material. However, they are still suitable for study using standard surface science techniques, such as electron-based spectroscopies (e.g. Auger electron spectroscopy, low energy electron diffraction, electron energy loss spectroscopy, x-ray photoelectron spectroscopy) and molecular beams. From early work on "real" catalysts, it was discovered that reducible supports (e.g. TiO_2, Fe_2O_3, MgO) result in the best activity for CO oxidation on gold catalysts, while insulating supports, like SiO_2 and Al_2O_3, are not as active.[23] Specifically, TiO_2 was found to be a very active support and for this reason it has been extensively studied. Gold particles supported on TiO_2(110) have been a popular model catalyst system[29-31,39] and this system is the subject of the work presented here. Figure 1.1 shows a scanning tunneling microscopy (STM) image of a Au/TiO_2 model catalyst used by Goodman and coworkers to study the CO oxidation reaction.[39] The model catalyst sample was prepared by evaporating gold on a single crystal TiO_2(110)-(1×1) sample. The Au particles are seen as light protrusions while the TiO_2(110) crystal rows and terraces are also resolved in the image (Ti cations are generally resolved in STM[39]). From the STM image, an average particle size of ~2.6 nm was determined for the scan shown.

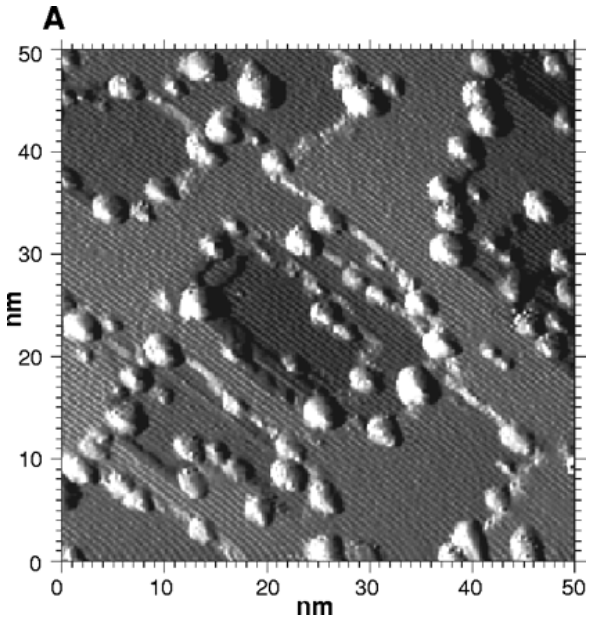

Figure 1.1: STM image of $Au/TiO_2(110)$-(1×1) model catalyst from Goodman and coworkers.[39] The Au coverage is 0.25 ML, which corresponds to an average cluster diameter of ~2.6 nm.

One of the most interesting, and still poorly understood, observations regarding gold catalysis is the dependence of the catalytic activity on gold particle size. As was mentioned previously, Haruta discovered that the activity of gold catalysts was strongly dependent on the Au particle size. Figure 1.2 shows turn-over-frequency (TOF) data taken by the Haruta group on Au/TiO_2 catalysts, which reveals the dependence of the reaction on Au particle size. Curve A shows the results of Haruta's work while Curve B shows turn-over-frequency results of a Au/TiO_2 model catalyst study performed by the Goodman group that will be discussed below. As can be seen in Curve A of Figure 1.2, a maximum in the reactivity of the catalyst was observed for particle sizes of ~2.5 - 3 nm. Particles larger than ~5 nm show negligible activity for the reaction. From transmission electron microscopy (TEM) images of the catalyst samples, Haruta noted that the perimeter contact area of small, active particles was larger (i.e. wet better) than the

contact area of larger, less active particles. From this observation, Haruta argued that the reaction occurred at the perimeter edge of the gold particles and therefore the smaller particles were more active than the larger particles. Vannice and coworkers tested this idea by depositing TiO_2 on 10 μm Au crystallites.[40] They observed CO oxidation on this system supporting Haruta's perimeter mechanism. Some theoretical investigations of Au supported on TiO_2 and MgO also support the idea of an active perimeter interface between the metal particle and the support.[28,35] However, other calculations of gold surfaces and unsupported gold particles indicate that low coordination sites could be the active centers for catalysis.[32-34] Perhaps these results can be viewed as complementary as the edge of the particles on a catalyst sample will inherently present a low coordination site. However, a recent study by the Goodman group,[41] to be discussed below, indicates that it is not necessary to have a substrate/particle interface to have CO oxidation activity.

One of the seminal Au/TiO_2 model catalyst studies, which showed that model catalyst systems could be used to mimic the "real world" catalysts of Haruta and which addressed the particle size effect observed by Haruta, was performed by the Goodman group.[39] They showed that vapor deposited gold clusters on $TiO_2(110)$ exhibited a similar particle size dependence for the CO oxidation reaction that Haruta observed using porous catalyst samples. The TOF data taken by the Goodman group is shown in Curve B of Figure 1.2 for comparison with Haruta's data. As can be seen in Figure 1.2, the trend observed for the TOF on the model catalyst sample is similar to that observed by the Haruta group on porous catalyst samples. Goodman and coworkers were able to employ STM to address the particle size effect. Through the use of scanning tunneling spectroscopy, an increase in the band gap (i.e. transition from metal to nonmetal) of the gold particles was observed as the particle size decreased, coincident with the onset of catalytic activity. This change in the electronic properties of the gold particles was

suggested as the reason for the turn on of the catalytic activity of the particles. Goodman and coworkers argued that it was the thickness of the gold clusters that was important in regards to catalytic activity. They proposed that it was necessary to have 2 layer thick gold particles to have high catalytic activity. This hypothesis was recently tested by growing completely wetting monolayer and bilayer gold films (i.e. no substrate/gold interface was present) on a thin TiO_x film.[41] CO oxidation activity was reported on these films with a maximum in the activity occurring for a 1 ML Au film. This result indicates that the substrate/particle interface may not be a necessary factor in determining activity in contrast to the results discussed above.

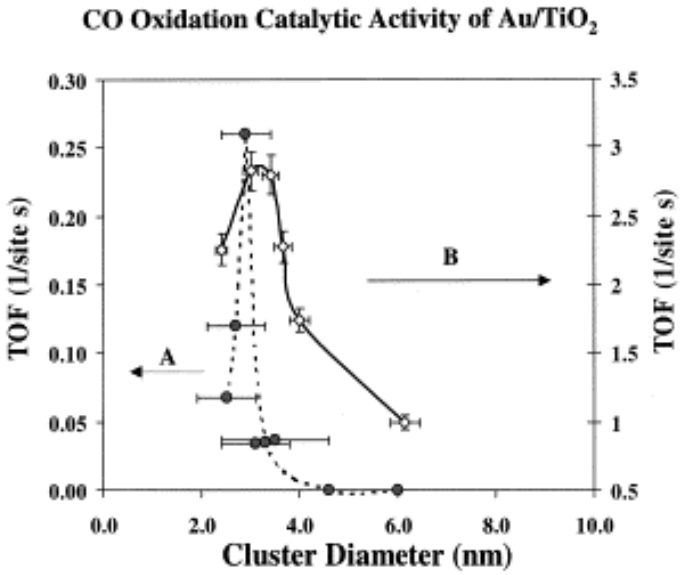

Figure 1.2: Turn-over-frequency (TOF) for CO oxidation on titania supported gold particles as a function of the cluster diameter. Curve A is data taken by the Haruta group[42] on "real" catalyst and Curve B is data taken by the Goodman group on a model catalyst sample.[39]

Another issue that has received considerable attention is the reaction mechanism for CO oxidation on Au catalysts. Some of the main issues that have been addressed regarding the mechanism are the active site(s) for reaction, including the oxidation state

of the active gold site and the nature of the active oxygen species. As was mentioned previously, the perimeter interface of the Au particle and support has been suggested as a possible active site for the reaction. However, results from theory, also mentioned previously, indicate that low coordination sites on unsupported gold could be active for CO oxidation. Another issue related to the active site for the reaction is the oxidation state of the Au. There is currently disagreement on whether metallic gold is responsible for the activity or if the Au(I) or Au(III) oxidation states of gold are active.[22,43,44]

The issue of the active oxygen species also continues to be a subject of debate. This issue has been somewhat puzzling to researchers due to the fact that gold in its bulk form does not activate the chemisorption of gas-phase molecular oxygen. Oxygen will not readily dissociate on bulk gold samples nor has molecularly chemisorbed oxygen been observed experimentally. Since many other metals that catalyze CO oxidation proceed through a reaction channel that requires the dissociation of oxygen, this has been considered as a possible mechanism for gold catalysts as well. It has been established that atomic oxygen on bulk gold samples (Au(110)-2×1[12,45] and Au(111)[46,47]) and model catalyst samples[27,29] is highly reactive with CO. In fact, it has been speculated that the particle size effect that has been observed is actually related to gold becoming active for oxygen dissociation as the particle dimensions decrease.[27] However, no experimental verification of oxygen dissociation on catalyst samples has been reported. Also, many theoretical investigations of oxygen dissociation on Au systems (e.g. surfaces, clusters, supported clusters) indicate that this process is highly activated (activation energies on the order of 1 eV are generally reported) and therefore not likely to occur under the conditions commonly used in catalysis.[32-35] Therefore, the idea of an atomic oxygen species being responsible for CO oxidation on Au catalysts is hard to reconcile. The

alternative of molecular chemisorption is also problematic as no evidence exists for molecular chemisorption when exposing bulk gold to gas-phase O_2.

Fortunately, the theoretical community has been very beneficial in trying to understand the issue of oxygen adsorption on gold systems. Theoretical calculations on defective gold samples and small gas phase gold clusters are starting to motivate the idea that a molecularly chemisorbed species can exist on gold under suitable conditions. Stable states of molecularly chemisorbed oxygen have been found on defective gold surfaces[32-34] as well as small gold clusters.[31,32,34] There is even experimental evidence showing that oxygen will molecularly chemisorb on gas-phase anionic gold clusters smaller than ~22 atoms with an odd number of valence electrons.[37,48-50] Evidence has also been presented indicating CO oxidation with a molecularly chemisorbed oxygen species on a Au_2^- cluster.[37]

As might be apparent from the preceding discussion, there are still unresolved issues concerning CO oxidation that need to be addressed with further research. In this dissertation, an attempt is made to provide insight into the mechanistic details of the CO oxidation reaction on Au/TiO_2 model catalysts, as well as to study the particle size effect that has been observed. The work presented here employs Au/TiO_2 model catalysts to study the CO oxidation reaction using molecular beam techniques. The experiments are all performed under ultrahigh vacuum conditions where adsorption of gas-phase oxygen (ground state) is immeasurable. Therefore, a radio frequency (RF) generated plasma-jet is used to populate the model catalyst samples with atomic oxygen. As will be shown in Chapters 3 and 4, the process of dosing the plasma-jet on the sample also results in the population of a molecularly chemisorbed oxygen state on the sample. This finding allows the unique opportunity to study the reactivity of atomically chemisorbed oxygen and molecularly chemisorbed oxygen.

In Chapter 2, results are presented of the reactivity of atomically chemisorbed oxygen on Au/TiO_2 model catalyst samples. A systematic study of the temperature dependence, gold coverage dependence, and the oxygen atom coverage dependence is presented. Atomically chemisorbed oxygen is found to be very reactive for the CO oxidation reaction. CO_2 production is observed at a temperature of 65 K if atomic oxygen species are present on the sample. The reaction of CO with atomically chemisorbed oxygen is found to be relatively independent of the gold coverage on the sample and hence the gold particle size. This finding is in contrast to results that have been found on real catalyst systems, suggesting that if the real reaction proceeds through the dissociation of oxygen to form adatoms, the dissociation process is likely the rate-limiting step. The reaction is observed to be strongly dependent on the oxygen coverage and on the surface temperature, with the adsorption/desorption kinetics of CO playing a large role in determining the reactivity of the sample.

In Chapters 3 and 4, the identification of a molecularly chemisorbed oxygen state ($O_{2,a}$) on the catalyst samples is discussed. Although ground state, gas-phase O_2 does not adsorb on the model catalyst samples under ultrahigh vacuum conditions, exposure of the model catalyst samples to a plasma-jet of oxygen results in the population of molecularly chemisorbed oxygen species and atomically adsorbed species. In Chapter 3, evidence is presented from thermal desorption, collision-induced desorption, and adsorption/reaction-induced desorption, identifying the molecular oxygen state on the catalyst samples studied. An $O_{2,a}$ desorption feature peaked at ~145 K, corresponding to an adsorption energy of ~0.35 eV, is observed following exposure of the sample to the plasma-jet. Chapter 4 presents results of a study of the formation of $O_{2,a}$. It is shown that some of the $O_{2,a}$ forms via recombination of O atoms on the surface during the plasma-jet exposure. However, this does not appear to be the dominant mechanism for the formation of $O_{2,a}$.

Evidence is also presented showing that adsorption of an oxygen atom can assist in the molecular chemisorption of gas-phase molecular oxygen. As the plasma-jet is only ~40% efficient (i.e. only ~40% of molecules in plasma-jet are dissociated), gas-phase oxygen molecules that strike the surface during simultaneous atomic oxygen adsorption might have an enhanced probability of adsorbing molecularly on the sample. Other possible adsorption routes such as adsorption of excited (electronically or vibrationally) oxygen species are discussed.

In Chapter 5, an experimental protocol is presented for testing the reactivity of molecularly chemisorbed oxygen. It is found that molecularly chemisorbed oxygen does react efficiently with impinging CO at 77 K. Although it is not possible to determine the reaction probability of the molecularly chemisorbed oxygen, it appears that it is at least as reactive as the atomically chemisorbed species. The existence of a reaction channel with molecularly chemisorbed oxygen indicates that dissociation of oxygen may not be necessary for CO oxidation on gold-based catalysts. Also, the fact that the reaction appears to be relatively facile suggests that the particle size effects that have been observed for the CO oxidation reaction could be due to small particles being able to activate the molecular chemisorption of oxygen more efficiently than larger particles and bulk gold.

In Chapter 6, I summarize the major findings of my studies and discuss their implications on the current understanding of gold catalysis. I also present some recommendations for future research projects.

REFERENCES

1. B. M. W. Trapnell, Proc. R. Soc. A **218**, 566 (1953).
2. D. A. Outka, R. J. Madix, Surf. Sci. **179**, 351 (1987).
3. D. H. Parker, B. E. Koel, J. Vac. Sci. Technol. A **8**, 2585 (1990).
4. N. Saliba, D. H. Parker, B. E. Koel, Surf. Sci. **410**, 270 (1998).
5. J. M. Gottfried, K. J. Schmidt, S. L. M. Schroeder, K. Christmann, Surf. Sci. **511**, 65 (2002).
6. B.Hammer, J. K. Nørskov, Nature **376**, 238 (1995).
7. A. G. Sault, R. J. Madix, C. T. Campbell, Surf. Sci. **169**, 347 (1986).
8. G. C. Bond, J. Mol. Catal. A: Chemical **156**, 1 (2000).
9. K. S. Pitzer, Acc. Chem. Res. **12**, 271 (1979).
10. P. Pyykko, J.-P. Desclaux, Acc. Chem. Res. **12**, 276 (1979).
11. N. Bartlett, Gold Bulletin **31**, 22 (1998).
12. D. Thompson, Gold Bulletin **31**, 111 (1998).
13. G. C. Bond, D. T. Thompson, Catal. Rev.-Sci. Eng. **41**, 319 (1999).
14. G. C. Bond, Gold Bulletin **34**, 117 (2001).
15. P. Pyykko, Angew. Chem. Int. Ed. **41**, 3537 (2002).
16. M. Haruta, T. Kobayashi, H. Sano, N. Yamada, Chem. Lett. **4**, 405 (1987).
17. W. A. Bone, G. W. Andrew, Proc. R. Soc. A **109**, 459 (1925).
18. G. C. Bond, P. A. Sermon, Gold Bulletin **6**, 102 (1973).
19. D. Y. Cha, G. Parravano, J. Catal. **18**, 200 (1970).
20. S. Galvano, G. Parravano, J. Catal. **55**, 178 (1978).
21. H. Huber, D. McIntosh, G. A. Ozin, Inorg. Chem. **16**, 975 (1977).
22. G. C. Bond, D. T. Thompson, Gold Bulletin **33**, 41 (2000).

23. M. Haruta, Catal. Today **36**, 153 (1997); CATTECH **6**, 102 (2002).

24. R. Meyer, C. Lemire, Sh. K. Shaikhutdinov, H. J. Freund, Gold Bulletin **37**, 72 (2004).

25. D. R. Rainer, C. Xu, D. W. Goodman, J. Mol. Catal. A: Chemical **119**, 307 (1997).

26. D. R. Rainer, D. W. Goodman, J. Mol. Catal. A: Chemical **131**, 259 (1998).

27. V. A. Bondzie, S. C. Parker, C. T. Campbell, Catal. Lett. **63**, 143 (1999).

28. A. Sanchez, S. Abbet, U. Heiz, W.-D. Schneider, H. Häkkinen, R. N. Barnett, U. Landman, J. Phys. Chem. A **103**, 9573 (1999).

29. T. S. Kim, J. D. Stiehl, C. T. Reeves, R. J. Meyer, C. B. Mullins, J. Am. Chem. Soc. **125**, 2018 (2003).

30. S. Lee, C. Fan, T. Wu, S. L. Anderson, J. Am. Chem. Soc. **126**, 5682 (2004).

31. N. Lopez, J. K. Nørskov, J. Am. Chem. Soc. **124**, 11262 (2002).

32. Z.-P. Liu, P. Hu, A. Alavi, J. Am. Chem. Soc. **124**, 14770 (2002).

33. Y. Xu, M. Mavrikakis, J. Phys. Chem. B **107**, 9298 (2003).

34. G. Mills, M. S. Gordon, H. Metiu, J. Chem. Phys. **118**, 4198 (2003).

35. Z.-P. Liu, X.-Q. Gong, J. Kohanoff, C. Sanchez, P. Hu, Phys. Rev. Lett. **91**, 266102 (2003).

36. D. Stolcic, M. Fischer, G. Ganterför, Y. D. Kim, Q. Sun, P. Jena, J. Am. Chem. Soc. **125**, 2848 (2003).

37. L. D. Socaciu, J. Hagen, T. M. Bernhardt, L. Wöste, U. Heiz, H. Hakkinen, U. Landman, J. Am. Chem. Soc. **125**, 10437 (2003).

38. Y. D. Kim, M. Fischer, G. Ganteför, Chem. Phys. Lett. **377**, 170 (2003).

39. M. Valden, X. Lai, D. W. Goodman, Science **281**, 1647 (1998).

40. M. A. Bollinger, M. A. Vannice, Appl. Catal. B: Environ. **8**, 417 (1996).

41. M. S. Chen, D. W. Goodman, Science **306**, 252 (2004).

42. G. R. Bamwenda, S. Tsubota, T. Nakamura, M. Haruta, Catal. Lett. **44**, 83 (1997).

43. G. J. Hutchings, Gold Bulletin **37**, 3 (2004).

44. M. C. Kung, C. K. Costello, H. H. Hung, Catal. **17**, 152 (2004).

45. J. M. Gottfried, K. Christmann, Surf. Sci. **566-568**, 1112 (2004).

46. T. S. Kim, J. D. Stiehl, S. M. McClure, P. L. Tanaka, C. B. Mullins, Catal. Lett., submitted for publication.

47. M. A. Lazaga, D. T. Wickham, D. H. Parker, G. N. Kastanas, B. E. Koel, ACS Sym. Ser. **523**, 90 (1993).

48. D. Stolcic, M. Fischer, G. Ganteför, Y. D. Kim, Q. Sun, P. Jena, J. Am. Chem. Soc. **125**, 2848 (2003).

49. Y. D. Kim, M. Fischer, G. Ganterför, Chem. Phys. Lett. **377**, 170 (2003).

50. Q. Sun, P. Jena, Y. D. Kim, M. Fischer, G. Ganteför, J. Chem. Phys. **120**, 6510 (2004).

Chapter 2: Reactive Scattering of CO from an Oxygen-Atom-Covered Au/TiO_2 Model Catalyst

INTRODUCTION

Gold has historically been regarded as a highly inert material with little or no reactivity.[1] This characteristic of bulk gold has made the discovery of catalytically active gold nanoclusters somewhat surprising.[2,3] Of particular interest to many researchers has been the discovery that gold can catalyze CO oxidation at temperatures well below room temperature. An early glimpse into the unique properties of gold was provided by Huber et al. who showed that co-condensed gold atoms in a matrix of CO and O_2 catalyzed CO_2 formation at temperatures as low as 30-40 K.[2] Subsequent experiments by Haruta and co-workers showed that small, highly dispersed gold nanoclusters on metal oxide supports were highly active for CO oxidation below room temperature.[3] Haruta's pioneering discovery of the catalytic properties of supported gold nanoclusters toward CO oxidation has led to an extensive amount of research focused on understanding the unique behavior of gold clusters of nanometer scale.[4-7]

The CO oxidation activity of gold nanoclusters on porous TiO_2 supports, as well as on planar TiO_2 samples (Au/TiO_2), has been extensively studied over the past several years.[3-15] Some of the issues that have been examined include CO adsorption, oxygen adsorption, the nature of the relevant oxygen species, the origin of particle size effects, and the reactive site or sites on the catalyst. The main objective of the majority of the studies to date has been to elucidate the mechanistic details of the CO oxidation reaction. However, despite all the work completed to date, a microscopic-level description of the CO oxidation reaction on TiO_2-supported Au nanoclusters has proved somewhat elusive with differing accounts of the reaction pathway being postulated.[15]

One particularly controversial issue regarding the reaction mechanism is the nature of the oxygen species involved in the CO oxidation reaction. Oxygen is known to molecularly chemisorb on highly defective TiO_2 samples[16] but not to chemisorb on bulk gold metal samples.[17] Neither bulk Au[18] nor TiO_2 is known to catalyze the reaction of CO with O_2 to form CO_2 under ambient conditions. However, atomic oxygen precovered Au(110)[17,19,20] and Au(111)[21,22] have been shown to oxidize CO readily. Atomic oxygen covered Au/TiO_2 model catalysts samples have also been shown to oxidize CO readily at room temperature.[12] From the work of Haruta,[23] Goodman,[13] and co-workers, the dissociative chemisorption probability of O_2 on the catalysts studied can be estimated to be $\sim 10^{-8}$, assuming that oxygen dissociation is the rate-limiting step in the reaction. This low dissociative adsorption probability of oxygen on gold-titania catalysts has raised much speculation as to whether the reaction on this surface proceeds via reaction of CO with an adsorbed oxygen atom or if molecularly chemisorbed oxygen is the rate-limiting intermediate in the reaction. No conclusive evidence has been presented regarding the nature of the oxygen intermediate involved in the CO oxidation reaction on TiO_2-supported gold nanoclusters.

In contrast to Au/TiO_2 catalyst systems, it has been experimentally established that oxygen adsorbs molecularly on small, gas-phase, anionic gold clusters (model systems for supported gold nanoparticles). Recent experimental results of oxygen adsorption on small gas-phase gold clusters, Au_n ($n < 20$), reveal that oxygen adsorbs molecularly on clusters with an odd number of valence electrons.[24-27] Reports of cooperative adsorption of both O_2 and CO have also been reported on gas-phase anionic clusters (n = 2-19).[28-30] Socaciu et al. have even observed CO oxidation by free Au_2^- clusters, which are known to adsorb oxygen molecularly.[30] Further, Madix et al.,[31] Burghaus et al.,[32] and Barth et al.[33] showed convincingly that CO oxidation can occur

with a molecularly chemisorbed species on Ag(110). These reports, along with the low probability of O_2 dissociation on gold clusters, have given some credence to the possibility of a similar reaction mechanism on TiO_2-supported gold catalysts.[2-4,14,15,30]

In addition to details concerning the mechanistic steps of the CO oxidation reaction on gold-titania catalysts, another issue that has received attention is the origin of the gold particle size effect.[3,13] The properties and catalytic activity of gold nanoparticles have been observed to be strongly dependent on the size of the gold clusters when employing gas phase O_2 as a reactant at or near room temperature. Haruta and co-workers observed that the activity of their Au/TiO_2 catalyst was a strong function of the size of the gold clusters.[3] They discovered that the activity of the catalyst reached a maximum for gold particle sizes ~2.5 nm in diameter and that the activity of the catalyst severely decreased if the gold particles exceeded ~5 nm in diameter. Valden et al.[13] recently investigated the origin of the gold particle size effect observed by Haruta. They concluded that the observed gold particle size effect correlated well with quantum properties related to the two-dimensional character of the small gold particles. Using Scanning Tunneling Spectroscopy (STS), Valden et al. showed that gold particles undergo a metal to nonmetal transition in the size range where the increased catalytic activity is observed.

Bondzie et al.[12] studied oxygen adsorption on a Au/TiO_2 model catalyst as a function of gold particle size, which they controlled by varying the gold coverage on the sample, in an attempt to understand the particle size effect described by Haruta and co-workers[3] and by Valden et al.[13] In their study, they report that the adsorption of molecular oxygen on Au/TiO_2 under ultrahigh vacuum (UHV) conditions was undetectable. Because of the difficulty in detecting O_2 adsorption, they chose to dose atomic species on their sample by cracking oxygen molecules with a hot filament. In

their investigation, they observed, via temperature-programmed desorption (TPD), that the smallest gold particles bound oxygen atoms more strongly than did the larger particles. This higher binding of oxygen manifested itself in CO oxidation as a decrease in CO_2 production with decreasing particle size. Using Brønsted relations, they argued that the results of their study suggested that small gold particles will be more "efficient" at dissociating oxygen molecules than larger clusters and hence the particle size effect observed by Haruta and Valden et al. was likely related to enhanced oxygen dissociation by small particles.

Speculation exists about whether the activity of the gold particles is actually related to their enhanced ability to dissociate oxygen. Recent theoretical investigations have indicated that the activation energy for dissociation of oxygen on various gold systems is on the order of ~1 eV and thus highly unlikely to occur under conditions relevant to the reported experimental investigations.[34-37] Liu et al. recently reported on a density functional theory (DFT) calculation in which they investigated the energetics of O_2 dissociation on perfect single-crystal surfaces, stepped single-crystal surfaces, and 12 and 29 atom gold clusters.[34] On the basis of the results of their calculations, they suggested that the dissociation probability of O_2 on a supported gold catalyst is at best on the order of $\sim 10^{-21}$. Mavrakakis et al. have also reported that although molecular adsorption becomes favorable on strained and stepped macroscopic gold surfaces, dissociation of oxygen is still highly activated.[35] Mills et al. also showed that surface roughness enhances the adsorption of molecular oxygen due to a localization of highest occupied molecular orbital electrons.[36] In a recent DFT study of CO oxidation on TiO_2-supported Au, Liu et al. report that the interface between gold and the titania support was instrumental in activating molecular adsorption of oxygen, which subsequently could react with CO with a very small activation barrier.[38] In contrast to the investigations just

discussed, Lopez and Nørskov recently showed, via DFT calculations, that gold particles consisting of 10 atoms are able to easily dissociate oxygen and the activation barrier for reaction of the atomically adsorbed oxygen with CO is small.[39] However, Lopez and Nørskov also showed that molecularly chemisorbed oxygen is stable on 10-atom gold clusters and that the activation barrier for reaction of CO with molecularly chemisorbed oxygen is comparable to the activation barrier for reaction of CO with atomic oxygen.

As has been noted, some issues regarding the CO oxidation activity of Au-based catalysts (e.g., nature of active oxygen species, particle size effects) still remain unresolved. In this paper we report on results obtained during the investigation of CO oxidation on a Au/TiO_2 model catalyst system with preadsorbed oxygen atoms employing molecular beam techniques in an attempt to shed light on some of the unresolved questions. Regardless of which oxygen species (atomic or molecular) is the active species involved in the catalytic reaction, atomic oxygen is likely to participate in the reaction at some point in the process, whether it be in the form of the rate-limiting species or whether it be a secondary reactant following reaction of CO with molecularly adsorbed oxygen that subsequently leaves behind an oxygen atom. Therefore, studying the reactivity of an atomic oxygen species on Au/TiO_2 will be useful in helping understand the catalytic CO oxidation reaction.

The successful utilization of molecular beam methods by Henry,[40-44] Freund,[45-49] Matolin[50-52] and their co-workers in studying planar model catalysts motivated us to employ similar techniques for exploring the catalytic nature of the Au/TiO_2 system. Parameters such as gold coverage, oxygen-atom coverage, and surface temperature were all varied in our investigation. Atomic oxygen was preadsorbed on the Au/TiO_2 sample using a radio-frequency-generated plasma-jet because adsorption of gaseous molecular oxygen was undetectable under UHV conditions or for exposures of molecular oxygen as

high as 200 Torr for 2 minutes. CO was observed to react with preadsorbed oxygen atoms, O_a, to form CO_2 at temperatures as low 65 K. The reaction of CO + O_a was also observed to be relatively independent of gold coverage and even independent of the presence of titania if oxygen atoms were supplied to a bulk gold film. A brief account of some of this work has been published previously.[53]

EXPERIMENTAL

All experiments reported in this paper were performed in a molecular beam surface-scattering apparatus that has been described in detail elsewhere.[53,54] Briefly, the apparatus consists of an UHV surface-scattering chamber with a base pressure of ~1×10^{-10} Torr and a quadruply differentially pumped molecular beam source. The scattering chamber is equipped with an Auger electron spectrometer (AES), low-energy electron diffraction optics (LEED), a quadrupole mass spectrometer (QMS), an ion gun, a quartz crystal microbalance (QCM), and a custom-built gold deposition system. The molecular beam source chamber is equipped with an alumina, radio frequency (RF) plasma-jet atom source[55-57] (200 μm) used for depositing atomic oxygen on the surfaces studied. An 8% O_2 in argon mixture was used for generating atomic oxygen in the RF plasma-jet source. An oxygen dissociation fraction of ~40%, as determined via time-of-flight techniques, is achieved.[55-57] Oxygen coverages reported in this study are defined as the coverage of oxygen relative to saturation for the gold coverage of interest and were obtained by integration of thermal desorption spectra of O_2 from the catalyst sample. The oxygen coverage on the catalyst was varied by controlling the exposure time of the sample to the O-atom beam. Pure CO was dosed through the 200 μm nozzle with the RF power off. A typical CO beam intensity of ~9×10^{13} molecules/cm^2·s was employed. In experiments in which it was desirable to remove CO from the model catalyst surface without heating the sample, collision-induced desorption was employed.[58-60] Collision-induced desorption of

CO was accomplished by bombarding the CO-covered surface with an energetic (~1 eV) beam of Kr. High-kinetic-energy beams of krypton are generated by expanding a dilutely seeded Kr (2%) in helium gas mixture through the 200 μm nozzle with the RF power off. The apertures which shape the molecular beams result in a beam spot of ~3 mm which is smaller than the dimensions of the sample, as will be discussed below.

Following exposure of the sample to the oxygen plasma-jet, the sample is known to be populated with molecularly chemisorbed oxygen.[60] To ensure that the sample was solely populated with atomic oxygen, either the sample was heated to 300 K to desorb the oxygen or the molecularly chemisorbed oxygen was removed via collision-induced desorption. Although these two methods were both suitable for the removal of molecular oxygen from the sample, they did result in differing reactivities of the atomic oxygen. Heated samples resulted in a lower reactivity than the samples that were cleared of adsorbed molecular oxygen via collision-induced desorption. Unless otherwise noted, heating to 300 K to desorb molecularly chemisorbed oxygen was used.

Gold was vapor deposited on a TiO_2(110) single crystal (10 mm × 10 mm × 0.5 mm thick) using a procedure described in detail by Lai et al.[61] A custom-built gold doser was used to evaporate gold on the TiO_2(110) sample by resistively heating a small piece of gold attached to a tungsten filament to 900 ^{o}C. The gold deposition rate was determined using a QCM, and various gold coverages were obtained by varying the deposition time. The typical gold deposition rate used was ~0.1 Å/s. In this study, 1 ML of gold refers to a single atomic layer of close-packed gold (1.387×10^{15} atoms/cm^2), which has a thickness of approximately 2.35 Å. Lai et al. have performed an extensive characterization study of vapor-deposited gold on TiO_2(110),[61] and we expect our samples to closely resemble theirs in regards to gold particle size and distribution for the various gold coverages employed in this investigation. The TiO_2 sample used in this

study is mounted on a tantalum plate (16.25 mm × 12.5 mm × 1 mm), and a Au(111) single crystal (not used in this study) is mounted on the face of the tantalum plate opposite the TiO_2 crystal in a 0.5 mm deep recess 0.5 in. in diameter. Both samples are held in place with two 0.5 mm tungsten wire clips. A 0.1 mm thick gold foil is sandwiched between the tantalum plate and the TiO_2 crystal for improved thermal contact.[62] Two tantalum wires are spot-welded to the tantalum plate to allow for computer-controlled, resistive heating of the sample. The tantalum heating wires are attached to two copper posts mounted on the sample probe that are in thermal contact with a liquid nitrogen reservoir. A type K thermocouple is spot-welded to the top edge of the tantalum plate for measurement of temperature. A sample temperature as low as 65 K is attainable by pumping on the headspace above the liquid nitrogen reservoir with a mechanical pump.

RESULTS

Oxygen Adatom Coverage Dependence of CO Oxidation

The kinetics of surface reactions are typically directly related to the surface population of the reactants. For the CO oxidation reaction on Au/TiO_2, the oxygen-atom coverage was one parameter that could be easily varied in this investigation and which proved useful in understanding the details of the observed catalytic behavior. The effect of oxygen adatom coverage on the CO oxidation reaction was studied by varying the O-atom exposure times to the surface. Since the saturation oxygen coverage varied for different Au coverages, all oxygen coverages reported in this paper are relative to the saturation coverage at the gold coverage of interest and are determined by integration of the O_2 thermal desorption spectra, as discussed earlier.

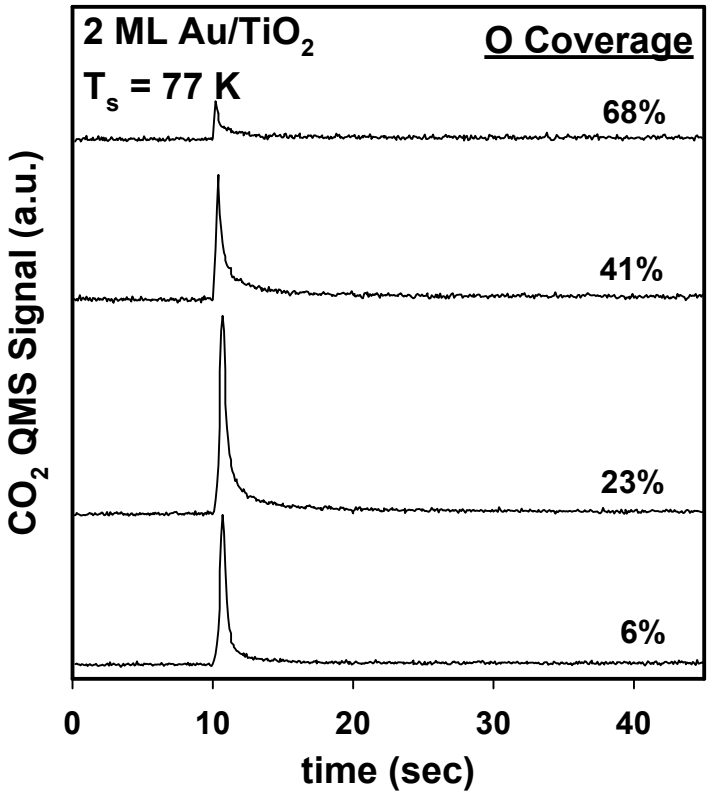

Figure 2.1: Oxygen-atom coverage dependence of the CO oxidation reaction at 77 K on a 2 ML Au/TiO_2 sample. A molecular beam of CO is impinged on the sample at t = 10 s for all the data shown.

The trends in the O-atom coverage dependence of the reaction varied as a function of the surface temperature. As will be discussed later, there are two temperature regimes which result in differing behavior of the catalyst. The two regimes are roughly demarcated by the peak desorption temperature of CO (~180 K) from the Au/TiO_2 sample. For temperatures well below the peak desorption temperature of CO, CO_2 production is observed to decrease with increasing O-atom coverage above a threshold value. For all oxygen coverages, the reaction is observed to increase rapidly when the sample is exposed to CO and then to abruptly decrease as the sample saturates with CO. Figure 2.1 shows a series of experiments performed at 77 K with 2 ML coverage of gold

and a variable oxygen adatom coverage (6-68%). Similar results for a 0.5 ML coverage have been presented previously.[53] At time t = 10 s, a beam of CO is impinged on the oxygen-covered samples and the CO_2 production is monitored with the QMS. The peak CO_2 production is observed to decrease as the oxygen adatom coverage is increased above 23% in Figure 2.1. For coverages of oxygen approaching saturation (68% in Figure 2.1), the CO_2 production is decreased drastically in intensity when compared to the CO_2 production for an oxygen coverage of 23%. If an inert flag is placed in front of the sample blocking direct impingement of the CO beam, no CO_2 production is observed.

For temperatures well below the peak CO desorption temperature, CO adsorption measurements provide another tool for studying the reaction details. The adsorption behavior of CO at 77 K was investigated as a function of O-atom coverage to determine its influence on the observed catalytic behavior discussed above. Specifically, the CO uptake by the sample was measured as a function of O-atom coverage. The uptake of CO by the surface was observed to decrease with increasing oxygen coverage for all gold coverages studied, partly explaining the drop in reactivity observed. As the oxygen-atom coverage increases, less adsorbed CO is available for reaction. Figure 2.2 shows a series of King and Wells adsorption measurements[63] made on a 0.5 ML Au/TiO_2 sample at 77 K with varying oxygen coverages. For comparison, measurements of the adsorption of CO on a bare TiO_2 sample (i.e., no gold) with equivalent oxygen exposure times to those used for the 0.5 ML Au/TiO_2 sample are shown. A King and Wells measurement consists of detecting the particles (i.e., CO) that reflect from the surface during beam impingement. By comparing the reflected signal from the sample with the reflected signal from an inert surface or the saturated sample (which reflect all species in the beam), quantitative measurements of the adsorption probability and uptake by the sample can be

obtained. As can be seen in Figure 2.2, the initial CO adsorption probability (~0.8) on the sample is

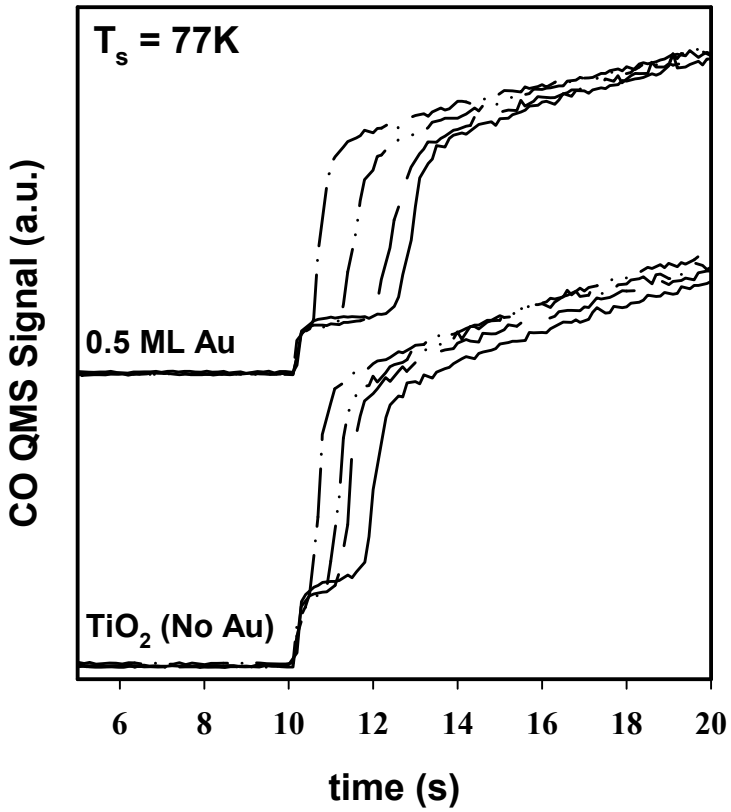

Figure 2.2: CO King and Wells adsorption measurements at 77 K on a 0.5 ML Au/TiO_2 sample and a bare TiO_2 (no gold) sample as a function of oxygen coverage. Measurements for oxygen coverages of 0% (solid), 9% (dashed), 17% (dash-dot-dot-dash) and 100% (dash-dot-dash) on the 0.5 ML Au/TiO_2 are shown. For the bare TiO_2 measurements, the sample was given equivalent oxygen exposures as the 0.5 ML Au/TiO_2 sample. For all measurements, the initial CO adsorption probability is ~0.8.

relatively independent of the oxygen coverage. However, the total uptake of CO by the catalyst is observed to be greatly suppressed as the oxygen-atom coverage approaches saturation, as indicated by the decreasing time for the onset of CO saturation (abrupt increase in reflected CO signal) of the sample. Similar trends are observed on the bare

TiO_2 sample with the exception that no CO_2 is produced (not shown) on the gold-free titania crystal. It should be pointed out that for the experiments shown in Figure 2.2, the sample was neither heated nor bombarded with Kr to remove molecularly adsorbed oxygen prior to performing the experiments. However, additional experiments reveal that the trends observed in Figure 2.2 are independent of sample heating or Kr bombardment.

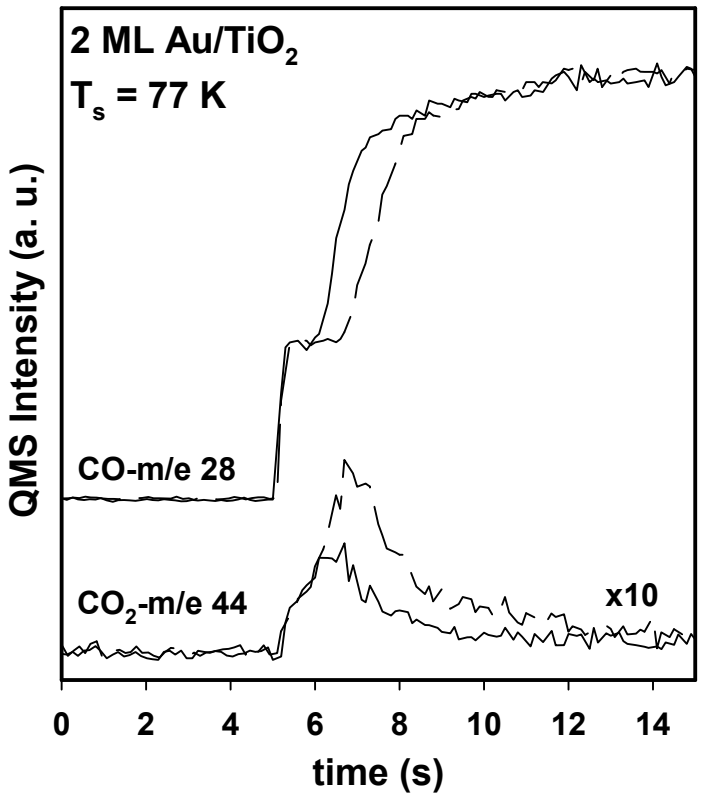

Figure 2.3: King and Wells reflectivity measurement of CO (*m*/*e* 28) and CO_2 (*m*/*e* 44) production for 20% (dashed line) and 38% (solid line) O-atom coverages on a 2 ML Au/TiO_2 sample at 77 K. CO beam impinges the sample at t = 5 s.

From the CO adsorption studies mentioned above, we have discovered that the production of CO_2 is observed to abruptly decrease coincident with the apparent onset of saturation of the surface with CO. Shown in Figure 2.3 is the CO_2 production

simultaneously monitored along with the King and Wells uptake measurements of the CO beam for two initial O-atom coverages, 38% and 20%, at 77 K on a 2 ML Au/TiO_2 sample. The measurements of the reflected CO intensity during the reaction reveal that the time for the onset of saturation, characterized by the sharp increase in the CO reflected signal, differs by ~1 s for the two initial O_a coverages shown in Figure 2.3. Closer examination of the reaction reveals that the peak in the production of CO_2 coincides with the onset of CO saturation. The shorter time available for reaction, as well as the decrease in the uptake of CO by the sample, results in a decrease in the CO_2 production for the sample with the 38% O coverage compared to the sample with a 20% O coverage. Although the CO_2 production is strongly affected by CO saturation, the initial (i.e., zero CO coverage limit) reaction probability is on the order of ~5% per adsorbed CO molecule.

Considering the prompt reaction that is observed upon impingement of the CO beam on the sample, it is interesting that the reaction is essentially poisoned by accumulation of CO on the sample. The observation that less CO_2 is made with increasing O-atom coverage indicates that there is still a large oxygen-atom population on the sample after the reaction is suppressed. Evidence that the reaction is suppressed by the accumulation of CO and not due to a loss of activity of the oxygen atoms comes from experiments that show the reactivity of the sample can be partially recovered by removal of CO and reexposure of the sample to the CO beam. Two approaches for clearing the sample of CO were explored, thermal desorption and collision-induced desorption, and both methods gave similar results. Figure 2.4a shows the CO_2 production from a 2 ML Au/TiO_2 sample with a ~10% oxygen coverage. Following the CO exposure in Figure 2.4a, the sample was heated to 300 K to desorb the excess CO on the sample. After cooling back to 77 K, the sample was once again exposed to the beam of CO, and the

CO_2 production is shown in Figure 2.4b. As can be seen in Figure 2.4b, CO_2 production is once again observed, indicating that oxygen atoms remain on the surface.

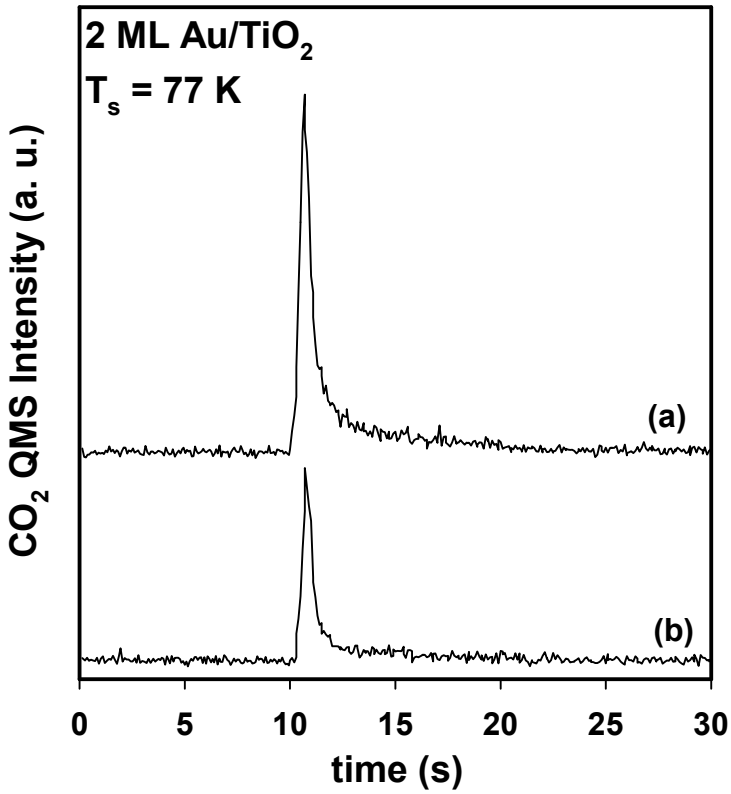

Figure 2.4: CO_2 production: (a) 2 ML Au/TiO_2 sample with a ~10% relative O-atom coverage at 77 K and (b) following heating to 300 K to desorb CO adsorbed in (a) and cooling to 77 K.

Heating the sample to 300 K to desorb CO also provides sufficient thermal energy to the adsorbed oxygen atoms on the surface to make them mobile, thus resulting in a redistribution of the oxygen atoms via diffusion. A redistribution of the oxygen atoms might result in an enhancement in the reactivity of the surface. In an attempt to minimize any effects due to thermally activated diffusion of oxygen atoms occurring during the heating ramp to 300 K, collision-induced desorption was employed.[58-60] Using an energetic beam (~1.0 eV) of Kr atoms impinging on the surface at normal incidence, the

sample could be cleared of CO rapidly at T_s = 77 K.[60] The collision-induced desorption of CO is expected to result in minimal disruption to the adsorbed oxygen atoms, thus allowing a determination of whether the recovery of the reactivity of the sample (as shown in Figure 2.4) is a result of oxygen-atom diffusion or whether it results from an absence of CO on the surface. Figure 2.5 shows a typical experiment in which an O- and a CO- covered surface was bombarded with a ~1.0 eV beam of Kr at normal incidence. The sample that was bombarded in the experiment shown in Figure 2.5 was a 2 ML Au/TiO_2 sample that was precovered with a 20% relative O-atom coverage and was titrated with a CO beam for 10 s at 77 K. Following the CO titration, the Kr beam was allowed to impinge on the sample at t = 10 s (Figure 2.5), at which time a sharp peak in the mass 28 signal was observed which decreased as the sample was cleared of CO. Also shown in Figure 2.5 is the mass 44 (CO_2) signal that was monitored during the Kr bombardment. A small increase in the mass 44 signal is observed when the Kr beam impinges on the sample. The mass 44 signal is believed to result from a collision-induced reaction between O atoms and CO molecules on the surface. Retitration of the sample following the collision-induced desorption measurement shown in Figure 2.5 resulted in the formation of CO_2 (not shown) in accord with the behavior shown in Figure 2.4. We have shown in recent experiments on Au(111) that 1 eV Kr atoms do not measurably perturb the oxygen atoms on the surface.[64]

Collision-induced desorption of CO can be used as a tool for indirectly investigating the O-atom surface population. Since the oxygen-atom mobility is not expected to be significant at 77 K, the reactivity of the oxygen remaining after titration with CO can be studied by clearing the sample of CO, via collision-induced desorption, with minimal disruption to the adsorbed oxygen atoms, and re-titrating the catalyst with CO. Figure 2.6a shows the CO_2 production obtained from a 2 ML Au/TiO_2 catalyst at 77

K with an initial oxygen coverage of ~10%. It should be noted that the sample was cleared of molecularly chemisorbed oxygen via collision-induced desorption prior to the CO exposure shown in Figure 2.6a and not by heating the sample to 300 K. Following the experiment shown in Figure 2.6a, the sample was bombarded with a high-kinetic-energy (~1.0 eV) beam of Kr at 30^{o} incidence to induce desorption of CO, as was shown in Figure 2.5. The sample was then re-titrated with CO, and the evolution of CO_2 is shown in Figure 2.6b. This procedure of titrating with CO followed by collision-induced desorption of CO was repeated until the CO_2 production was only a small fraction of the amount made in the experiment shown in Figure 2.6a. The results are shown in curves c-f in Figure 2.6. CO_2 production is observed when titrating the sample with CO following each collision-induced desorption experiment. However, following the fifth collision-induced desorption measurement, the amount of CO_2 produced (curve 2.6f) during CO titration is only a small fraction of the amount initially produced. After the experiment shown in Figure 2.6f, the sample was heated to 300 K to allow any oxygen that might be remaining on the sample to redistribute on the catalyst. The sample was then allowed to cool to 77 K and a CO titration, Figure 2.6g, was performed. Only a small increase in the CO_2 production, compared to Figure 2.6f, is observed indicating that only a small quantity of "new" oxygen was made available for reaction during the heating ramp to 300 K. To determine if there was any reactive oxygen remaining on the sample following the experiment shown in Figure 2.6g, the sample was once again heated to 300 K, followed by cooling back to 77 K and then retitrated with CO, Figure 2.6h. A negligible amount of CO_2 is produced on reexposure to the CO beam, indicating that all of the oxygen atoms on the surface have been consumed. This conclusion is also supported by a thermal desorption measurement (not shown) following the experiments shown in Figure 2.6 in which no recombinative desorption of oxygen atoms from the gold particles is evident.

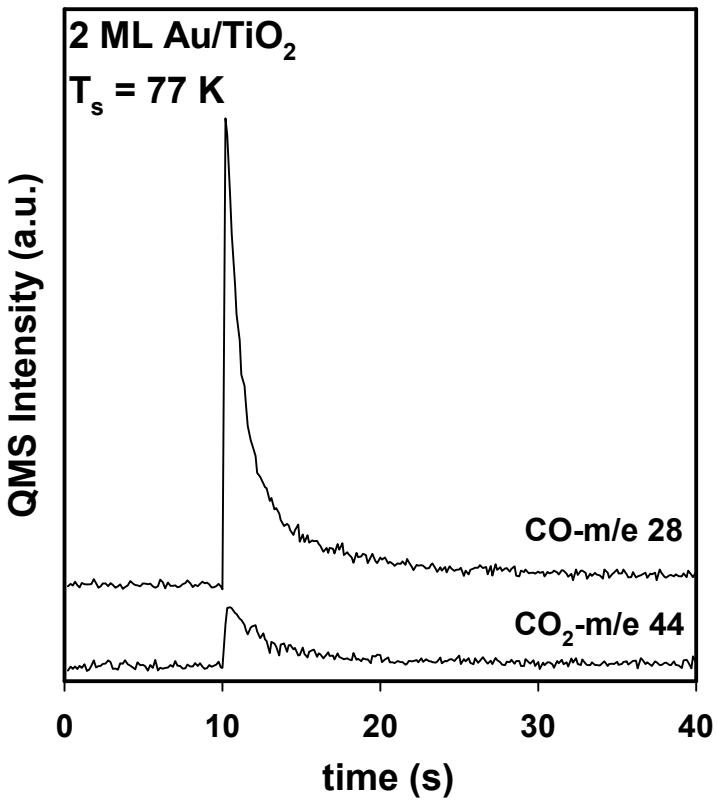

Figure 2.5: Evolution of the species *m*/*e* 28 (CO) and 44 (CO_2) during bombardment of a 2 ML Au/TiO_2 sample with a high-kinetic-energy (~1 eV) Kr beam, incident on the sample at 0^o at 77 K. Prior to Kr bombardment, the sample was precovered with a 20% relative O-atom coverage and titrated with a CO beam for 10 s.

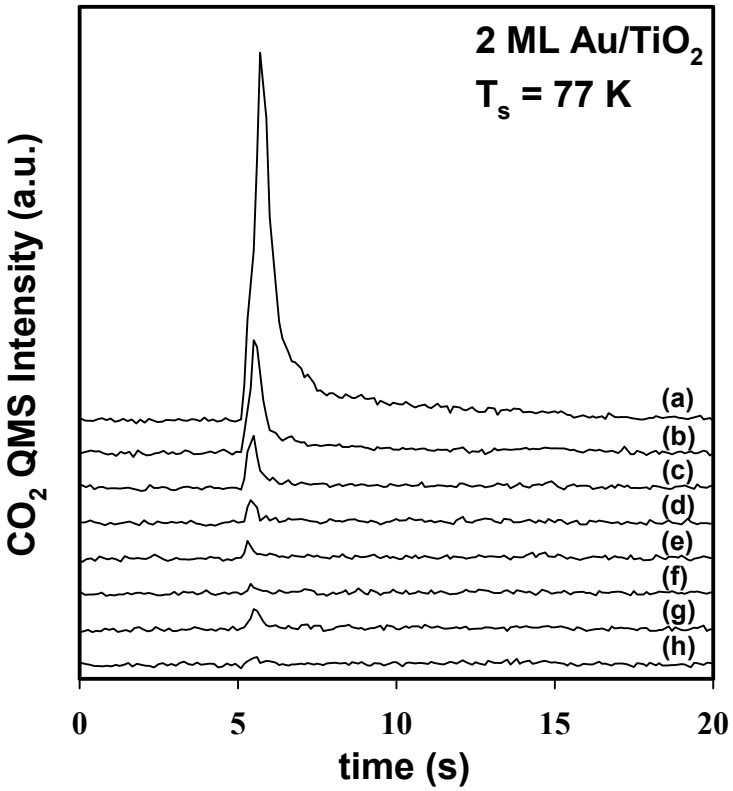

Figure 2.6: CO_2 production at 77 K from (a) CO titration (starts at t = 5 s) of a 2 ML Au/TiO_2 sample with a 10% relative O-atom coverage, (b) CO titration of sample following high-kinetic-energy (~ 1.0 eV) Kr bombardment at 30° incidence of sample following experiment shown in (a), (c)-(f) CO titration of sample following high-kinetic-energy (~ 1.0 eV) Kr bombardment at 30° incidence of sample following the preceding experiments, (g) CO titration of sample after heating of sample to 300 K following experiment shown in (f) and cooling to 77 K, and (h) CO titration of sample after heating of sample to 300 K following experiment shown in (g) and cooling to 77 K. Sample was kept at 30° throughout entire experiment to ensure that gas exposures were on the same spot of the sample. Also, the sample was cleared of molecularly chemisorbed oxygen via collision-induced desorption prior to the first CO exposure and not by heating the sample to 300 K.

More insight into the reaction details can be gained by studying the reaction at temperatures exceeding the desorption temperature of CO. Under these conditions, the issues regarding surface saturation by CO, which were discussed above, can be avoided since the lifetime of a CO molecule on the surface will be very short in comparison to the time scale of the experiment. Since CO does not accumulate on the surface and impede the reaction, as is seen for temperatures well below 180 K, the reaction is able to proceed until all the oxygen on the surface has been consumed. Also, the effect of surface temperature on the adsorbed oxygen-atom layer can be investigated.

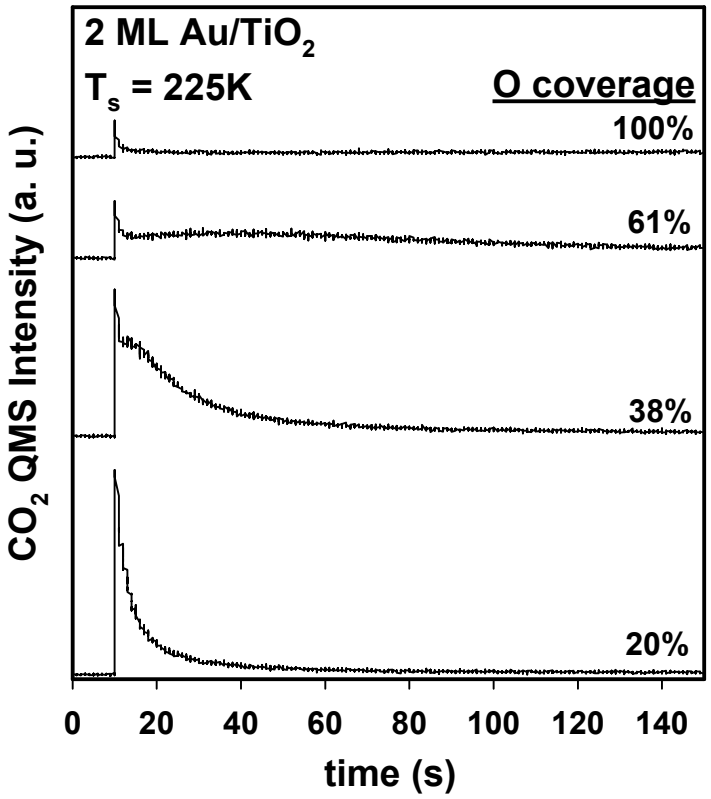

Figure 2.7: CO_2 production at 225 K from a 2 ML Au/TiO_2 sample as a function of O-atom coverage. O-atom coverages shown range from 20% to 100%.

For temperatures exceeding the desorption temperature of CO, the CO_2 production also varies as a function of the oxygen coverage. Figure 2.7 shows the CO_2

production as a function of oxygen coverage from a 2ML Au/TiO_2 surface at 225 K. The oxygen-atom coverages shown in Figure 2.7 range from 20% to 100% of saturation. For low coverages of oxygen, the reaction is characterized by a sharp rise in the CO_2 production upon impingement of CO followed by a decay in the reaction rate as the oxygen is consumed. For intermediate coverages of oxygen on the 2 ML Au/TiO_2 sample, bimodal curves are observed. For coverages approaching saturation, the reaction is characterized by a smaller, sharp initial rise in CO_2 production followed by a rapid decrease.

Figure 2.8 shows a similar set of data to that presented in Figure 2.7 with the exception that the oxygen coverage dependence of the CO oxidation reaction was studied on a 0.5 ML Au/TiO_2 sample at 225 K. The oxygen coverages shown in Figure 2.8 range from 17% to 67%. The CO oxidation reaction at low and high oxygen coverages is qualitatively similar to the behavior shown in Figure 2.7. For low oxygen coverages, there is an initial rapid rise in the CO_2 production on impingement of the CO beam (10 s) followed by a decay in the CO_2 production as the oxygen on the sample is consumed. For oxygen coverages approaching saturation, there is a rapid increase in the CO_2 production upon impingement of the CO beam, followed by an abrupt decrease in the reaction. However, for intermediate coverages of oxygen on the 0.5 ML sample, no bimodal curves are observed, in contrast to the behavior seen on the 2 ML Au/TiO_2 sample shown in Figure 2.7. It is worth noting that, based on the work of Lai et al.,[61] a 0.5 ML Au coverage results in an average gold particle size of ~2.5 nm, a size that is known to be active for CO oxidation under high-pressure conditions employing gaseous CO and O_2, whereas a 2 ML gold coverage results in an average particle size of ~4.5 nm, a size which is known to be relatively inactive for the CO oxidation reaction.

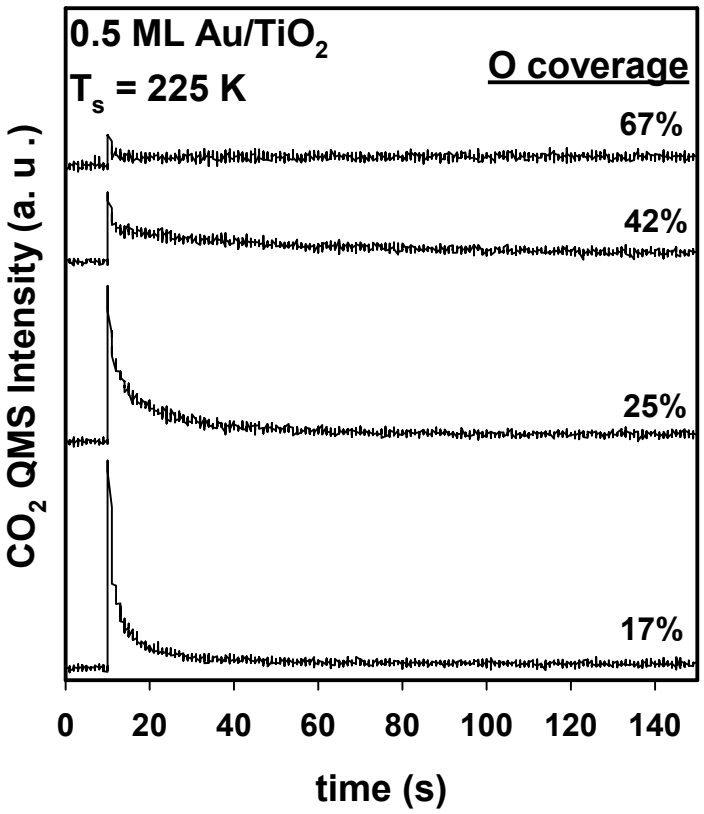

Figure 2.8: CO_2 production at 225 K from a 0.5 ML Au/TiO_2 sample with variable oxygen coverage. Measurements for oxygen coverages ranging from 17% to 67% are shown.

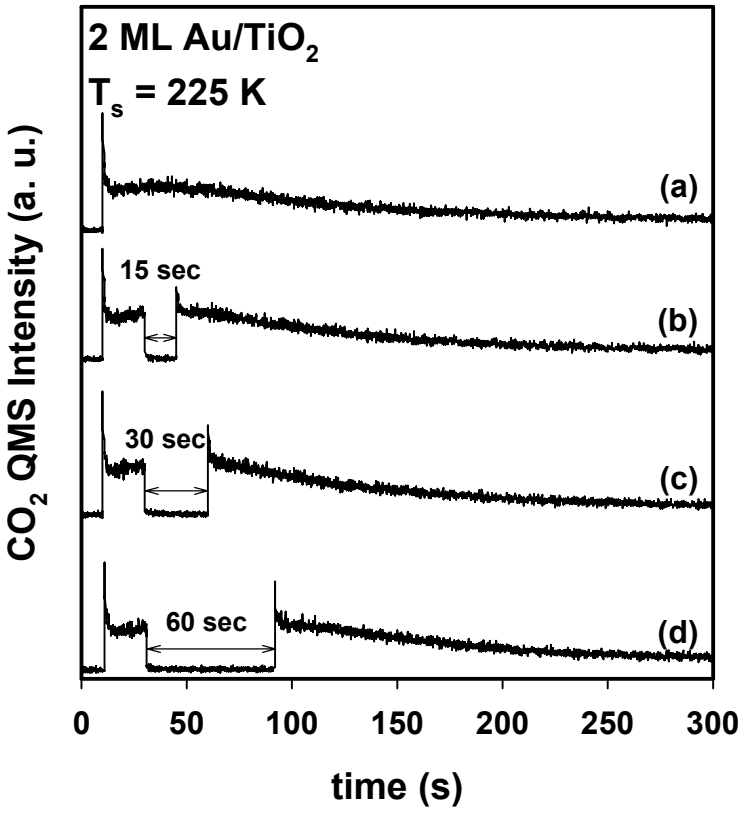

Figure 2.9: CO_2 production at 225 K from a 2 ML Au/TiO_2 sample with a 61% relative O-atom coverage. (a) Continuous beam of CO was impinged on the sample at t = 10 s. (b)-(d) CO beam was impinged on the sample at t = 10 s, and the reaction was allowed to proceed for 20 s, at which time the CO beam was blocked from impinging on the sample. The sample was held at the reaction temperature for (b) 15, (c) 30, and (d) 60 s before reexposing the sample to the CO beam once again.

The lack of CO accumulation on the sample for temperatures above 180 K also allows for an investigation into the mobility of oxygen atoms on the surface. The effect of oxygen mobility on the surface was studied by titrating an oxygen-precovered surface (intermediate coverage) with CO at a temperature exceeding the desorption temperature of CO. As was mentioned above, for intermediate coverages of oxygen, a bimodal trend is observed in the CO_2 production curves. To investigate whether the observed behavior

is due to oxygen mobility on the surface, the CO beam was blocked before the maxima of the second feature in the CO_2 production curve was evident. The sample was then held at the reaction temperature for a given amount of time, after which the sample was reexposed to the CO beam. Figure 2.9 shows a series of experiments performed in the manner described above on a 2 ML Au/TiO_2 sample with an initial relative O-atom coverage of 61% at 225 K. In all data shown, the CO beam is impinged on the sample at t = 10 s and the reaction is allowed to proceed for 20 s, at which time the CO beam is shuttered from entering the scattering chamber. The anneal time after the CO beam is blocked from impinging on the sample is varied before re-exposing the sample to CO. Figure 2.9a shows the CO_2 production for a continuous exposure of CO as a reference spectrum. A bimodal CO_2 production curve is observed as was discussed previously. Parts b, c, and d of Figure 2.9 show the CO_2 production curves for samples that were annealed at the reaction temperature for 15, 30, and 60 s respectively, following an initial 20 s CO exposure. On reexposing the sample to CO following the anneal, a slight increase in the CO_2 production above its value prior to the CO beam being blocked is observed for all three anneal times. Due to experimental uncertainties in the O-atom dose and variations in the CO flux during the three experiments, it is difficult to attribute the slight differences observed in the CO_2 production following the three different anneal times to oxygen mobility. The behavior shown in Figure 2.9 might simply be attributed to an initially transient CO surface population when reexposing the sample to the CO beam.

Surface Temperature Dependence of CO Oxidation

As seen in the previous section, the reaction of CO with atomically adsorbed oxygen on a Au/TiO_2 surface is a strong function of the surface temperature. The surface temperature dependence of the CO oxidation reaction with preadsorbed oxygen atoms on

a Au/TiO_2 model catalyst has been investigated over the temperature range 65-250 K. Most notably in this study, CO oxidation with preadsorbed oxygen atoms is observed to occur at temperatures as low as 65 K. CO_2 production is not observed from (i) an oxygen-atom-precovered TiO_2 sample without gold or (ii) from a Au/TiO_2 sample without preadsorbed oxygen atoms, at any temperature studied.

As previously mentioned, the results of this portion of the study can generally be divided into two temperature regimes with the peak desorption temperature of CO from Au/TiO_2 (~180 K) demarcating the boundary between the two regimes. Figure 2.10 shows the CO_2 production from a 2 ML Au/TiO_2 sample precovered with a 38% relative O-atom coverage at various surface temperatures ranging from 65 to 250 K. For the experiments shown in Figure 2.10, the sample was heated to 300 K to desorb any adsorbed molecular oxygen prior to reaction. As can be seen in Figure 2.10, the trends in the CO_2 production curves vary between the two temperature regimes studied. For temperatures well below the peak desorption temperature of CO from Au/TiO_2 (~180 K), there is a rapid rise in the production of CO_2 upon impingement of the CO beam followed by an abrupt decrease in the CO_2 production, as shown in Figure 2.10 for 65 and 77 K. For temperatures exceeding the peak desorption temperature of CO, the trends of the CO_2 production curves are strong functions of the oxygen-adatom coverage on the surface, as discussed in the previous section. For intermediate coverages of oxygen adatoms on 2 ML Au/TiO_2, as shown in Figure 2.10, the CO_2 production curves are observed to be bimodal. A fast initial rise and reduction in the CO_2 QMS signal is observed at early times, followed by a slow, broad peak whose maximum location is also a function of the oxygen-adatom coverage. As was mentioned in the previous section, for low coverages of gold (e.g., 0.5 ML) no bimodal CO_2 production curves are observed. For low oxygen-adatom coverages, the CO_2 production curves are not bimodal as seen in Figure 2.7. For

high oxygen coverages, approaching saturation, there is a quick rise in the CO_2 production followed by an abrupt decrease in the CO_2 production. Even at temperatures where CO does not accumulate, a saturation coverage of O renders the surface relatively unreactive.

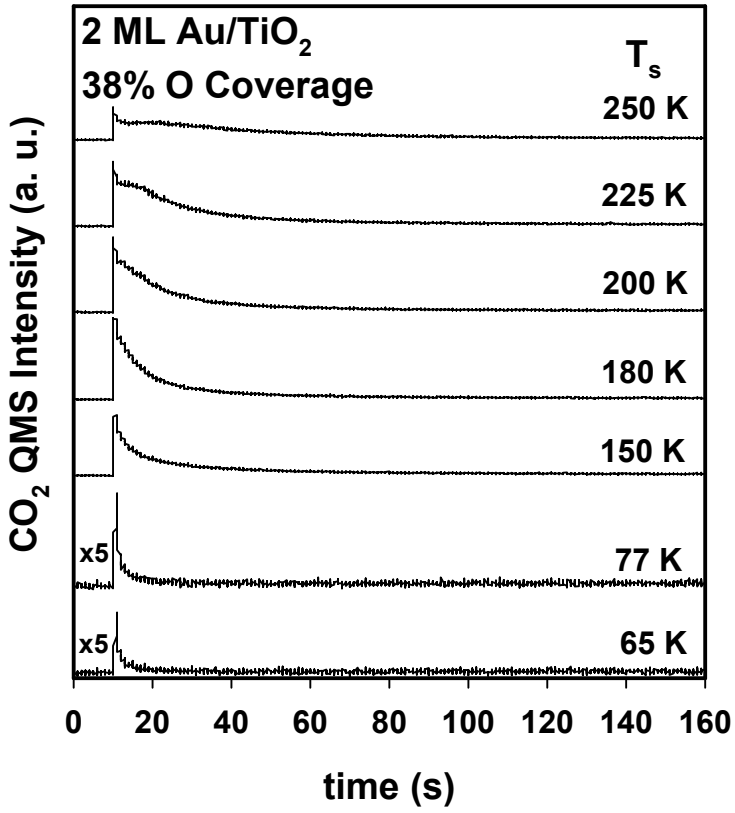

Figure 2.10: Temperature dependence of the CO oxidation reaction on a 2 ML Au/TiO_2 sample. Data shown are for temperatures ranging from 65 to 250 K. The data shown are for an initial oxygen coverage of 38%, and the CO beam is impinged on the sample at t = 10 s for all the data shown.

Au Coverage Dependence of CO Oxidation

The effect of particle size on the CO oxidation reaction with preadsorbed oxygen atoms at 77 K has also been investigated.[53] As was mentioned earlier, previous studies have found the CO oxidation reaction kinetics, when employing molecular oxygen as a

reactant, to be a strong function of gold particle size. A maximum in reactivity has been observed for particle sizes approximately 2.5 nm in diameter, while the reaction has been observed to be severely suppressed as the gold particle size increases above approximately 6 nm.[3,4,13] The effect of particle size on the reaction of CO with O atoms may provide some insight into which aspect of the mechanism, for the reaction employing molecular oxygen at higher pressures, might be affected by the gold particle size.

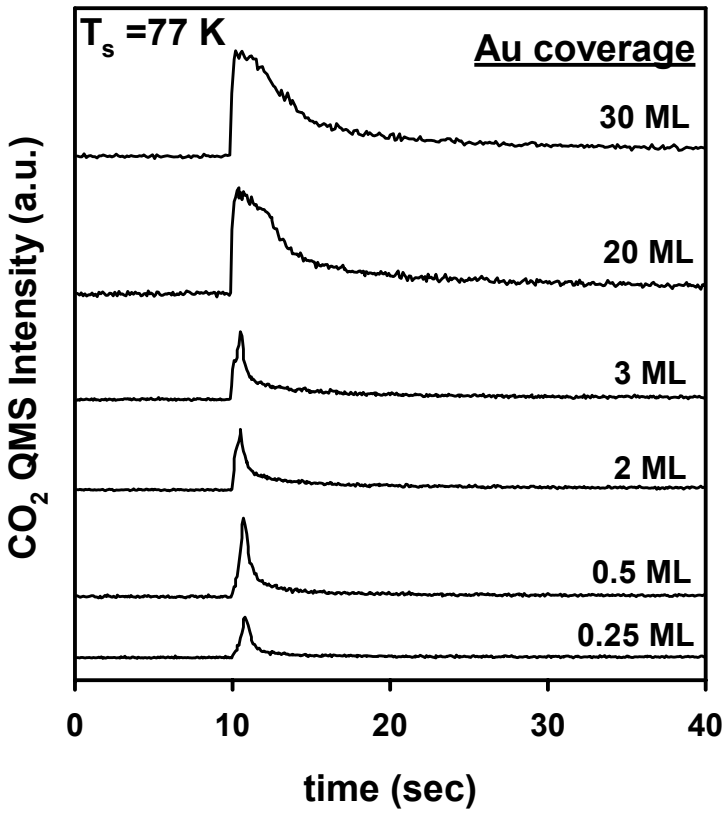

Figure 2.11: CO_2 production at 77 K from Au/TiO_2 samples of varying gold coverage. CO beam is impinged on the surface at t = 10 s for all the data shown.

Figure 2.11 shows a series of CO oxidation experiments performed at 77 K on Au/TiO_2 samples with varying gold coverages.[53] The gold coverages shown in Figure

2.11 range from 0.25 to 30 ML, with the 20 and 30 ML coverages being nominally continuous gold films. Unlike the lower Au-coverage samples, the 20 and 30 ML gold films were deposited at 77 K because heating of the films resulted in agglomeration of the gold and exposure of the underlying TiO_2 substrate, as determined via AES. The oxygen coverage on all the samples ranged between 50% and 70%, and the samples were neither heated nor bombarded with Kr to remove any molecular oxygen present on the surface prior to measurements. The 20 and 30 ML gold films were given the same oxygen exposure as the 3 ML gold sample. From Figure 2.11 it is evident that the CO oxidation reaction with preadsorbed oxygen atoms occurs readily on all the surfaces regardless of the Au coverage. The reaction is even observed to occur on a nominally continuous gold film (titanium Auger signal is greatly suppressed), strongly suggesting the Au/TiO_2 interface is not critical for CO oxidation by oxygen atoms.[17,22,53] Although the amount of CO_2 produced changes with increasing gold coverage, CO_2 production is observed for gold coverages that correspond to particle sizes larger than 5-6 nm in diameter, unlike previous studies[3,13] employing gaseous molecular oxygen as a reactant.

O_2 Adsorption

As was mentioned in the Introduction, the dissociation probability of O_2 on Au/TiO_2 catalysts is expected to be very small and practically immeasurable under UHV conditions.[12,34-37] No detectable dissociation of oxygen on Au/TiO_2 was observed under UHV conditions employing a high intensity room temperature molecular beam of pure O_2 with an average kinetic energy of ~0.1 eV. In another attempt to measure the dissociation of oxygen on a Au/TiO_2 model catalysts, a 0.5 ML Au/TiO_2 sample was exposed to pressures as high as 200 Torr of O_2 for 2 min, at a sample temperature of 300 K in a high-pressure cell, which can be isolated from the UHV-scattering chamber with a gate valve. After the O_2 exposure, the high-pressure cell was evacuated and pumped with

a turbo pump for approximately 2 hours until the pressure decreased to ~10^{-8} Torr. The gate valve separating the high-pressure cell and the UHV-scattering chamber was then opened and the sample was transferred back into the UHV chamber. The sample was then cooled to 77 K and exposed to a molecular beam of CO, while the production of CO_2 was monitored with a QMS. No CO_2 production was observed, indicating that dissociation of O_2 was not detectable.

A similar experiment to the one described above was performed to determine if any oxygen that might dissociate could "survive" in an environment of O_2 at 200 Torr. A 0.5 ML Au/TiO_2 sample was precovered with 4% relative ^{18}O-atom coverage employing the plasma source prior to exposing the sample to 200 Torr of $^{16}O_2$ in the high-pressure cell. After the high-pressure exposure, the sample was exposed to a molecular beam of CO and mass 46, corresponding to $C^{16}O^{18}O$, was monitored with a QMS. No mass 46 was detectable indicating that the contamination level in the background during the 200 Torr O_2 exposure (or at some point during the process) was sufficient for scrubbing off the ^{18}O on the sample and hence too high to allow for measurement of O_2 dissociation.[12]

DISCUSSION

The reaction of CO with preadsorbed atomic oxygen on a Au/TiO_2 model catalyst has been studied over the temperature range 65-250 K as a function of gold and oxygen-atom coverage. Prompt CO_2 production is observed for moderate oxygen coverages, even at 65 K, providing further evidence that the activation barrier for reaction of CO with atomic oxygen on the model catalyst surface is very low as has been suggested by Bondzie et al.[12] and as has been calculated using DFT.[34,39] The investigation of the Au-coverage dependence of the CO oxidation reaction has shown that the reaction is relatively independent of gold coverage, and hence particle size, if atomic oxygen is supplied to the catalyst prior to exposure to a beam of CO. The reaction is independent

of the gold coverage in the sense that there is no deactivation of the catalyst as the gold loading increases, in contrast to the studies of Haruta,[3] Goodman,[13] and co-workers. The low activation barrier for reaction and the particle size independence observed in this study indicate that if atomic oxygen is the active species during catalytic reactions on Au/TiO_2 employing molecular oxygen, then O_2 dissociation is likely the rate-limiting step and the observed particle size effect is likely due to enhanced O_2 dissociation by small (~3 nm) gold particles as was suggested by Bondzie et al.[12] The observation of the high reactivity on nominally continuous gold films also indicates that the TiO_2 support is unnecessary for catalyzing CO oxidation if atomic oxygen is supplied to the gold surface, and hence, the gold-titania interface does not play a special role in the observed reactivity. This claim is also consistent with ongoing studies of CO oxidation with atomically adsorbed oxygen atoms on Au(111) that reveal similar behavior to the model catalyst samples.[22] This result suggests that if the rate-limiting active oxygen species involved in the reaction is an oxygen atom, then the role of the support during CO oxidation employing molecular oxygen may only be important in the adsorption and dissociation of O_2.

As was mentioned in the Introduction, there is no experimental evidence[12] for dissociation of molecular oxygen on Au/TiO_2 and theory[34-37] suggests that the barrier for dissociation is on the order of ~1 eV. Therefore, it is possible that molecularly chemisorbed oxygen is the rate-limiting species in the reaction. If molecularly chemisorbed oxygen is the active species in the CO oxidation reaction, an adsorbed atomic oxygen species will likely be generated during the reaction, which will readily react with CO to form CO_2.

The results of this investigation indicate that there are two distinct reaction regimes over the temperature range studied. The reaction behavior of the catalyst differs

for temperatures well below the peak desorption temperature of CO and temperatures exceeding the peak desorption temperature of CO. The observed difference between the two temperature regimes appears to be a direct result of the accumulation of CO on the catalyst for temperatures well below 180 K.

For surface temperatures well below the desorption temperature of CO (e.g., 77 K), the reaction is drastically suppressed by CO saturation despite an abundance of oxygen atoms still present on the surface. If the accumulated CO is removed from the surface, either by collision-induced desorption or thermal desorption, CO_2 production is once again observed if the sample is reexposed to a CO beam. CO adsorption measurements at 77 K have also shown that the CO uptake by the sample decreases with increasing oxygen coverage. This effect combined with the observation that CO saturation of the surface drastically impedes the reaction works to decrease the CO_2 production as the oxygen coverage increases above a threshold value.

One possible explanation for the observed catalytic behavior for temperatures well below the desorption temperature of CO is that there is a distribution of sites on the model catalyst with differing reactivities, some of which may be completely inactive at temperatures as low as 77 K. Thus, once the "active" oxygen is consumed, the reaction stops despite the coexistence of O and CO on the surface. The distribution of sites might be edge sites[8,38] of the particles and sites on the terraces of the particles or simply sites of variable coordination number.[39] However, the observation that all the oxygen atoms can be consumed by reaction at 77 K, if steps are taken to keep the surface clear of CO (Figure 2.6), suggests that the reaction of CO with preadsorbed atomic oxygen is not exclusive to the edge sites of the particles, as has been suggested by Liu et al. from DFT calculations regarding the reactivity of molecular oxygen on Au/TiO_2,[38] and that there are no catalytically inactive sites populated by oxygen atoms on the gold surface. Also,

recent findings from a study of CO oxidation with preadsorbed oxygen atoms on a Au(111) single crystal cast doubt on the observed behavior being a result of reaction at the edges of the particles since similar behavior is seen on the single-crystal sample.[22] In Lopez et al.'s recent study of Au_{10} particles, they determined that low-coordinated geometries on the gold particle are highly reactive for CO oxidation.[39] In their calculations, they determined the energetics of an oxygen molecule dissociating and then reacting with CO on the particle. Since we are dosing atomic oxygen we are likely also populating high-coordination sites on the surface that are less reactive than oxygen atoms on low-coordinated sites and may not be reactive at 77 K. This picture, however, is hard to reconcile with the drop in CO adsorption with increasing O coverage. Also, as mentioned earlier, the observation that it is possible to remove CO from the surface via collision-induced desorption without altering the adsorbed atomic oxygen and still recover the reactivity argues against any effects resulting from variable coordination sites. The catalytic behavior could just be a matter of CO adsorption site blocking with increasing O coverage. This interpretation is consistent with the observation that the CO uptake by the sample is reduced as the oxygen coverage is increased (Figure 2.2).

An alternate explanation for the observed catalytic behavior at low temperatures is that under the O-exposure conditions employed, some oxygen atoms might be driven into the bulk of the particles, thus making them inaccessible to CO. Gottfried et al. recently reported on a study in which they were able to populate a Au(110)2×1 single crystal with atomic oxygen by sputtering the sample with 1, 2, and 5 keV oxygen ions.[65] In their study they observed four distinct peaks in the desorption spectra of oxygen from the sample. One of the peaks in the spectra was attributed to subsurface oxygen species whose desorption is limited by diffusion to the surface. After exposing the sample to 8000 L of CO at 300 K, the desorption peak attributed to the subsurface oxygen was

unperturbed. Although the oxygen deposition method that we employed in this study is drastically different than the method employed by Gottfried et al., it might be possible that the high exposure of O atoms from the plasma-jet source is causing some of the oxygen atoms on the surface to diffuse into the subsurface region of the particles when the coverage exceeds some critical value. Subsurface oxygen has been formed during exposures of a Rh(111) single crystal to an oxygen plasma source similar to the one employed in this study.[66,67] However, the experimental evidence, as shown in Figure 2.6, suggests that the existence of subsurface oxygen species in our gold nanoclusters is highly unlikely. The results shown in Figure 2.6 indicate that the oxygen on the sample can be depleted at 77 K if accumulation of CO can be minimized by collision-induced desorption.

Results for temperatures exceeding the desorption temperature of CO are also somewhat suggestive of a distribution of sites on the catalyst with varying reactivities. For intermediate coverages of oxygen, the bimodal peaks observed during the reaction on 2 ML Au/TiO_2 samples could be interpreted as reaction of two distinct oxygen species. In fact, XPS studies of the oxidation of bulk gold samples reveal that there is a coexistence of chemisorbed oxygen atoms and an oxide phase present after exposure to ozone.[68] Perhaps the coexistence of these phases on the 2 ML Au/TiO_2 samples could be responsible for the reactivity trends that are observed. However, the fact that these bimodal reaction curves are not observed on the 0.5 ML Au/ TiO_2 sample, which has particles more in the range of the size seen on active, high surface area catalysts, might indicate that the bimodal features are actually characteristic of bulk gold chemistry, as observed on Au(111),[22] and not really relevant to Au/TiO_2 catalysis.

CONCLUSION

The purpose of this study was to gain some insight into the microscopic-level details regarding the CO oxidation reaction on titania-supported gold catalysts. Due to the difficulties inherent in populating the Au/TiO_2 with gaseous molecular oxygen under UHV conditions, a RF plasma jet source was used for populating the sample with atomic oxygen. The reactivity of the oxygen-atom-precovered sample was systematically studied as a function of temperature, oxygen-atom coverage, and gold coverage. The most notable results from this study are the observation of CO_2 production from oxygen-precovered Au/TiO_2 at temperatures as low as 65 K, and the observation that the reaction is facile on all samples studied, independent of the gold coverage and hence the gold particle size.

The catalytic behavior of the Au/TiO_2 model catalyst was found to be a strong function of surface temperature and oxygen-atom coverage. For temperatures well below the desorption temperature of CO (~180 K), the reaction was characterized by a sharp rise in the CO_2 production followed by an abrupt decrease as the sample became saturated with CO. Adsorbed CO and O were observed to coexist on the sample despite the apparent low activation energy for abstraction of an O atom by CO to form CO_2. Removal of the accumulated CO from the sample, either by heating to 300 K or by bombarding the sample with a high-kinetic-energy beam of Kr, and then reexposing the sample to CO once again resulted in CO_2 production. The amount of CO_2 produced at temperatures well below the desorption temperature of CO was observed to decrease with increasing O-atom coverage above a threshold value. For saturation coverages of oxygen, the sample was rendered essentially inactive for CO oxidation. CO adsorption measurements at 77 K revealed that the absolute uptake of CO by the sample decreased

as the oxygen-atom coverage increased, partly explaining the observed decrease in CO_2 production with increasing O-atom coverage.

Like the low-temperature regime, the reaction at temperatures above 180 K is also a strong function of the oxygen coverage. Low coverages of oxygen resulted in prompt CO_2 production upon CO impingement followed by a decay in the reaction rate as the oxygen atoms were consumed. For intermediate coverages of oxygen and relatively high Au coverages (e.g., 2 ML Au), bimodal CO_2 production curves were observed when impinging CO on the O-atom-covered sample. For intermediate coverages of oxygen and low Au coverages (e.g., 0.5 ML Au), results qualitatively similar to the low-oxygen-coverage data were observed. High oxygen coverages, near saturation, also resulted in a decrease in the CO_2 production at surface temperatures exceeding the peak desorption temperature of CO.

REFERENCES

1. B. Hammer, J. K. Nørskov, Nature **376**, 238 (1995).
2. H. Huber, D. McIntosh, G. A. Ozin, Inorg. Chem. **16**, 975 (1977).
3. M. Haruta, Catal. Today **36**, 153 (1997).
4. M. Haruta, CATTECH **6**, 102 (2002).
5. T. V. Choudhary, D. W. Goodman, Top. Catal. **21**, 25 (2002).
6. G. C. Bond, D. T. Thompson, Catal. Rev.-Sci. Eng. **41**, 319 (1999).
7. R. Meyer, C. Lemire, Sh. K. Shaikhutdinov, H. J. Freund, Gold Bull. **37**, 72 (2004).
8. M. A. Bollinger, M. A. Vannice, Appl. Catal. B: Environ. **8**, 417 (1996).
9. J.-D. Grunwaldt, A. Baiker, J. Phys. Chem. B **103**, 1002 (1999).
10. F. Boccuzzi, A. Chiorino, M. Manzoli, P. Lu, T. Akita, S. Ichikawa, M. Haruta, J. Catal. **202**, 256 (2001).
11. F. Boccuzzi, A. Chiorino, J. Phys. Chem. B **104**, 5414 (2000).
12. V. A. Bondzie, S. C. Parker, C. T. Campbell, Catal. Lett. **63**, 143 (1999).
13. M. Valden, X. Lai, D. W. Goodman, Science **281**, 1647 (1998).
14. H. Liu, A. I. Kozlov, A. P. Kozlova, T. Shido, K. Asakura, Y. Iwasawa, J. Catal. **185**, 252 (1999).
15. G. C. Bond, D. T. Thompson, Gold Bull. **33**, 41 (2000).
16. M. A. Henderson, W. S. Epling, C. L. Perkins, C. H. F. Peden, U. Diebold, J. Phys. Chem. B **103**, 5328 (1999).
17. D. A. Outka, R. J. Madix, Surf. Sci. **179**, 351 (1987).
18. W. A. Bone, G. W. Andrew, Proc. R. Soc. A **109**, 459 (1925).
19. J. M. Gottfried, K. J. Schmidt, S. L. M. Schroeder, K. Christmann, Surf. Sci. **525**, 184 (2003).

20. J. M. Gottfried, K. J. Schmidt, S. L. M. Schroeder, K. Christmann, Surf. Sci. **252**, 197 (2002).

21. M. A. Lazaga, D. T. Wickham, D. H. Parker, G. N. Kastanas, B. E. Koel, ACS Sym. Ser. **523**, 90 (1993).

22. T. S. Kim, J. D. Stiehl, S. M. McClure, C. B. Mullins, Manuscript submitted for publication.

23. G. R. Bamwenda, S. Tsubota, T. Nakamura, M. Haruta, Catal. Lett. **44**, 83 (1997).

24. T. H. Lee, K. M. Ervin, J. Phys. Chem. **98**, 10023 (1994).

25. B. E. Salisbury, W. T. Wallace, R. L. Whetten, Chem. Phys. **262**, 131 (2000).

26. D. Stolcic, M. Fischer, G. Ganterför, Y. D. Kim, Q. Sun, P. Jena, J. Am. Chem. Soc. **125**, 2848 (2003).

27. Y. D. Kim, M. Fischer, G. Ganterför, Chem. Phys. Lett. **377**, 170 (2003).

28. W. T. Wallace, R. L. Whetten, J. Am. Chem. Soc. **124**, 7499 (2002).

29. J. Hagen, L. D. Socaciu, M. Elijazyfer, U. Heiz, T. M. Bernhardt, L. Wöste, Phys. Chem. Chem. Phys. **4**, 1707 (2002).

30. L. D. Socaciu, J. Hagen, T. M. Bernhardt, L. Wöste, U. Heiz, H. Häkkinen, U. Landman, J. Am. Chem. Soc. **125**, 10437 (2003).

31. A. J. Capote, T. J. Roberts, R. J. Madix, Surf. Sci. **209**, L151 (1989).

32. U. Burghaus, H. Conrad, Surf. Sci. **364**, 109 (1996).

33. J. V. Barth, T. Zambelli, Surf. Sci. **513**, 359 (2002).

34. Z.-P. Liu, P. Hu, A. Alavi, J. Am. Chem. Soc. **124**, 14770 (2002).

35. Y. Xu, M. Mavrikakis, J. Phys. Chem. B **107**, 9298 (2003).

36. G. Mills, M. S. Gordon, H. Metiu, J. Chem. Phys. **118**, 4198 (2003).

37. B. Yoon, H. Hakkinen, U. Landman, J. Phys. Chem. A **107**, 4066 (2003).

38. Z.-P. Liu, X.-Q. Gong, J. Kohanoff, C. Sanchez, P. Hu, Phys. Rev. Lett. **91**, 266102 (2003).

39. N. Lopez, J. K. Nørskov, J. Am. Chem. Soc. **124**, 11262 (2002).

40. C. R. Henry, C. Chapon, C. Duriez, J. Chem. Phys. **95**, 700 (1991).

41. C. H. Henry, Surf. Sci. Rep. **31**, 231 (1998).

42. C. Becker, C. R. Henry, Catal. Lett. **43**, 55 (1997).

43. C. Goyhenex, M. Croci, C. Claeys, C. R. Henry, Surf. Sci. **352-354**, 475 (1996).

44. L. Piccolo, C. Becker, C. R. Henry, Appl. Surf. Sci. **164**, 156 (2000).

45. J. Libuda, I. Meusel, J. Hoffmann, J. Hartmann, H. J. Freund, J. Vac. Sci. Technol. A **19**, 1516 (2000).

46. I. Meusel, J. Hoffmann, J. Hartmann, J. Libuda, H.-J. Freund, J. Phys. Chem. B **105**, 3567 (2001).

47. J. Hoffmann, I. Meusel, J. Hartmann, J. Libuda, H.-J. Freund, J. Catal. **204**, 378 (2001).

48. T. Dellwig, J. Hartmann, J. Libuda, I. Meusel, G. Rupprechter, H. Unterhalt, H.-J. Freund, J. Mol. Catal. A **162**, 51 (2000).

49. I. Meusel, J. Hoffmann, J. Hartmann, M. Heemeier, M. Bäumer, J. Libuda, H.-J. Freund, Catal. Lett. **71**, 5 (2001).

50. I. Stara, V. Matolin, Surf. Sci. **313**, 99 (1994).

51. I. Stará, V. Nehasil, V. Matolín, Surf. Sci. **331-333**, 173 (1995).

52. I. Stará, V. Nehasil, V. Matolín, Surf. Sci. **365**, 69 (1996).

53. T. S. Kim, J. D. Stiehl, C. T. Reeves, R. J. Meyer, C. B. Mullins, J. Am. Chem. Soc. **125**, 2018 (2003).

54. M. C. Wheeler, D. C. Seets, C. B. Mullins, J. Chem. Phys. **105**, 1572 (1996).

55. J. E. Pollard, Rev. Sci. Instrum. **63**, 1771 (1992).

56. M. C. Wheeler, D. C. Seets, C. B. Mullins, J. Chem. Phys. **107**, 1672 (1997).

57. M. C. Wheeler, C. T. Reeves, D. C. Seets, C. B. Mullins, J. Chem. Phys. **108**, 3057 (1997).

58. J. D. Beckerle, A. D. Johnson, S. T. Ceyer, Phys. Rev. Lett. **62**, 685 (1989).

59. J. D. Beckerle, A. D. Johnson, S. T. Ceyer, J. Chem. Phys. **93**, 4047 (1990).

60. J. D. Stiehl, T. S. Kim, S. M. McClure, C. B. Mullins, J. Am. Chem. Soc. **126**, 1606 (2004).

61. X. Lai, T. P. St. Clair, M. Valden, D. W. Goodman, Prog. Surf. Sci. **59**, 25 (1998).

62. D. Brinkley, M. Dietrich, T. Engel, P. Farral, G. Gantner, A. Schafer, A. Szumacher, Surf. Sci. **395**, 292 (1998).

63. D. A. King, M. G. Wells, Proc. R. Soc. London. A **339**, 245 (1974).

64. J. D. Stiehl, T. S. Kim, S. M. McClure, C. B. Mullins, Manuscript in preparation.

65. J. M. Gottfried, N. Elghobashi, S. L. M. Schroeder, K. Christman, Surf. Sci. **523**, 89 (2003).

66. K. D. Gibson, M. Viste, E. C. Sanchez, S. J. Sibener, J. Chem. Phys. **110**, 2757 (1999).

67. K. D. Gibson, M. Viste, E. C. Sanchez, S. J. Sibener, J. Chem. Phys. **112**, 2470 (2000).

68. A. Krozer, M. Rodahl, J. Vac. Sci. Technol. A **15**, 1704 (1997).

Chapter 3: Evidence for Molecularly Chemisorbed Oxygen on TiO_2 Supported Gold Nanoclusters and Au(111)

INTRODUCTION

It is well documented from experiment that O_2 does not readily chemisorb on gold single crystals[1,2,3] or titania supported gold clusters larger than ~1 nm[4] either dissociatively or molecularly. Additionally, and consistent with experiment, density functional theory (DFT) calculations suggest that the barrier to dissociative chemisorption of oxygen on gold is very high and also that molecularly chemisorbed oxygen is not stable on clean Au(111).[5,6] However, some DFT calculations indicate that molecularly chemisorbed oxygen is stable on strained gold surfaces and steps, as well as on small gold clusters.[5-9] Indeed, ultraviolet photoemission spectroscopy measurements have indicated that small *gas-phase* gold clusters, Au_n (n = 2-20), will adsorb molecular oxygen.[10,11] The nature of chemisorbed oxygen on gold, either atomically or molecularly adsorbed, is important in elucidating the unique chemistry that has been observed over *supported* gold catalysts in the 1-5 nm diameter range (such as the oxidation of carbon monoxide).[12] It is known from experiment that atomically adsorbed oxygen will readily oxidize CO[4,13] and DFT calculations regarding gold clusters suggest that molecularly chemisorbed oxygen is stable and oxidizes CO with virtually no activation barrier.[7,9] However, no conclusive experimental evidence has been presented regarding the existence, stability, or reactivity of molecularly chemisorbed oxygen on extended gold surfaces or on supported gold clusters larger than ~20 atoms. Herein we present evidence from thermal desorption (TDS), adsorption/reaction induced desorption, and collision-induced desorption (CID) spectra indicating the presence of molecularly chemisorbed

oxygen ($O_{2,a}$) on both gold clusters supported on TiO_2(110) as well as on Au(111), after exposure to an oxygen plasma-jet molecular beam.

EXPERIMENTAL

The experiments were performed in an ultra high vacuum molecular beam surface scattering apparatus that has been described in detail previously.[14] The sample assembly consists of Au(111) and TiO_2(110) single crystals which are mounted on opposite faces of a tantalum plate that is in thermal contact with a liquid nitrogen reservoir and that can be resistively heated. Titania supported Au nanoclusters are created by vapor deposition of gold on the TiO_2(110) sample.[13] Oxygen is dosed via a supersonic, radio frequency generated plasma-jet source with a dissociation fraction of ~40% as determined via time-of-flight.[19] A 60% relative oxygen coverage is used in all the experiments reported for the 2 ML Au/TiO_2 sample and the experiments reported on the Au(111) single crystal were given an equivalent oxygen exposure (~1.3 ML). A high kinetic energy beam of Kr (~1 eV), formed by supersonic expansion of a 2% Kr in He mixture, is used for the CID experiments.[15] The same apertures are used for defining beams of CO, Kr, and the O-plasma-jet and the spot size produced is much smaller than the crystal faces in order to minimize exposure of these gases to surfaces other than the sample.

RESULTS AND DISCUSSION

Figure 3.1a shows the TDS obtained immediately after exposing the 2 ML Au/TiO_2 sample, held at 77 K, to the oxygen plasma-jet source. A low temperature desorption feature indicative of molecularly chemisorbed oxygen is evident in the spectrum. Figure 3.1b shows a TDS taken after the same oxygen exposure as in Figure 3.1a but with removal of the $O_{2,a}$ via CID (as discussed later). The TDS feature observed in 3.1b is significantly decreased in intensity compared to 3.1a. Figure 3.1c shows the

difference spectrum of the two TDS and clearly reveals a desorption peak at ~145 K, which, assuming first order desorption, corresponds to a binding energy of approximately 0.35 eV. This peak desorption temperature is comparable to that measured in $O_{2,a}$ desorption from Pt(111) (150 K)[16] and Ag(110) (190 K).[17] The quantity of $O_{2,a}$ is only ~10% of the amount of O_2 that desorbs as a result of recombinative desorption of O atoms from the 2 ML Au/TiO_2 surface.

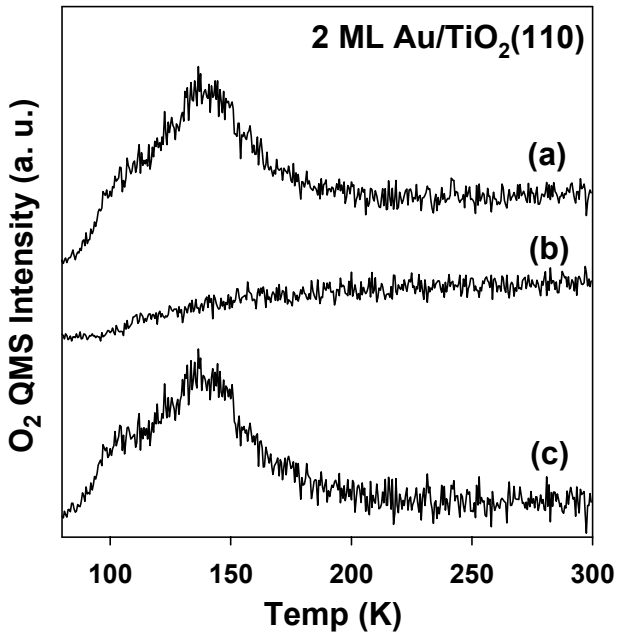

Figure 3.1: TDS from 2 ML Au/TiO_2 (a) following exposure to the oxygen plasma-jet, (b) following exposure to the plasma-jet and then CID of $O_{2,a}$ and (c) difference spectra of (a) and (b).

Figure 3.2 shows a series of experiments that further suggest the existence of an $O_{2,a}$ species on the samples following exposure to the plasma-jet. Figure 3.2a shows a CID measurement of an oxygen covered 2 ML Au/TiO_2 sample. At time t = 10 sec the Kr beam was directed at the sample and a prompt increase in the mass 32 quadrupole

mass spectrometer (QMS) signal is observed, followed by a decay to the background level. Either (i) $O_{2,a}$ is desorbed upon impingement of the Kr beam, or (ii) two oxygen adatoms recombine and desorb due to the Kr-surface collision. Evidence for the former mechanism is depicted in Figure 3.2b which shows the results of a CID measurement following (i) exposure of the sample to the plasma-jet followed by (ii) heating the sample to 300 K prior to (iii) impingement of the Kr beam. Note that a mass 32 signal is not observed in Figure 3.2b indicating that heating to 300 K, a temperature ~300 K below the recombinative *thermal* desorption temperature of O_a from gold, was sufficient to remove the $O_{2,a}$. Finally, further support for CID of $O_{2,a}$ and not recombination of O adatoms was obtained by re- exposing the sample to the Kr beam following the experiment shown in Figure 3.2a: no further CID of a mass 32 species is observed. Additionally, we note that TDS measurements in the 300-700 K range reveal that the O_a population is unchanged, within experimental uncertainty, by CID of $O_{2,a}$. Also, the quantity of $O_{2,a}$ observed during CID is consistent with the amount seen in low temperature TDS, within the experimental uncertainties. CID of $O_{2,a}$ has been observed previously in a study on Pt(111).[15]

Figure 3.2c shows the mass 32 signal detected while dosing CO (CO beam impinges on sample at t = 10 s) on an oxygen covered 2 ML Au/TiO_2 surface. Interestingly, a small amount of mass 32 evolves from the surface upon impingement of CO. Apparently, the heat of adsorption of CO and/or the heat of reaction of CO with adsorbed oxygen is sufficient to induce desorption of weakly bound di-oxygen. No mass 32 signal is observed in similar experiments if either (i) Kr CID or (ii) annealing of the sample to ~ 300 K is performed to remove $O_{2,a}$ prior to CO beam impingement. Adsorption/reaction induced desorption of $O_{2,a}$ is also observed on Au(111) (not shown) when impinging a CO beam on the oxygen plasma-jet exposed Au(111) surface. We

note that adsorption induced desorption of $O_{2,a}$ has been observed on Pt(111) previously.[18,19]

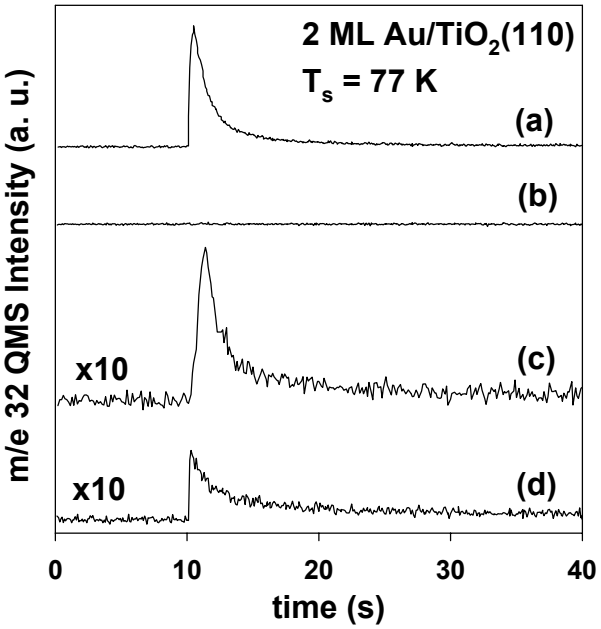

Figure 3.2: O_2 evolution at 77 K (a) from CID from a 2 ML Au/TiO_2 after exposure to O_2 plasma-jet, (b) from CID from a 2 ML Au/TiO_2 after exposure to O_2 plasma-jet and heating to 300 K, (c) during impingement of a CO beam on an oxygen covered 2 ML Au/TiO_2 sample, and (d) from CID from Au(111) following exposure to plasma-jet.

Oxygen is known to adsorb molecularly on TiO_2[20] and impingement of Kr on the oxygen plasma-jet dosed, Au-free TiO_2(110) surface results in CID of $O_{2,a}$. Thus, it is important to determine if any of the oxygen evolving during the CID measurement on the Au/TiO_2 sample shown in Figure 3.2a is associated with Au clusters. Although the time-integrated quantity of $O_{2,a}$ on the bare TiO_2 sample is ~30% greater than from a 2 ML Au/TiO_2 sample for equivalent exposures of oxygen, 2 ML of Au is expected to cover ~70% of the TiO_2(110) crystal (based on STM data from Lai, et al.[21]) strongly suggesting

that some of the $O_{2,a}$ is associated with gold clusters. Low temperature TDS of $O_{2,a}$ from gold-free TiO_2 compared with 2 ML Au/TiO_2 shows similar behavior to that just discussed regarding the CID measurements. Further proof of $O_{2,a}$ being associated with gold is evidence for adsorption/reaction induced desorption of $O_{2,a}$ from Au(111) as mentioned previously. CID of di-oxygen is also observed from the Au(111) single crystal upon impingement by energetic Kr as shown in Figure 3.2d. The amount of mass 32 species that evolves from the Au(111) single crystal in CID is much smaller than from the 2 ML Au/TiO_2 sample for equivalent plasma jet exposures. Perhaps $O_{2,a}$ adsorbs much more readily on the Au particles than on the Au(111) surface due to an increased concentration of low coordination sites compared to Au(111).[5,6]

Attempts to populate $O_{2,a}$ on the Au/TiO_2 sample without using the plasma-jet were unsuccessful. A 2 ML Au/TiO_2 sample was exposed to 100 L (1 L = $1x10^{-6}$ Torr·s) of O_2 at a surface temperature of 77 K and $O_{2,a}$ was undetectable in CID experiments (as was O_a). Additionally, the 2 ML Au/TiO_2 sample was (i) exposed to the plasma-jet of oxygen followed by (ii) heating to 300 K to desorb any $O_{2,a}$ and then (iii) exposed to 100 L of oxygen followed by (iv) CID in an attempt to determine if pre-adsorbed oxygen adatoms would enhance adsorption and/or stabilize $O_{2,a}$. This experiment also resulted in no detectable $O_{2,a}$.

Finally, the mechanisms for formation of $O_{2,a}$ on the samples studied upon exposure to the plasma-jet oxygen source are the subject of Chapter 4.

CONCLUSIONS

In conclusion, we have shown evidence for the presence of $O_{2,a}$ on Au(111) and on Au clusters supported on a TiO_2(110) surface following exposure of these samples to a plasma-jet source of oxygen. We have detected and identified $O_{2,a}$ from thermal

desorption spectra, collision induced desorption spectra, and heat of adsorption/reaction induced desorption spectra.

REFERENCES

1. D. A. Outka, R. J. Madix, Surf. Sci. **179**, 351 (1987).

2. D. H. Parker, B. E. Koel, J. Vac. Sci. Technol. A **8**, 2585 (1990).

3. J. M. Gottfried, K. J. Schmidt, S. L. M. Schroeder, K. Christmann, Surf. Sci. **511**, 65 (2002).

4. V. A. Bondzie, S. C. Parker, C. T. Campbell, Catal. Lett. **63**, 143 (1999).

5. Y. Xu, M. Mavrakakis, J. Phys. Chem. B **107**, 9298 (2003).

6. G. Mills, M. S. Gordon, H. Metiu, J. Chem. Phys. **118**, 4198 (2003).

7. N. Lopez, J. K. Nørskov, J. Am. Chem. Soc. **124**, 11262 (2002).

8. Z.-P. Liu, P. Hu, A. Alavi, J. Am. Chem. Soc. **124**, 14770 (2002).

9. A. Sanchez, S. Abbet, U. Heiz, W.-D. Schneider, H. Häkkinen, R. N. Barnett, U. Landman, J. Phys. Chem. A **103**, 9573 (1999).

10. D. Stolcic, M. Fischer, G. Ganterför, Y. D. Kim, Q. Sun, P. Jena, J. Am. Chem. Soc. **125**, 2848 (2003).

11. Y. D. Kim, M. Fischer, G. Ganterför, Chem. Phys. Lett. **377**, 170 (2003).

12. M. Haruta, Catal. Today **36**, 153 (1997); CATTECH **6**, 102 (2002).

13. T. S. Kim, J. D. Stiehl, C. T. Reeves, R. J. Meyer, C. B. Mullins, J. Am. Chem. Soc. **125**, 2018 (2003).

14. M. C. Wheeler, D. C. Seets, C. B. Mullins, J. Chem. Phys. **105**, 1572 (1996).

15. C. Åkerlund, I. Zorić, B. Kasemo, J. Chem. Phys. **104**, 7359 (1996).

16. J. Gland, Surf. Sci. **93**, 487 (1980).

17. M. A. Barteau and R. J. Madix, in *The Chemical Physics of Solid Surfaces and Heterogeneous Catalysis*, Vol. 4, edited by D. A. King and D. P. Woodriff (Elsevier, Amsterdam, 1982).

18. C. T. Rettner, J. J. Lee, J. Chem. Phys. **101**, 10185 (1994).

19. M. C. Wheeler, D. C. Seets, C. B. Mullins, J. Chem. Phys. **107**, 1672 (1997).

20. M. A. Henderson, W. S. Epling, C. L. Perkins, C. H. F. Peden, U. Diebold, J. Phys. Chem. B **103**, 5328 (1999).

21. X. Lai, T. P. St. Clair, M. Valden, D. W. Goodman, Prog. Surf. Sci. **59**, 25 (1998).

Chapter 4: Formation of Molecularly Chemisorbed Oxygen on TiO_2 Supported Gold Nanoclusters and Au(111) from Exposure to an Oxygen Plasma-Jet

INTRODUCTION

The discovery that properly prepared gold clusters that are 2 - 5 nm in size can facilitate the CO oxidation reaction,[1-3] a reaction that requires the activation of an oxygen species, has led to a renewed interest in oxygen adsorption on gold systems. After all, it is bulk gold's inability to react with simple molecules, such as hydrogen[4] and oxygen, that has historically characterized this precious metal and therefore, the observation of catalytic CO oxidation by gold was quite surprising. The nature of chemisorbed oxygen on gold, either atomically or molecularly adsorbed, is important in understanding the unique chemistry that has been observed over supported gold catalysts.[1] Despite gold's inert character, the adsorption of oxygen on bulk gold has been studied previously,[3] but issues regarding oxygen adsorption on metal-oxide supported, gold catalyst surfaces remain unresolved.[5]

Experiments have shown that room temperature, gas-phase O_2 does not readily chemisorb on macroscopic gold single crystals[6-8] or supported gold clusters larger than ~1 nm in diameter[9,10] either dissociatively or molecularly. This property of gold has made the determination of the active oxygen species during the CO oxidation reaction difficult. Although it has been shown experimentally that atomically adsorbed oxygen on gold will readily react with CO to form CO_2,[6-12] the lack of experimental evidence regarding the dissociation of O_2 casts doubt on whether dissociation is the rate-limiting step in the oxidation reaction over gold catalysts. The alternative of a molecularly chemisorbed oxygen species is starting to be regarded as a worthy candidate for the

active oxygen species during the CO oxidation reaction.[13-16] However, there has been no experimental verification of a stable, molecularly chemisorbed oxygen state on extended gold systems or supported gold clusters larger than ~20 atoms when employing gaseous molecular oxygen.

Although adsorption studies on extended gold systems have provided little evidence for the existence of a molecularly chemisorbed oxygen state, work on small gold clusters have been very influential in propagating the idea of a molecularly chemisorbed oxygen species on gold.[17-21] The first suggestion that molecularly chemisorbed oxygen might be active in gold catalysis was provided by Huber et al. in their study of the chemistry of single gold atoms for CO oxidation.[17] From IR measurements, they suggested a mechanism for the reaction which involved molecularly chemisorbed oxygen. Recent experiments on small gas-phase gold clusters have complimented these results. Specifically, ultraviolet photoelectron spectroscopy (UPS) measurements of oxygen adsorbed on gas-phase anionic gold clusters, Au_n (n = 2-20), have revealed fine structure in the spectra for n = even clusters consistent with an oxygen-oxygen bond indicating the presence of molecularly chemisorbed oxygen on the clusters.[18,19,21] Experiments performed on two-atom gas-phase anionic gold clusters have also established that molecularly chemisorbed oxygen will react with CO.[20]

Results from theory also lend support to the idea of molecularly chemisorbed oxygen existing on gold under suitable conditions and suggest that the dissociation of oxygen on gold is highly activated. Consistent with the lack of measurable dissociation of oxygen on gold, theoretical studies on many different gold systems have concluded that the barrier to dissociation of O_2 is on the order of ~1 eV.[22-25] Strained gold surfaces and steps, as well as some small gold clusters, have been found to provide a suitable platform for molecular chemisorption of oxygen.[14,22-28] Of more relevance to catalysis,

stable molecular chemisorption states have been calculated at the metal-oxide/metal interface for Au_8 on MgO[13] and for Au/TiO_2. [15,16]

In Chapter 3, we presented evidence for the existence of a molecularly chemisorbed oxygen species ($O_{2,a}$) on a Au/TiO_2 model catalyst and a Au(111) single crystal following exposure of these surfaces to a plasma-jet of oxygen.[29] In this paper, we report on an extension of this study in which further insight into the mechanism of formation of $O_{2,a}$ on these surfaces can be gleamed. In particular, we present evidence that suggests that some of the $O_{2,a}$ is formed by recombination of atomic oxygen species on the sample surface during the plasma-jet exposure. However, we are not able to rule out molecular adsorption directly from the gas-phase and we speculate on other mechanisms by which molecular oxygen could adsorb on the surfaces studied. We also show evidence that adsorption of an atomic species directly influences adsorption of molecular oxygen on the Au/TiO_2 samples.

EXPERIMENTAL

The experiments reported in this study were performed in an ultrahigh vacuum (UHV) molecular beam surface scattering apparatus that has been described in detail previously.[10,11,29] The sample assembly consists of Au(111) and TiO_2(110) single crystals which are mounted on opposite faces of a tantalum plate that is in thermal contact with a liquid nitrogen reservoir and that can be resistively heated. Gold is vapor deposited on the TiO_2 sample closely following a procedure described in detail by Lai et al.[30] and coverages of gold are calibrated with a Quartz Crystal Microbalance.[10,11] The Au(111) single crystal was cleaned by argon ion sputtering, followed by annealing in UHV to eliminate surface impurities. The cleaning cycle was performed until impurity levels were below Auger Electron Spectroscopy (AES) detection limits. The crystallinity of the TiO_2(110) and Au(111) samples was verified with low energy electron diffraction.

Mixtures of 8% oxygen in Ar are dosed via a supersonic, RF-generated plasma-jet with a dissociation fraction of ~40% as determined via time-of-flight.[31-33] The purities of the oxygen gases used were 99.4% for $^{18}O_2$ and 99.93% for $^{16}O_2$. Ionic species are deflected out of the beam line using a charged plate biased at 3 kV. No adsorption of oxygen, either dissociative or molecular, is observed if a thermal beam of O_2 is dosed (equivalent exposure of ~50 L) on the samples (RF power off) or if the sample is given a 100 L (1 L = 1×10^{-6} Torr·s) exposure of room-temperature oxygen by backfilling. Coverages of oxygen on the Au/TiO_2 model catalysts are determined by integration of the oxygen atom recombinative desorption spectra from the gold particles and are reported as coverages relative to saturation. Oxygen coverages on the Au(111) single crystal are determined from the O/Au AES peak ratios as described by Kim et al.[34] High kinetic energy beams of Kr (~1 eV) and Ar (~0.5 eV), formed by supersonic expansion of 2% rare gas in He mixtures, are used for collision-induced desorption (CID) experiments.[35-38] The Kr and Ar beams are generated employing the same nozzle that is used for dosing oxygen, except with the RF power off. For experiments employing ozone, ozone was generated using a commercial ozone generator, Ozotech (Yreka, CA) Model OZ2PCS, through which pure oxygen was flowed, and the gas was dosed from the same nozzle used for dosing atomic oxygen (with the RF power off). A lower limit on the ozone flux of ~1.4×10^{12}/cm^2·s was determined by comparing the recombinative oxygen desorption spectra from Au(111) following exposure to the beam formed using the ozone generator to the desorption spectra from a known coverage of oxygen on Au(111). Beam shaping apertures ensure that the molecular beam spot size (~3 mm in diameter) is smaller than the samples to avoid directly exposing areas of the sample assembly other than the TiO_2 or Au(111) crystals.

RESULTS AND DISCUSSION

Previously we presented evidence from thermal desorption, collision-induced and adsorption/reaction-induced desorption of molecularly chemisorbed oxygen on a Au/TiO_2 model catalyst system exposed to an oxygen plasma-jet source.[29] From thermal desorption measurements, we estimated the binding energy of the molecularly chemisorbed oxygen on Au/TiO_2 to be ~0.35 eV (corresponding to a peak desorption temperature of ~145 K). We also showed via collision-induced desorption and reaction/adsorption-induced desorption that a molecularly chemisorbed state could also be populated on the Au(111) sample, albeit with much less $O_{2,a}$, following exposure of the sample to the plasma source. Since collision-induced desorption has proven to be a very sensitive tool for detecting small quantities of weakly bound adsorbates and since it will be used extensively in this study, we briefly review some of the data that have been previously presented.[29] Figure 4.1 shows data from collision-induced desorption experiments that were performed on both the Au/TiO_2 and the Au(111) samples. Figure 4.1a shows the mass 32 signal observed during a collision-induced desorption measurement from a 2 ML Au/TiO_2 sample that has been exposed to the $^{16}O_2$ oxygen plasma-jet (60% relative O coverage). A sharp mass 32 peak is seen upon impingement of the Kr beam (t = 10 s) that decays to the background level as the $O_{2,a}$ on the sample is removed. Experiments performed on bare TiO_2 (no gold) result in spectra similar to those shown in Figure 4.1a indicating that some of the mass 32 species that desorb are associated with the titania substrate. However, as mentioned in Chapter 3, although the time-integrated quantity of $O_{2,a}$ on the bare TiO_2 sample is ~30% greater than from a 2 ML Au/TiO_2 sample for equivalent exposures of oxygen, 2 ML of Au is expected to cover ~70% of the TiO_2(110) crystal (based on STM data from Lai, et al.[30]) strongly suggesting that some of the $O_{2,a}$ is associated with gold clusters.[29] Collision-induced desorption

experiments with lower energy (~0.5 eV) Ar atoms also result in the evolution of O_2 from the surface providing some evidence for dismissing the signal observed with Kr as due to impulsively driven recombination of oxygen atoms. Figure 4.1b shows a collision-induced desorption measurement from a 2 ML Au/TiO_2 sample with a ~30% relative coverage performed using a ~0.5 eV Ar beam. Evolution of mass 32 is clearly observed indicating desorption of molecular oxygen from the surface. Due to the lower energy of the impinging Ar beam, longer exposure times are required to remove all of the $O_{2,a}$. Figure 4.1c shows a similar collision-induced desorption measurement from the Au(111) single crystal following an equivalent exposure to the oxygen plasma-jet as provided to the 2 ML Au/TiO_2 sample shown in Figure 4.1a (~1.3 ML O coverage). Once again, a peak in the mass 32 signal is observed when impinging the Kr beam (t = 10 s) on the sample. Note the scale on the signal from the Au(111) indicating that the surface population is much smaller on this sample than on the 2 ML Au/TiO_2 sample. The observation of $O_{2,a}$ on the Au(111) single crystal also provides support for $O_{2,a}$ being associated with the gold particles on the model catalyst samples. The difference in the $O_{2,a}$ population might be a result of an increased number of defects or low coordination sites on the catalyst sample in comparison to the Au(111) single crystal.[14,24,25] The presence of $O_{2,a}$ on the TiO_2 crystal also accounts for some of the difference.[29,39]

Also presented in Figure 4.1 is an adsorption/reaction-induced desorption measurement from a 2 ML Au/TiO_2 sample. During the experiment shown in Figure 4.1d, a beam of CO impinges (t = 10 s) on an oxygen-covered (60% relative O coverage), 2 ML Au/TiO_2 sample and the evolution of mass 32 is monitored with the quadrupole mass spectrometer. The heat of adsorption/reaction of CO on the oxygen covered sample is sufficient to induce desorption of a weakly bound mass 32 species. This experiment suggests that the mass 32 species observed during CID is not a result of recombinative

oxygen desorption resulting from impulsive collisions of Kr with O atoms. Adsorption/reaction-induced desorption of $O_{2,a}$ is also observed (not shown) from Au(111) when impinging CO on the oxygen covered surface.

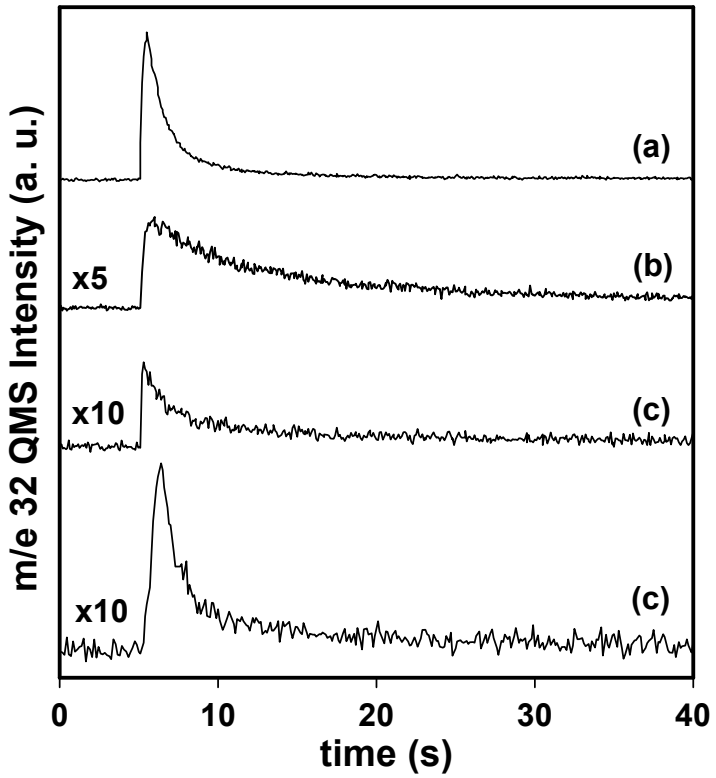

Figure 4.1: $^{16}O_2$ evolution (a) from Kr CID (Kr beam starts at t = 5 s) from a 2 ML Au/TiO_2 sample at 77 K after exposure to a $^{16}O_2$ plasma-jet (60% relative coverage), (b) from Ar CID (Ar beam starts at t = 5 s) from a 2 ML Au/TiO_2 sample at 77 K after exposure to a $^{16}O_2$ plasma-jet (~30% relative coverage), (c) from Kr CID (Kr beam starts at t = 5 s) from Au(111) at 77 K following an exposure to a $^{16}O_2$ plasma-jet equivalent to the exposure in (a), and (d) during impingement of a CO beam (CO beam starts at t = 5 s) on an oxygen-covered, 2 ML Au/TiO_2 sample (60% relative coverage) at 77 K.

Through the use of isotopically labeled oxygen species we have been able to discern some details regarding how molecular oxygen forms on the surface of the sample during exposure to the oxygen plasma-jet. Figure 4.2 shows a collision-induced

desorption measurement from a 2 ML Au/TiO_2 sample prepared in the following manner: (i) exposure of the sample (T_s = 77 K) to a plasma-jet formed using $^{18}O_2$ to give an oxygen atom coverage of ~66%, (ii) heating to 300K to desorb any adsorbed molecular oxygen, and then, after cooling to 77 K, (iii) exposure to a plasma-jet formed using $^{16}O_2$ (exposure equivalent to ~27% relative oxygen atom coverage on a clean 2 ML Au/TiO_2 surface). The three possible isotopic combinations of oxygen, corresponding to $^{16}O_2$ (m/e 32), $^{18}O_2$ (m/e 36) and $^{16}O^{18}O$ (m/e 34), are shown. As can be seen in Figure 4.2, the major species evolving from the surface during the collision-induced desorption measurement is mass 32. However, it should be noted that a small amount of mass 34 is seen evolving from the sample suggestive of the recombination of an ^{18}O atom with a ^{16}O atom (i.e. impinging ^{16}O reacts with the ^{18}O present on the surface). As will be discussed later, the impurity levels of the gases are not high enough to be responsible for the observed mass 34 signal.

Figure 4.3 shows the result of a collision-induced desorption experiment similar to the one shown in Figure 4.2 with the exception that the order of the oxygen isotopes was reversed. From Figure 4.3 it is evident that the major species desorbing from the surface is mass 36, corresponding to $^{18}O_2$ species. However, as was the case for the reverse experiment shown in Figure 4.2, a small amount of mass 34 is also seen evolving from the sample during the collision-induced desorption measurement, suggestive of oxygen atom recombination during the second plasma-jet exposure.

The results of Figures 4.2 and 4.3 provide additional evidence for discounting a recombinative desorption mechanism during CID. If a recombinative desorption mechanism was responsible for the observed signal, one would expect the mass 34 species, corresponding to $^{16}O^{18}O$, to be the major species desorbing from the surface since ^{18}O atoms are being deposited into a large matrix of surface ^{16}O adatoms in Figure

4.3, and vice versa for Figure 4.2. However, only a small amount of $^{16}O^{18}O$ desorbs from the sample during both experiments suggesting that molecularly adsorbed oxygen is formed on the surface prior to CID.

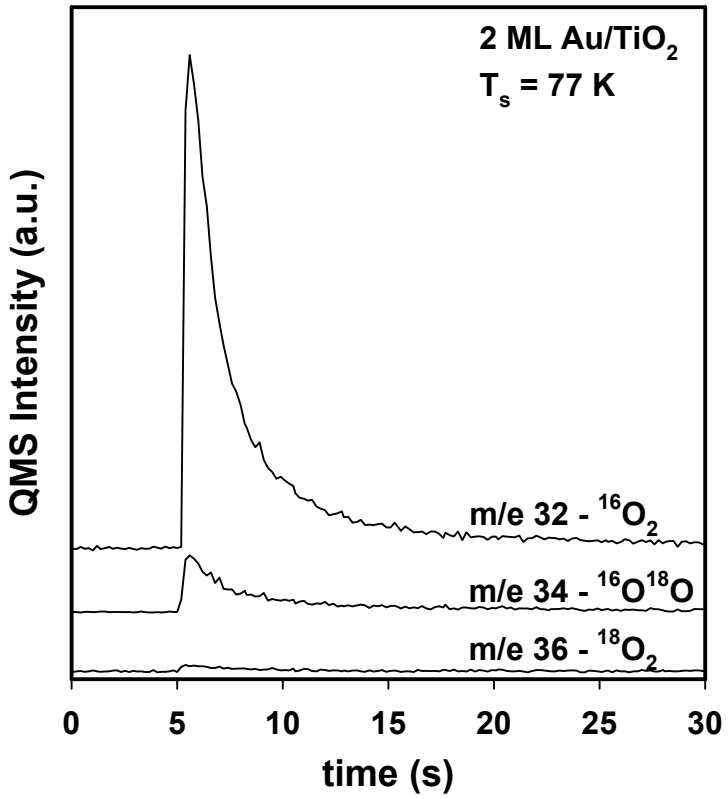

Figure 4.2: Kr CID measurement from a 2 ML Au/TiO_2 sample at 77 K of $^{16}O_2$ (m/e 32), $^{18}O_2$ (m/e 36), and $^{16}O^{18}O$ (m/e 34) following (i) exposure to a $^{18}O_2$ plasma-jet (66% relative coverage) at 77 K, followed by (ii) heating to 300 K, and after cooling to 77 K (iii) exposure to a $^{16}O_2$ plasma-jet (exposure equivalent to 27% relative coverage on a clean 2 ML Au/TiO_2 sample). Kr beam impinges on the sample at t = 5 s.

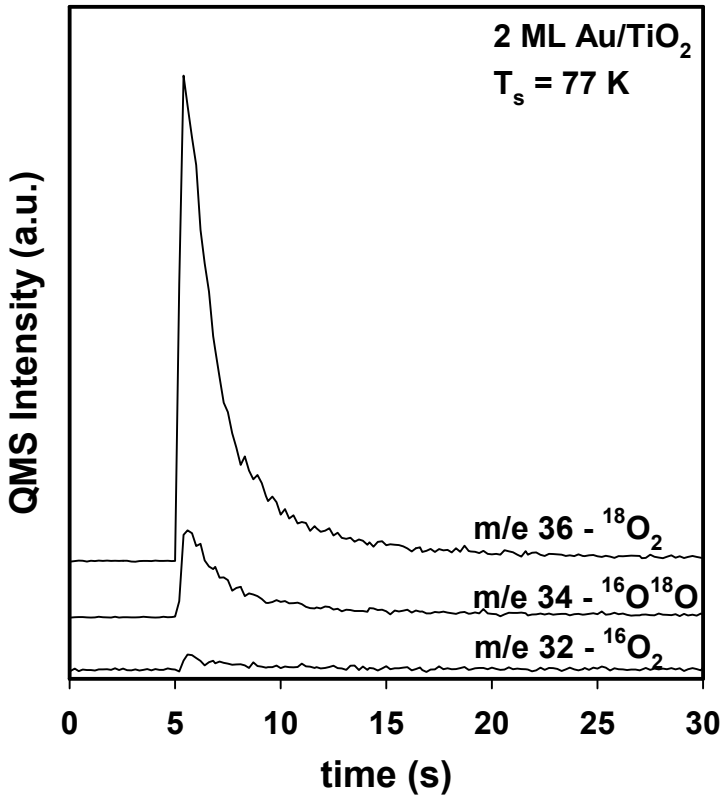

Figure 4.3: Kr CID measurement from a 2 ML Au/TiO_2 sample at 77 K of $^{16}O_2$ (m/e 32), $^{18}O_2$ (m/e 36), and $^{16}O^{18}O$ (m/e 34) following (i) exposure to a $^{16}O_2$ plasma-jet (66% relative coverage) at 77 K, followed by (ii) heating to 300 K, and after cooling to 77 K (iii) exposure to a $^{18}O_2$ plasma-jet (exposure equivalent to 27% relative coverage on a clean 2 ML Au/TiO_2 sample). Kr beam impinges on the sample at t = 5 s.

Experiments performed on bare TiO_2 (no gold) reveal that some of the mass 34 species observed during experiments like the ones shown in Figures 4.2 and 4.3 results from oxygen exchange between ^{16}O atoms in the TiO_2 lattice and ^{18}O atoms in the impinging beam. To determine if any of the mass 34 signal that is observed during the CID measurements is associated with the gold particles, similar experiments to the ones

shown in Figures 4.2 and 4.3 were performed on a Au(111) single crystal to unambiguously determine if this phenomena is also associated with the gold.

Three separate experiments were performed on the Au(111) single crystal to determine if there was precedence for some of the mass 34 signal shown in Figures 4.2 and 4.3 being associated with the gold particles. Figure 4.4 shows the results of the three experiments. The first two experiments were intended to determine whether there were significant impurities in the gas mixtures used to form the plasma-jet that might be responsible for the observed behavior shown in Figures 4.2 and 4.3. The natural abundance of ^{18}O in oxygen is 0.2% atomic and is therefore expected to play a negligible role during experiments with $^{16}O_2$. However, the purity of the $^{18}O_2$ we employed could play a more significant role as this gas is only ~99.4% pure ^{18}O. Figure 4.4a shows a collision induced desorption measurement following exposure of the Au(111) crystal to the $^{16}O_2$ plasma-jet (1.89 ML coverage). All three of the possible isotopic combinations of oxygen monitored with the QMS are shown (m/e 32, 34, and 36). Only the mass 32 species is seen desorbing from the sample upon impingement of the Kr beam (t = 10 s). Figure 4.4b shows a similar experiment to Figure 4.4a except that in this experiment the sample is exposed exclusively to the $^{18}O_2$ plasma-jet. Only the mass 36 species is observed during the collision-induced desorption measurement shown in Figure 4.4b. Figure 4.4c shows the CID results from a mixed isotope experiment in which (i) the sample was exposed to the plasma-jet formed with the $^{18}O_2$ isotope (1.89 ML coverage), followed by (ii) heating of the sample to 300 K to desorb the mass 36 species that populate the sample, and then after cooling back to 77 K, (iii) the sample was further exposed to the plasma-jet formed using the $^{16}O_2$ isotope (exposure equivalent to 1.89 ML on clean Au(111)). The predominant species seen evolving from the sample during CID is the mass 32 isotope of oxygen. However, in contrast to the experiments shown in

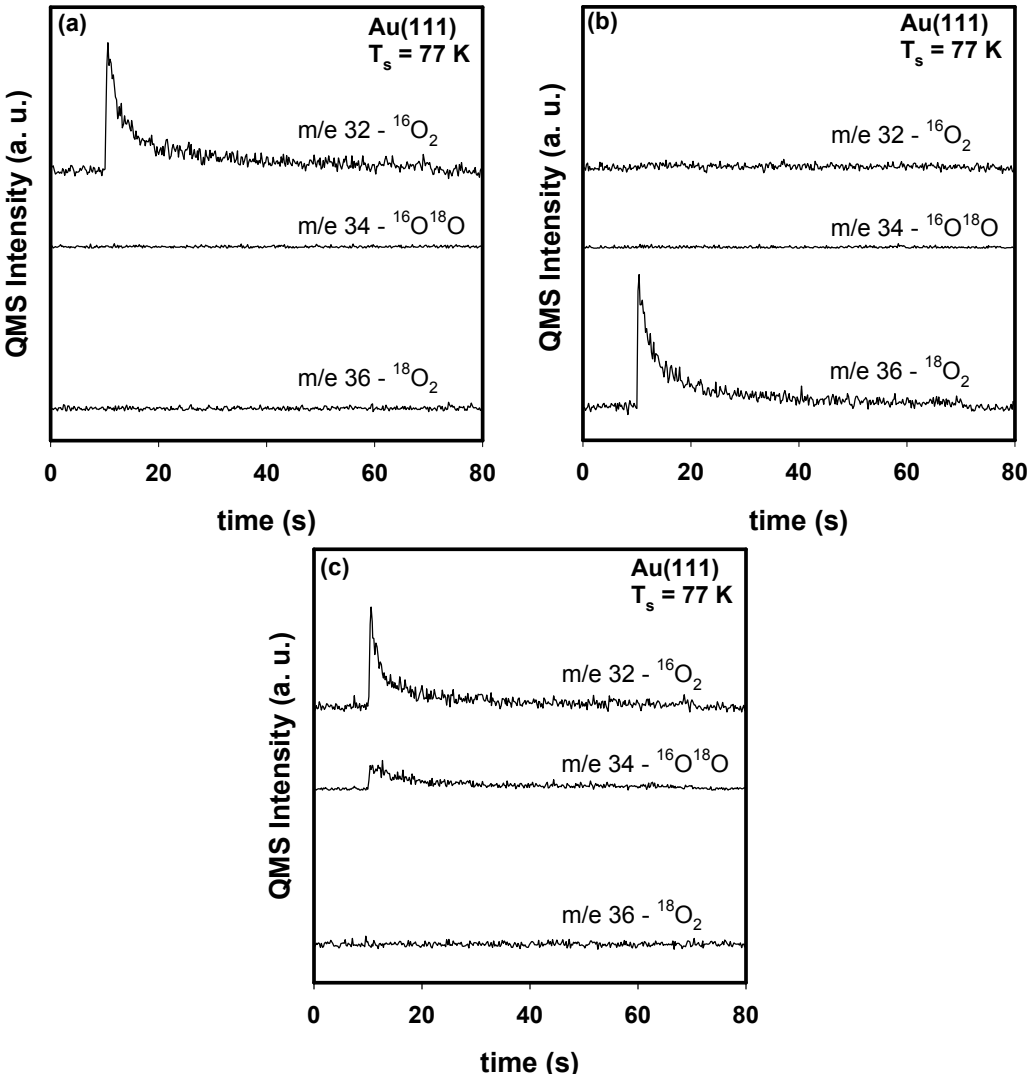

Figure 4.4: (a) Kr CID measurement at T_s = 77 K from Au(111) following exposure to the $^{16}O_2$ plasma-jet (1.89 ML O coverage), (b) Kr CID measurement at T_s = 77 K from Au(111) following exposure to the $^{18}O_2$ plasma-jet (1.89 ML O coverage), and (c) Kr CID measurement at 77 K from Au(111) following exposure to the $^{18}O_2$ plasma-jet (1.89 ML O coverage), followed by heating to 300 K, then, on cooling back to 77 K, exposure to the $^{16}O_2$ plasma-jet (exposure equivalent to 1.89 ML O coverage on clean Au(111)). Kr beam impinges on the samples at t = 10 s for all the data shown.

Figures 4.4a and 4.4b, a mass 34 species is seen evolving from the sample suggesting that a ^{16}O atom and an ^{18}O atom recombined to form $^{16}O^{18}O$ during the $^{16}O_2$ plasma-jet exposure.

Similar results to those shown in Figure 4.4 are seen if adsorption/reaction-induced desorption measurements are performed with CO as shown in Figure 4.5. Figure 4.5a shows the adsorption/reaction-induced desorption of mass 32 following the exposure of the Au(111) sample at 77 K to the plasma-jet formed using $^{16}O_2$ (0.85 ML $^{16}O_a$ coverage). A small rise in the mass 32 signal is seen on impingement of the CO beam (t = 10 s) on the oxygen-covered sample. No mass 34 and 36 species are observed as expected. Figure 4.4b shows the adsorption/reaction-induced desorption of a mass 36 species following exposure of the Au(111) sample at 77 K to the plasma-jet formed using $^{18}O_2$ (0.85 ML $^{18}O_a$ coverage). Once again, a small rise in the mass 36 signal is seen on impingement of the CO beam (t = 10s). No mass 32 or 34 species are seen desorbing during the experiment. Figure 4.5c shows the adsorption/reaction-induced desorption from a mixed isotope experiment in which (i) the sample was exposed to the plasma jet formed with the $^{16}O_2$ isotope (0.85 ML $^{16}O_a$ coverage), followed by (ii) heating of the sample to 300 K to desorb the mass 32 species that populate the sample, and then after cooling back to 77 K, (iii) the sample was further exposed to the plasma-jet formed using the $^{18}O_2$ isotope (exposure equivalent to 0.85 ML on clean Au(111)). On impingement of the CO beam (t = 10 s), a small rise is observed in the mass 36 and mass 34 signal but no rise is seen in the mass 32 signal. Once again, the mass 34 signal is evidence of a recombination of $^{16}O_a$ with an impinging ^{18}O during the second plasma-jet exposure. The yield of oxygen species desorbing from the sample during adsorption/reaction-induced desorption is smaller than the yield during collision-induced desorption since the reaction

does not proceed long enough to desorb all of the oxygen species,[10,11] contrary to the collision-induced desorption experiments.

Evidence for the formation of a gas-phase mass 34 oxygen species on impingement of the $^{16}O_2$ plasma-jet on an $^{18}O_a$ covered Au(111) surface is shown in Figure 4.6. Figure 4.6 shows the mass 34 evolving during the exposure of the $^{16}O_2$ plasma-jet on a surface that has been precovered with ~0.23 ML of $^{18}O_a$. For background reference, the mass 34 signal that is observed when bouncing the beam off a nominally inert flag placed in front of the sample is also shown. Measurements of the ratio of mass 34 to mass 32 seen with the RF power off are consistent with the natural abundance of ^{18}O atoms in oxygen and therefore we ascribe the mass 34 background seen in Figure 4.6 to naturally occurring mass 34 species in the beam. However, as can be seen in Figure 4.6, mass 34 production upon impingement of the ^{16}O atom beam is observed providing evidence that ^{16}O will react with preadsorbed ^{18}O to form gaseous $^{16}O^{18}O$.

Based on the data presented in this paper, it appears that the recombination of impinging oxygen atoms with preadsorbed atoms on the surface is not the primary channel for the formation of molecularly chemisorbed oxygen on the sample. It is useful to speculate on other possible pathways by which molecularly chemisorbed oxygen could form on the surface and account for the observed isotopic mixing seen in Figures 4.4 and 4.5. From the observation that exposure to a thermal beam of gaseous molecular oxygen or background dosing of molecular oxygen results in no detectable adsorption, we can conclude that the adsorption of molecular oxygen on the samples studied likely proceeds through a nonequilibrium channel. We can exclude adsorption of ionic species from our RF powered atomic beam since we deflect all ions out of the beam line using an electric field, as discussed earlier. Perhaps impinging oxygen atoms are more apt to react with

other "hot," nascently adsorbed atoms on the surface than they are to react with

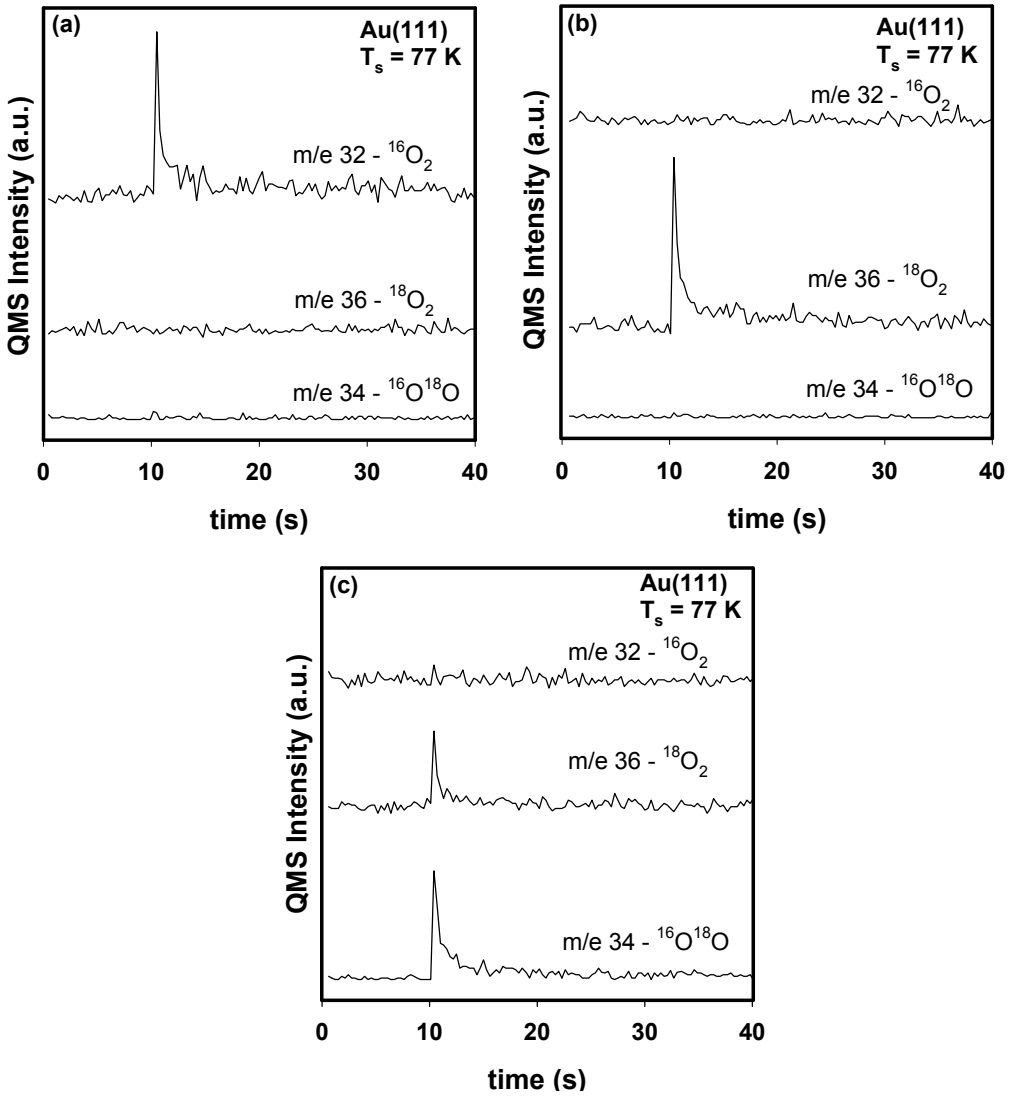

Figure 4.5: (a) CO adsorption/reaction-induced desorption measurement at T_s = 77 K from Au(111) following exposure to the $^{16}O_2$ plasma-jet (0.85 ML O coverage), (b) CO adsorption/reaction-induced desorption measurement at T_s = 77 K from Au(111) following exposure to the $^{18}O_2$ plasma-jet (0.85 ML O coverage), and (c) CO adsorption/reaction-induced desorption measurement at 77 K from Au(111) following exposure to the $^{16}O_2$ plasma-jet (0.85 ML O coverage), followed by heating to 300 K, then, on cooling back to 77 K, exposure to the $^{18}O_2$ plasma-jet (exposure equivalent to 0.85 ML O coverage on clean Au(111)). CO beam impinges on the samples at t = 10 s for all the data shown.

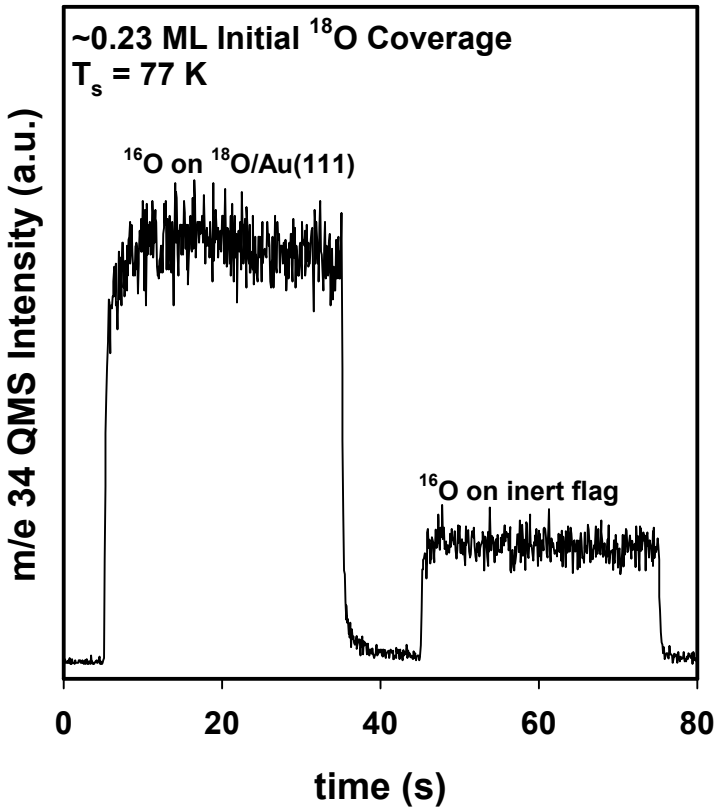

Figure 4.6: $^{16}O^{18}O$ (m/e 34) signal observed while exposing a 0.23 ML ^{18}O covered Au(111) surface to a $^{16}O_2$ plasma-jet (exposure starts at t = 5 s and proceeds until t = 35 s) and while exposing the $^{16}O_2$ plasma-jet on a nominally inert flag (exposure starts at t = 45 s and proceeds until t = 75 s).

a preadsorbed, equilibrated atom. This picture would reconcile the large amount of mass 32 observed in comparison to mass 34 in Figure 4.4 and still be consistent with a recombination mechanism. Although this scenario might seem unlikely from an energetic point of view, in that the molecules formed might be expected to retain a large amount of energy which could be used to escape the surface potential, Sharpless et al.

have observed that gold is very efficient at forming electronically excited oxygen

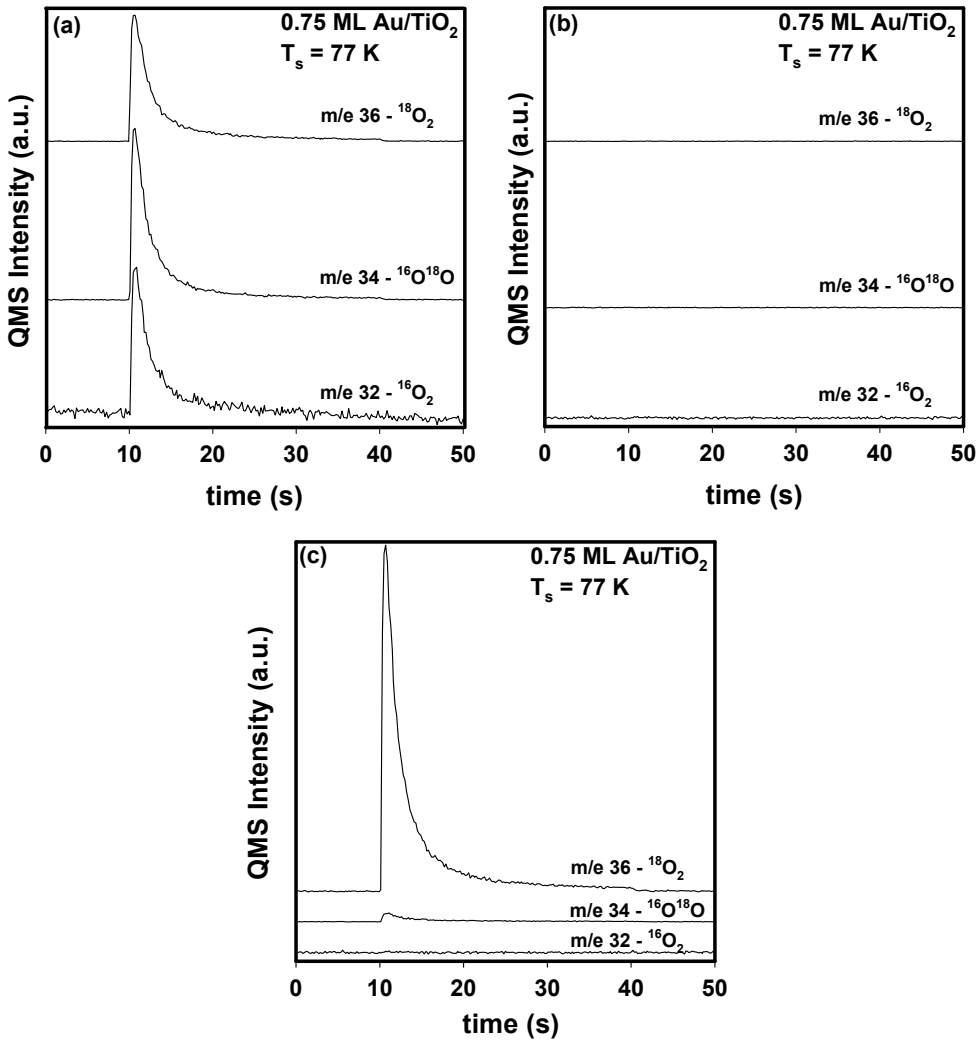

Figure 4.7: (a) Kr CID measurement of $^{16}O_2$ (m/e 32), $^{16}O^{18}O$ (m/e 34), and $^{18}O_2$ (m/e 36) from a 0.75 ML Au/TiO_2 surface at T_s = 77 K following a ~100 L background dose of $^{16}O_2$ while simultaneously dosing an $^{18}O_2$ plasma-jet to saturation (3 minute exposure). (b) Kr CID measurement of $^{16}O_2$ (m/e 32), $^{16}O^{18}O$ (m/e 34), and $^{18}O_2$ (m/e 36) from a 0.75 ML Au/TiO_2 surface at T_s = 77 K following a ~100 L background dose of $^{16}O_2$. (c) Kr CID measurement of $^{16}O_2$ (m/e 32), $^{16}O^{18}O$ (m/e 34), and $^{18}O_2$ (m/e 36) from a 0.75 ML Au/TiO_2 surface at T_s = 77 K following (i) a saturation exposure to an $^{18}O_2$ plasma-jet, followed by (ii) a ~100 L background dose of $^{16}O_2$. Note, the Y-axis of graphs (a)-(c) are all the same scale.

molecules (electronically excited states 4-5 eV above the ground state have been observed) through recombination of oxygen atoms.[40] These nascent, electronically excited states might have an enhanced probability of adsorbing molecularly on the gold surface.

Through the use of isotopically labeled oxygen, we also investigated the influence of adsorption of oxygen atoms on the model catalyst surface on the simultaneous adsorption of ground-state molecular oxygen. As the dissociation fraction of the plasma-jet is only ~40%, impinging, intact oxygen molecules could be influenced by the simultaneous adsorption of atomic species. Figure 4.7a shows a CID measurement of $^{16}O_2$, $^{18}O_2$, and $^{16}O^{18}O$ following a ~100 L background dose of $^{16}O_2$ while simultaneously dosing a plasma-jet formed with $^{18}O_2$ to saturation. Interestingly, all three isotopic mixtures observed have nearly equal intensities. Figure 4.7b shows a reference experiment where the sample was given a ~100 L background dose of $^{16}O_2$ and then a CID measurement was performed; no mass 32 species are observed and, as might be expected, no mass 34 or 36 species are observed during the CID measurement. Finally, Figure 4.7c shows a CID measurement following (i) a saturation exposure of the sample to an $^{18}O_2$ plasma-jet, followed by (ii) a ~100 L background dose of $^{16}O_2$. Only mass 34 and 36 species are observed during the CID measurement. It should be noted that the mass 34 produced is related to the $^{18}O_2$ plasma-jet exposure (mixing with TiO_2 lattice oxygen), as shown in Figure 4.3, and not due to background dosing of $^{16}O_2$. As is apparent from Figure 4.7c, preadsorbed, equilibrated oxygen atoms do not play a role in the molecular chemisorption of oxygen. The results of the experiments shown in Figure 4.7c indicate that preadsorbed atoms do not assist in the molecular chemisorption of oxygen from the gas phase. The large population of mass 34 species seen during the experiment shown in Figure 4.7a is not currently understood. It should be noted that a

similar experiment to the one shown in Figure 4.7a performed on Au(111) resulted in no detectable $^{16}O_2$ adsorption. While experiments performed on bare TiO_2 (i.e. no gold) gave similar results to those shown in Figure 4.7a. Nienhaus et al. recently showed that adsorption of H or D atoms on Ag and Cu surfaces resulted in the generation of hot electrons.[41] Perhaps hot electrons are formed during adsorption of O atoms on the samples studied here. Based on the results shown in Figure 4.7, it seems plausible that hot electrons, resulting from the generation of electron hole pairs, formed during ^{18}O atom adsorption could lead to adsorption of the impinging $^{16}O_2$.

An experiment was performed to determine if reaction of CO with preadsorbed oxygen atoms at 77 K assisted in the adsorption of background molecular oxygen (possibly through electron-hole pair generation from heat of reaction). No molecular adsorption was observed with Kr CID following CO exposure on an oxygen atom covered sample while simultaneously backfilling $^{16}O_2$ at $\sim 1\times10^{-7}$ Torr. However, the reaction only proceeds for a short time (~1 s) due to CO saturation of the surface.[10,11] Perhaps the short reaction time precludes any measurable adsorption of molecular oxygen.

Vibrationally excited molecular oxygen in the plasma-jet may have an enhanced adsorption probability. From time-of-flight measurements of the Ar in the plasma-jet, a nozzle temperature of ~1300 K was estimated. However, due to the nonequilibrium nature of the plasma-jet, the oxygen molecules in the jet are likely to be "hotter" vibrationally than 1300 K and thus there would be a high population of vibrationally excited oxygen molecules in the beam. Since a molecularly chemisorbed oxygen species is likely to have a stretched oxygen-oxygen bond compared to the gas-phase value, a vibrationally excited molecule might have a greater probability of adsorbing molecularly on the gold sample. This could also explain the large amount of mass 32 and 36 species

seen in comparison to the mass 34 species when exposing the sample to the plasma-jets. Another possibility for adsorption directly from the gas-phase is the molecular chemisorption of the low-lying (0.98 eV above ground state) electronically excited, single delta oxygen (SDO) state, $O_2(a^1\Delta_g)$, of molecular oxygen. SDO has been observed to react in some metal complex systems forming metastable oxygenated compounds, which are not formed with ground state oxygen.[42] Walker and coworkers have also suggested that SDO is responsible for the formation of subsurface oxygen on Pt{100}(1×2) during molecular beam exposures.[43] This excited state of oxygen is known to be populated in plasma discharges, sometimes to a high degree,[44] and it is likely present in our plasma-jet also, as suggested by Pollard.[31] SDO is known to have a very long lifetime (~72 minutes[45]), thus nearly every SDO created in the plasma-jet will encounter the surface before relaxing to the ground state (flight times are on the order of 100 μs). Ryskin et al. have measured the deactivation of SDO on a gold wire and observe that there is some deactivation indicating that the SDO does interact with the gold surface.[46] However, Sharpless et al. have also measured the deactivation of SDO on gold and observe very little interaction.[47] Perhaps a state-resolved study of $O_2(a^1\Delta_g)$ adsorption on Au is warranted based on the renewed interest in the chemistry of gold and the results presented here.

Finally, we address the possibility of the formation of molecularly chemisorbed oxygen on the surface by decomposition of ozone on the sample to yield an atomically chemisorbed oxygen species[7] and a molecularly chemisorbed oxygen species. Under the conditions persisting in the oxygen plasma-jet, ozone formation might be possible and its interaction with the surface is worthy of investigation. Parker et al. have shown that Au(111) can be populated with atomically adsorbed oxygen by exposure to ozone at 300 K.[7] We were unable to detect ozone in the plasma-jet employing our QMS. However,

ozone is difficult to detect with the QMS due to its weak intermolecular bonding (easily fragments during electron ionization in QMS), therefore its presence in the plasma-jet cannot be ruled out. To verify whether ozone could be responsible for the molecularly chemisorbed oxygen observed after plasma-jet exposures, we exposed both a 0.5 ML Au/TiO_2 sample and the Au(111) single crystal sample to ~5 L of ozone at 77 K. Kr CID measurements following the ozone exposures resulted in no detectable measurement of molecularly chemisorbed oxygen from either sample studied. Recombinative desorption of oxygen atoms from the Au(111) single crystal after dosing with ozone was observed, in agreement with the results of Parker et al.,[7] verifying that ozone was indeed being generated. Based on the results of these experiments, it can be concluded that ozone decomposition on the sample is not responsible for the presence of molecularly chemisorbed oxygen observed in these studies.

CONCLUSION

We have presented results of an investigation into the mechanism for formation of molecularly chemisorbed oxygen on Au/TiO_2 model catalysts and a Au(111) single crystal following exposure to an oxygen plasma-jet. We have shown evidence suggesting that some of the molecularly chemisorbed oxygen formed on the surfaces results from the recombination of adsorbed atoms with impinging atoms from the plasma-jet. However, this mechanism does not seem to dominate. We also presented results suggesting that nascent adsorption of oxygen atoms on the Au/TiO_2 surface assists in adsorption of gaseous, ground-state molecular oxygen (possibly through the generation of "hot" electrons during O atom adsorption). This process could be relevant during the plasma-jet exposure since a dissociation fraction of ~40% is achieved and hence intact molecules will also strike the surface during the adsorption of oxygen atoms. We cannot rule out adsorption of excited state molecular oxygen species directly from the gas phase, and we

speculate that perhaps singlet-delta oxygen or vibrationally excited oxygen may have enhanced probabilities of adsorbing molecularly. Exposure of the sample to ozone resulted in no detectable formation of molecularly chemisorbed oxygen.

REFERENCES

1. M. Haruta, Catal. Today **36**, 153 (1997); CATTECH 6, 102 (2002).
2. G. C. Bond, D. T. Thompson, Catal. Rev.-Sci. Eng. **41**, 319 (1999).
3. R. Meyer, C. Lemire, Sh. K. Shaikhutdinov, H. J. Freund, Gold Bulletin **37**, 72 (2004).
4. B. Hammer, J. K. Nørskov, Nature **376**, 238 (1995).
5. G. C. Bond, D. T. Thompson, Gold Bulletin **33**, 41 (2000).
6. D. A. Outka, R. J. Madix, Surf. Sci. **179**, 351 (1987).
7. D. H. Parker, B. E. Koel, J. Vac. Sci. Technol. A **8**, 2585 (1990).
8. J. M. Gottfried, K. J. Schmidt, S. L. M. Schroeder, K. Christmann, Surf. Sci. **511**, 65 (2002).
9. V. A. Bondzie, S. C. Parker, C. T. Campbell, Catal. Lett. **63**, 143 (1999).
10. J. D. Stiehl, T. S. Kim, C. T. Reeves, R. J. Meyer, C. B. Mullins, J. Phys. Chem. B **108**, 7917 (2004).
11. T. S. Kim, J. D. Stiehl, C. T. Reeves, R. J. Meyer, C. B. Mullins, J. Am. Chem. Soc. **125**, 2018 (2003).
12. M. A. Lazaga, D. T. Wickham, D. H. Parker, G. N. Kastanas, B. E. Koel, ACS Sym. Ser. **523**, 90 (1993).
13. A. Sanchez, A. Abbet, U. Heiz, W.-D. Schneider, H. Häkkinen, R. N. Barnett, U. Landman, J. Phys. Chem. A **103**, 9573 (1999).
14. N. Lopez, J. K. Nørskov, J. Am. Chem. Soc. **124**, 11262 (2002).
15. L. M. Molina, M. D. Rasmusen, B. J. Hammer, J. Chem. Phys. **120**, 7673 (2004).
16. Z.-P. Liu, X.-Q. Gong, J. Kohanoff, C. Sanchez, P. Hu, Phys. Rev. Lett. **91**, 266102 (2003).
17. H. Huber, D. McIntosh, G. A. Ozin, Inorg. Chem. **16**, 975 (1977).
18. D. Stolcic, M. Fischer, G. Ganterför, Y. D. Kim, Q. Sun, P. Jena, J. Am. Chem. Soc. **125**, 2848 (2003).

19. Y. D. Kim, M. Fischer, G. Ganterför, Chem. Phys. Lett. **377**, 170 (2003).

20. L. D. Socaciu, J. Hagen, T. M. Bernhardt, L. Wöste, U. Heiz, H. Häkkinen, U. Landman, J. Am. Chem. Soc. **125**, 10437 (2003).

21. Q. Sun, P. Jena, Y. D. Kim, M. Fischer, G. Ganteför, J. Chem. Phys. **120**, 6510 (2004).

22. Z.-P. Liu, P. Hu, A. Alavi, J. Am. Chem. Soc. **124**, 14770 (2002).

23. B. Yoon, H. Hakkinen, U. Landman, J. Phys. Chem. A **107**, 4066 (2003).

24. Y. Xu, M. Mavrikakis, J. Phys. Chem. B **107**, 9298 (2003).

25. G. Mills, M. S. Gordon, H. Metiu, J. Chem. Phys. **118**, 4198 (2003).

26. M. Mavrikakis, P. Stolze, J. K. Norskov, Catal. Lett. **64**, 101 (2000).

27. D. H. Wells Jr., W. N. Delgass, K. T. Thomson, J. Chem. Phys. **117**, 10597 (2002).

28. A. Franceschetti, S. J. Pennycook, S. T. Pantelides, Chem. Phys. Lett. **374**, 471 (2003).

29. J. D. Stiehl, T. S. Kim, S. M. McClure, C. B. Mullins, J. Am. Chem. Soc. **126**, 1606 (2004).

30. X. Lai, T. P. St. Clair, M. Valden, D. W. Goodman, Prog. Surf. Sci. **59**, 25 (1998).

31. J. E. Pollard, Rev. Sci. Instrum. **63**, 1771 (1992).

32. M. C. Wheeler, D. C. Seets, C. B. Mullins, J. Chem. Phys. **107**, 1672 (1997).

33. M. C. Wheeler, C. T. Reeves, D. C. Seets, C. B. Mullins, J. Chem. Phys. **108**, 3057 (1997).

34. T. S. Kim, J. D. Stiehl, S. M. McClure, C. B. Mullins, Catal. Lett. Manuscript submitted for publication **(**2004).

35. J. D. Beckerle, A. D. Johnson, S. T. Ceyer, Phys. Rev. Lett. **62**, 685 (1989).

36. J. D. Beckerle, A. D. Johnson, S. T. Ceyer, J. Chem. Phys. **93**, 4047 (1990).

37. C. Åkerlund, I. Zorić, B. Kasemo, J. Chem. Phys. **104**, 7359 (1996).

38. M. Asscher, Y. Zeiri, J. Phys. Chem. B **107**, 6903 (2003).

39. M. A. Henderson, W. S. Epling, C. L. Perkins, C. H. F. Peden, U. Diebold, J. Phys Chem. B **103**, 5328 (1999).

40. R. L. Sharpless, L. E. Jusinski, T. G. Slanger, J. Chem. Phys. **91**, 7936 (1989).

41. H. Nienhaus, H. S. Bergh, B. Gergen, A. Majumdar, W. H. Weinberg, E. W. McFarland, Phys. Rev. Lett. **82**, 446 (1999).

42. M. Selke, C. S. Foote, W. L. Karney, Inorg. Chem. **32**, 5425 (1993).

43. A. V. Walker, B. Klötzer, D. A. King, J. Chem. Phys. **112**, 8631 (2000).

44. M. Shibata, N. Nakano, T. Makabe, J. Appl. Phys. **80**, 6142 (1996).

45. S. M. Newman, A. J. Orr-Ewing, D. A. Newnham, J. Ballard, J. Phys. Chem. A **104**, 9467 (2000).

46. M. E. Ryskin, B. R. Shub, J. Pavlicek, Z. Knor, Chem. Phys. Lett. **99**, 140 (1983).

47. R. L. Sharpless, T. G. Slanger, J. Chem. Phys. **91**, 7947 (1989).

Chapter 5: Reaction of CO with Molecularly Chemisorbed Oxygen on TiO_2 Supported Gold Nanoclusters

INTRODUCTION

The chemistry of supported gold catalysts[1,2] has proven to be complex and details regarding a reaction as superficially simple as CO oxidation are still not fully understood. One important issue that remains unresolved is the identity of the active oxygen species involved in the reaction. It is well known that bulk gold will not readily dissociate oxygen,[3-5] yet atomic oxygen species adsorbed on gold surfaces have been observed to be highly reactive towards CO.[3-9] It has been speculated that the unique catalytic behavior of gold nanoclusters is related to their reduced dimensionality resulting in properties suitable for the dissociation of oxygen.[6,10] However, this picture is in contrast with (i) results from theory that show oxygen dissociation on any gold system, including small gold clusters, is highly activated (activation energies ~1 eV)[11-14] and (ii) null experimental results regarding the dissociation of oxygen on gold systems.[3-6,8]

Interestingly, some density functional theory (DFT) calculations indicate that molecularly chemisorbed oxygen is stable on strained gold surfaces and steps, as well as on small gold clusters[11-15] and ultraviolet photoemission spectroscopy measurements have indicated that small, gas-phase gold clusters, Au_n (n = 2-20), will adsorb oxygen molecularly.[16,17] Gas-phase gold clusters that are known to adsorb oxygen molecularly have also provided experimental evidence for oxidation of CO,[18] and DFT calculations regarding the reaction of CO with molecularly chemisorbed oxygen on gold have predicted that the reaction is relatively facile.[10,15,19,20] Liu et al. have calculated that molecularly chemisorbed oxygen at the Au-TiO_2 interface will readily react with CO to form CO_2.[19] Molina et al. have also presented similar results showing that CO will react

with molecularly chemisorbed oxygen at the Au-TiO_2 interface with an activation barrier of 0.15 eV.[20] Lopez and Nørskov report calculations that show that molecular oxygen adsorbed on a 10 atom gold cluster is as reactive as atomically adsorbed oxygen for CO oxidation.[10] Sanchez et al. have also presented DFT results in which they determine that CO will react spontaneously with molecularly chemisorbed oxygen on Au_8 clusters supported on MgO.[15]

As of yet, no conclusive experimental evidence has been presented regarding the reactivity of molecularly chemisorbed oxygen on extended gold surfaces or on supported gold clusters larger than ~20 atoms. In a previous study, we showed that exposing a Au/TiO_2 model catalyst sample to a radio frequency (RF)-generated plasma-jet resulted in the population of molecularly chemisorbed oxygen ($O_{2,a}$) species on the sample along with atomically adsorbed (O_a) species.[21] In this paper we present results from an investigation of the reactivity of $O_{2,a}$ on an oxygen covered Au/TiO_2 model catalyst. We observe that samples that are populated with both O_a and $O_{2,a}$ consistently result in greater CO_2 production than samples populated with an equivalent O_a coverage but without $O_{2,a}$. For the data presented in this paper, we observe a 41% difference in CO_2 production between a sample populated with only O_a and one populated with both O_a and $O_{2,a}$.

EXPERIMENTAL

The experiments were performed in an ultrahigh vacuum molecular beam surface scattering apparatus that has been described in detail previously.[9,21,22] The sample assembly consists of Au(111) and TiO_2(110) single crystals which are mounted on opposite faces of a tantalum plate that is in thermal contact with a liquid nitrogen reservoir and that can be resistively heated. Gold is vapor-deposited on the TiO_2(110) sample as described previously.[9,21] Mixtures of 8% oxygen in Ar are dosed via a

supersonic, RF generated plasma-jet source with a dissociation fraction of ~40% as determined via time-of-flight.[23] All oxygen coverages reported on Au/TiO_2 are defined as the coverage relative to saturation and are determined by integration of the recombinative thermal desorption spectra of oxygen from the Au particles. Energetic beams of Kr (~1 eV) and Ar (~0.5 eV), formed by supersonic expansion in a 98% He mixture, are used for the collision-induced desorption (CID) experiments.[21,24,25] The same apertures are used for defining beams of $C^{16}O$, Kr, and the oxygen-plasma-jet and the spot size produced is smaller than the crystal faces, thus minimizing direct exposure to surfaces other than the sample.

In our previous study,[21] we noted that the ratio of $O_{2,a}$ adsorbed on the sample during the plasma exposure to the O_a on the sample is relatively small (~10% for 2 ML [monolayers] Au/TiO_2). For the experiments presented in this paper, it was desirable to increase this ratio to facilitate measurement of the reactivity of $O_{2,a}$. A procedure utilizing isotopically labeled oxygen was devised: (i) the sample (T_s = 77 K) was exposed to a plasma-jet formed using $^{16}O_2$ to a coverage of ~50%; (ii) the sample was heated to 300 K to desorb $^{16}O_{2,a}$; and after cooling to 77 K, (iii) the $^{16}O_a$-covered sample was exposed to a plasma-jet formed using $^{18}O_2$ (exposure equivalent to ~25% coverage on a clean 1 ML Au/TiO_2 sample). By preadsorbing $^{16}O_a$ on the sample, we could limit the available sites for $^{18}O_a$ adsorption and thus increase the ratio of $^{18}O_{2,a}$ to $^{18}O_a$ on the sample. For the 1 ML Au/TiO_2 sample discussed here the ratio was increased from ~0.34 to ~0.75. We observe some formation of mass 34 species ($^{16}O^{18}O$) on the sample, but the quantity formed is small compared to the amount of mass 36 ($^{18}O_{2,a}$) species and its effect on the measurement of the reactivity of molecularly chemisorbed oxygen is immeasurable as is discussed below.

Following the preparation of the oxygen-covered sample described above, two separate experiments were performed to determine if $^{18}O_{2,a}$ reacted with $C^{16}O$. One experiment required the removal of $^{18}O_{2,a}$ via CID, followed by a $C^{16}O$ exposure to measure the amount of $C^{16}O^{18}O$ produced from reaction of $C^{16}O$ with $^{18}O_a$. The second experiment consisted of exposing the oxygen-covered sample to $C^{16}O$ to determine the quantity of $C^{16}O^{18}O$ produced from reaction with both $^{18}O_a$ and $^{18}O_{2,a}$. A difference in the $C^{16}O^{18}O$ produced during the two experiments could be associated with the presence of $^{18}O_{2,a}$ since both surfaces are populated with the same amount of $^{18}O_a$.

RESULTS AND DISCUSSION

Figure 5.1 shows the mass 46 ($C^{18}O^{16}O$) produced during experiments representative of both CO oxidation scenarios discussed above. The upper solid curve in Figure 5.1 shows the mass 46 production from the sample with both $^{18}O_a$ and $^{18}O_{2,a}$ species present on the sample and the lower dashed curve shows the mass 46 production from a surface that has been cleared of $^{18}O_{2,a}$ via CID. Both reactions show behavior typical of the CO oxidation reaction with preadsorbed oxygen atoms reported previously.[8,9] However, comparison of the two $C^{16}O^{18}O$ production curves in Figure 5.1 shows that the sample with both of the oxygen species present on the sample results in more $C^{16}O^{18}O$ production (average values and uncertainties from three identical experiments are shown in the inset). On average, a difference of 41 ± 2% in the $C^{16}O^{18}O$ production is observed between the two samples. Similar results have been obtained on a 2 ML Au covered TiO_2 surface (~18% difference). It should be noted that no mass 48 species is observed evolving from the sample indicating that the original $C^{16}O$ bond remains intact throughout the process.

In principle, the difference in the $C^{16}O^{18}O$ production shown above cannot be totally ascribed to reaction of $C^{16}O$ with $^{18}O_{2,a}$. When $^{18}O_{2,a}$ reacts with $C^{16}O$, the $^{18}O_a$

remaining could also react to make $C^{16}O^{18}O$. However, a large accumulation of additional $^{18}O_a$ on the sample reduces the reactivity of the sample in this O_a coverage regime, as shown previously.[8]

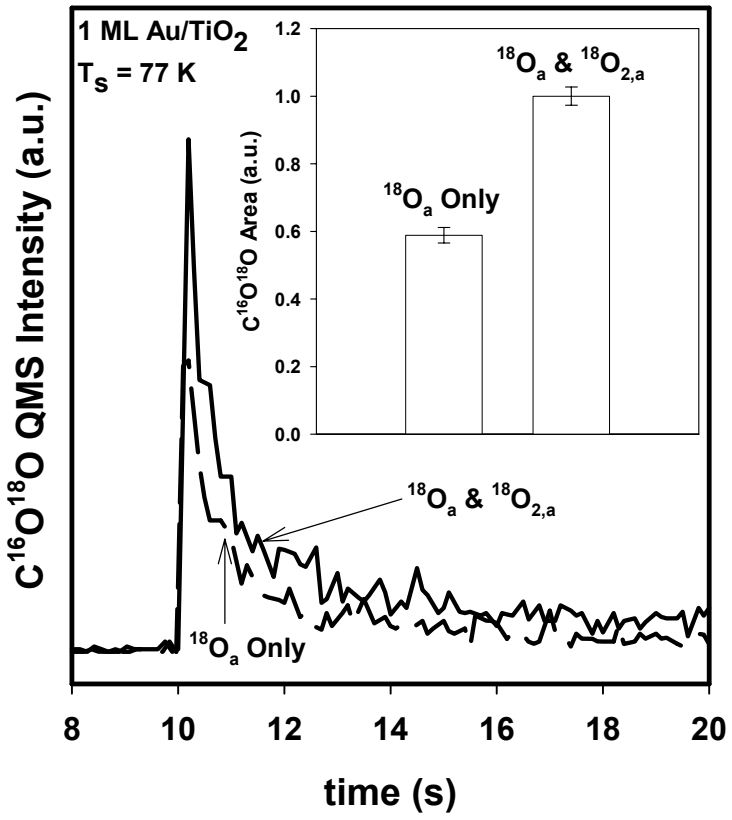

Figure 5.1: $C^{16}O^{18}O$ production at 77 K from a 1 ML Au/TiO_2 sample populated with both $^{18}O_a$ and $^{18}O_{2,a}$ (solid curve) and $^{18}O_a$ only (dashed curve) upon exposure to a pure CO beam at 10 s. Inset shows average values and uncertainties of $C^{16}O^{18}O$ produced from a series of three identical measurements like the ones shown.

A key assumption in the interpretation of our experimental results is that Kr CID does not affect the reactivity of the atomic oxygen overlayer. To verify the validity of this assumption, we repeated the experiments shown in Figure 5.1 using energetic Ar

(~0.5 eV) for CID measurments. Results essentially identical to those presented in Figure 5.1 were obtained.

To further address the effect of Kr CID on the reactivity of O_a, an experiment was performed on $^{16}O_a$ covered Au/TiO_2 in which the sample was (i) exposed to the plasma-jet at 77 K, (ii) heated to 170 K to desorb $^{16}O_{2,a}$ and after cooling to 77 K (iii) Kr CID was performed (as expected, no CID of $^{16}O_{2,a}$ was observed) and (iv) the CO_2 production was measured. For comparison, a similar experiment was conducted, with the exception that step iii was not performed. The difference in the CO_2 production between these two experiments was found to be negligible (< 3%), further verifying that Kr CID does not alter the reactivity of the atomic oxygen overlayer. Similar results are observed on Au(111).

Finally, in all the experiments used for the data in Figure 1, the mass 44 ($C^{16}O_2$) produced was the same (within ~5%), again suggesting that Kr CID does not measurably affect the reactivity of the preadsorbed, annealed ^{16}O atoms.

A determination of the reaction probability of the $O_{2,a}$ on the sample is difficult since both the TiO_2 and Au clusters are populated with $O_{2,a}$ as discussed in our previous publication.[21] However, considering its smaller population relative to the O_a species, it appears that $O_{2,a}$ is at least comparable in reactivity to the O_a on the sample.

CONCLUSIONS

In conclusion, we have investigated the CO oxidation reaction on a Au/TiO_2 model catalyst populated with both O_a and $O_{2,a}$ and compared it to the reactivity of a Au/TiO_2 model catalyst sample populated with only O_a. We observe that samples populated with both oxygen species consistently result in more CO_2 production than samples with only O_a. For the data shown in this paper, we observe a difference of 41 ± 2% in the CO_2 production from samples with both oxygen species compared to samples

with just atomic oxygen. We interpret this result as evidence that molecularly chemisorbed oxygen species directly participate in the CO oxidation reaction on Au/TiO_2 model catalyst systems with particles in the 2 – 5 nm size range, revealing a reaction channel that does not require the dissociation of oxygen.

REFERENCES

1. M. Haruta, Catal. Today **36**, 153 (1997); CATTECH **6**, 102 (2002).

2. R. Meyer, C. Lemire, Sh. K. Shaikhutdinov, H. J. Freund, Gold Bulletin **37**, 72 (2004).

3. D. A. Outka, R. J. Madix, Surf. Sci. **179**, 351 (1987).

4. D. H. Parker, B. E. Koel, J. Vac. Sci. Technol. A **8**, 2585 (1990).

5. J. M. Gottfried, K. J. Schmidt, S. L. M. Schroeder, K. Christmann, Surf. Sci. **511**, 65 (2002).

6. V. A. Bondzie, S. C. Parker, C. T. Campbell, Catal. Lett. **63**, 143 (1999).

7. T. S. Kim, J. D. Stiehl, S. M. McClure, P. L. Tanaka, C. B. Mullins, Manuscript submitted for publication.

8. J. D. Stiehl, T. S. Kim, C. T. Reeves, R. J. Meyer, C. B. Mullins, J. Phys. Chem. B **108**, 7917 (2004).

9. T. S. Kim, J. D. Stiehl, C. T. Reeves, R. J. Meyer, C. B. Mullins, J. Am. Chem. Soc. **125**, 2018 (2003).

10. N. Lopez, J. K. Nørskov, J. Am. Chem. Soc. **124**, 11262 (2002).

11. Y. Xu, M. Mavrakakis, J. Phys. Chem. B **107**, 9298 (2003).

12. G. Mills, M. S. Gordon, H. Metiu, J. Chem. Phys. **118**, 4198 (2003).

13. Z.-P. Liu, P. Hu, A. Alavi, J. Am. Chem. Soc. **124**, 14770 (2002).

14. B. Yoon, H. Häkkinen, U. Landman, J. Phys. Chem. A **107**, 4066 (2003).

15. A. Sanchez, S. Abbet, U. Heiz, W.-D. Schneider, H. Häkkinen, R. N. Barnett, U. Landman, J. Phys. Chem. A **103**, 9573 (1999).

16. D. Stolcic, M. Fischer, G. Ganterför, Y. D. Kim, Q. Sun, P. Jena, J. Am. Chem. Soc. **125**, 2848 (2003).

17. Y. D. Kim, M. Fischer, G. Ganterför, Chem. Phys. Lett. **377**, 170 (2003).

18. L. D. Socaciu, J. Hagen, T. M. Bernhardt, L. Wöste, U. Heiz, H. Häkkinen, U. Landman, J. Am. Chem. Soc. **125**, 10437 (2003).

19. Z.-P. Liu, X.-Q. Gong, J. Kohanoff, C. Sanchez, P. Hu, Phys. Rev. Lett. **91**, 266102 (2003).

20. L. M. Molina, M. D. Rasmusen, B. Hammer, J. Chem. Phys. **120**, 7673 (2004).

21. J. D. Stiehl, T. S. Kim, S. M. McClure, C. B. Mullins, J. Am. Chem. Soc. **126**, 1606 (2004).

22. M. C. Wheeler, D. C. Seets, C. B. Mullins, J. Chem. Phys. **105**, 1572 (1996).

23. J. E. Pollard, Rev. Sci. Instrum. **63**, 1771 (1992).

24. J. D. Beckerle, A. D. Johnson, S. T. Ceyer, Phys. Rev. Lett. **62**, 685 (1989).

25. C. Åkerlund, I. Zorić, B. Kasemo, J. Chem. Phys. **104**, 7359 (1996).

Chapter 6: Concluding Remarks

The perception of gold as a chemically active material has begun to take shape over the past couple of decades. Since the discovery by Haruta that supported gold clusters in the 2-5 nm size range can be catalytically active,[1-4] many studies have been performed to try and understand this unexpected property of gold. CO oxidation on gold based catalysts, despite its superficial simplicity, has proven to be a very complex system to study and has received much attention by the gold chemistry community. Many details regarding the fundamental steps of the reaction are not well understood.[5] The active site for reaction on the catalyst is not known and the nature of the oxygen species involved in the reaction has also not been identified. As in many studies of catalytic activity, answering fundamental questions such as these can be crucial to the design of catalysts, which might have potential for use in actual applications. In this dissertation, Au/TiO_2 model catalysts were used to explore some fundamental questions regarding the CO oxidation reaction. Through the use of molecular beam techniques, the reaction of CO with preadsorbed oxygen was studied under ultrahigh vacuum conditions in which the temperature of the catalyst could be varied, various gold coverages could be studied, and the effect of oxygen precoverage on the sample could be investigated.

In Chapter 2, a systematic study of the reactivity of atomically adsorbed oxygen on Au/TiO_2 model catalysts was reported. The reaction of CO with preadsorbed oxygen atoms was found to be a strong function of the surface temperature and the oxygen precoverage. The reaction was observed to occur at temperatures as low as 65 K, indicating that there is a low activation barrier associated with the reaction. This is in agreement with theoretical work that has shown that atomic oxygen will readily react with CO to form CO_2.[6,7] Another interesting observation from the results shown in

Chapter 2 is that the reaction of CO with a preadsorded atom is relatively particle size independent. The reaction was observed to occur on all the gold coverages studied, including nominally continuous films of gold. This result is in contrast to the observations of Haruta and Goodman for work on Au/TiO_2 catalyst systems under high-pressure conditions employing gas-phase O_2 as a reactant in which they observe a strong particle size dependence. The results from Chapter 2 suggest that under real catalytic conditions, if atomic oxygen is the active species, reaction of CO with an atomic oxygen species is not likely the rate-limiting step. Therefore, assuming that O_a is the active species, the particle size dependence observed by Haruta and Goodman is likely related to the adsorption of oxygen on the catalyst samples and its dependence on gold particle size.

In Chapters 3 and 4 of the dissertation, the identification of a molecularly chemisorbed oxygen state ($O_{2,a}$) on the catalyst samples was discussed. Although ground state, gas-phase O_2 does not adsorb on the model catalyst samples under ultrahigh vacuum, exposure of the catalyst samples to a plasma-jet of oxygen resulted in the population of molecularly chemisorbed oxygen species. In Chapter 3 evidence was presented from thermal desorption, collision-induced desorption, and adsorption/reaction-induced desorption, identifying the molecular oxygen state on the catalyst samples studied. An $O_{2,a}$ desorption feature peaked at ~145 K, corresponding to an adsorption energy of ~0.35 eV, was observed following exposure of the sample to the plasma-jet. Chapter 4 presented results of a study of the formation of $O_{2,a}$. It was shown that some of the $O_{2,a}$ forms via recombination of O atoms on the surface during the plasma-jet exposure. However, this does not appear to be the dominant mechanism for the formation of $O_{2,a}$. Evidence is also presented showing that adsorption of an oxygen atom can directly influence the molecular chemisorption of gas-phase molecular oxygen. As

the plasma-jet used for dosing oxygen is only ~40% efficient (i.e. only ~40% of molecules in plasma-jet are dissociated), gas-phase oxygen molecules that strike the surface during simultaneous atomic oxygen adsorption might have an enhance probability of adsorbing molecularly on the sample. Other possible adsorption routes such as adsorption of excited (electronically or vibrationally) oxygen species are discussed.

The population of a molecular state on the catalyst sample allowed for the unique opportunity to directly determine whether a reaction channel existed where CO could react with a molecularly chemisorbed oxygen species. Evidence was presented in Chapter 5 indicating that CO can directly react with $O_{2,a}$ on a Au/TiO_2 model catalyst surface. Although it is not possible to conclusively say that this is an active channel for reaction during real catalytic processes, this is the first direct evidence of such a channel on Au/TiO_2. This result indicates that dissociation of oxygen is not required for the oxidation reaction to occur. Thus, if reaction of CO with molecularly chemisorbed oxygen is responsible for the CO oxidation activity of gold-based catalysts, then the molecular chemisorption of oxygen is likely to be the rate-determining step and the particle size effects that have been observed are likely related to an enhanced activity of 2 - 5 nm diameter particles for molecular chemisorption of oxygen.

RECOMMENDATIONS FOR FUTURE RESEARCH

The understanding of catalysis by gold is still in its infancy and much work is still required to understand how this material, which is so inert in its bulk form, can be so reactive as its dimensions are decreased to nanometer scales. Fortunately, through the participation of several different scientific disciplines, the mysteries of gold chemistry are slowly becoming unraveled. As the understanding of this remarkable material increases so could its impact on technology. However, many avenues of study are still necessary for this to become a reality.

Some issues that are directly relevant to the work presented in this dissertation are worthy of attention. One issue involves the characterization of the model catalyst samples (likely with scanning tunneling microscopy) that were used for this study. The assumption has been made that the model catalyst samples mimic closely the samples prepared and characterized by the Goodman group.[4] This is likely a valid assumption for the freshly prepared catalyst samples, however, confirmation of this assumption is desirable. A characterization study of a Au/TiO_2 model catalyst sample that has been exposed to the extreme oxiding conditions used in this study is also desirable as this has not been performed. Goodman and coworkers observed that exposure of their samples to a high pressure O_2 dose resulted in the sintering of the gold particles. Perhaps a similar phenomenon occurs on exposure of the catalyst samples to the oxygen plasma-jet used in the studies presented here. Another aspect of the work presented here that requires more attention is the CO oxidation reaction with preadsorbed oxygen atoms at temperatures above the desorption temperature of CO. In Chapter 2, it was shown that for intermediate coverages of oxygen atoms, bimodal CO_2 production curves were observed for surface temperatures above the desorption temperature of CO. XPS studies of atomically adsorbed oxygen on Au single crystals have shown that there are two oxygen domains present, an oxidic gold domain and a domain where oxygen is chemisorbed. Perhaps the bimodal features could be related to varying reactivities of these two domains. Through a combined XPS and reaction kinetics study, the bimodal features shown in Chapter 2 might be more fully understood.

As has been mentioned in the previous chapters, most fundamental studies of gold chemistry have been performed using CO oxidation as a test reaction. There is likely still much more interesting chemistry to be discovered. In Haruta's early work, the propylene epoxidation reaction was also studied and it was found that Au catalysts might be

promising for this reaction as well. This reaction could have significant industrial impact as current routes for propylene epoxidation involve a two-step reaction process. Experiments similar to the ones discussed in this dissertation could be performed with propylene to see if this reaction occurs on Au/TiO_2 model catalysts. Also, McClure et al. recently showed that NO could be oxidized on a Au(111) single crystal at a temperature of 77 K.[8] A complimentary study of NO oxidation could be performed on the Au/TiO_2 model catalyst for comparison with the bulk single crystal study.

Another avenue that deserves investigation is the use of bimetallic catalysts. If Au could be incorporated in a catalyst with a metal, which readily dissociates oxygen, the reactivity of the catalyst could have the potential of being high. Since Au binds oxygen atoms weaker than, for example Ir or Pt (which are very reactive for oxygen dissociation), the reactivity could be high. Recently, Lang et al. showed that intimately mixed Pt-Au nanoparticles approximately 3 nm in size could be prepared via stabilization with dendrimers on a SiO_2 substrate.[9] The particles were observed to be active for CO oxidation at low temperatures (30-80 ^oC), exhibiting higher activity than Pt/SiO_2 and Au/SiO_2. A model catalyst study employing dendrimer stabilized Pt-Au particles could be performed to determine their activity for oxygen adsorption. If oxygen is observed to adsorb on these catalysts under UHV, a study of the CO oxidation activity of these catalysts at cryogenic temperatures could be performed similar to the studies presented here.

Another prospect for a bimetallic catalyst system is based on the results of Okada et al. who showed that Au layers grown epitaxially on Ir(111) could dissociate hydrogen.[10] This result is quite surprising as bulk Au(111) does not dissociate H_2 as has been mentioned previously. Ongoing work in the Korgel research lab at the University of Texas at Austin has shown promise for making colloidal stabilized Au/Ir nanoclusters.

Should attempts to synthesize these particles be successful, model catalyst studies on various supports, both reducible and nonreducible, could be initiated to determine if these particles exhibit properties similar to Au layers grown on Ir(111).

Finally, and more generally, through the investigation of different materials for supports and implementation of new deposition methods, perhaps far more interesting chemistry can still be discovered. The use of mixed metal oxides has recently been implemented in a model catalyst study to prevent the sintering of gold particles that is known to occur during interaction with oxygen.[11] Perhaps, mixed metal oxides can be developed which not only prevent sintering but which also perturb the electronic structure of the gold particles to enhance their reactivity. This would entail in depth characterization studies of the metal-oxide supports as well as the characterization of Au supported on the oxides.

REFERENCES

1. M. Haruta, T. Kobayashi, H. Sano, N. Yamada, Chem. Lett. **4**, 405 (1987).

2. G. C. Bond, D. T. Thompson, Catal. Rev.-Sci. Eng. **41**, 319 (1999).

3. R. Meyer, C. Lemire, Sh. K. Shaikhutdinov, H. J. Freund, Gold Bulletin **37**, 72 (2004).

4. M. Valden, X. Lai, D. W. Goodman, Science **281**, 1647 (1998).

5. G. C. Bond, D. T. Thompson, Gold Bulletin **33**, 41 (2000).

6. N. Lopez, J. K. Nørskov, J. Am. Chem. Soc. **124**, 11262 (2002).

7. Z.-P. Liu, P. Hu, A. Alavi, J. Am. Chem. Soc. **124**, 14770 (2002).

8. S. M. McClure, T. S. Kim, J. D. Stiehl, P. L. Tanaka, C. B. Mullins, J. Phys. Chem. B **108**, 17952 (2004).

9. H. Lang, S. Maldonado, K. J. Stevenson, B. D. Chandler, J. Am. Chem. Soc. **126**, 12949 (2004).

10. M. Okada, M. Nakamura, K. Moritani, T. Kasai, Surf. Sci. **523**, 218 (2003).

11. B. K. Min, W. T. Wallace, D. W. Goodman, J. Phys. Chem. B **108**, 14609 (2004).

Bibliography

C. Åkerlund, I. Zorić, B. Kasemo, J. Chem. Phys. **104**, 7359 (1996).

M. Asscher, Y. Zeiri, J. Phys. Chem. B **107**, 6903 (2003).

G. R. Bamwenda, S. Tsubota, T. Nakamura, M. Haruta, Catal. Lett. **44**, 83 (1997).

M. A. Barteau and R. J. Madix, in *The Chemical Physics of Solid Surfaces and Heterogeneous Catalysis*, Vol. 4, edited by D. A. King and D. P. Woodriff (Elsevier, Amsterdam, 1982).

J. V. Barth, T. Zambelli, Surf. Sci. **513**, 359 (2002).

N. Bartlett, Gold Bulletin **31**, 22 (1998).

C. Becker, C. R. Henry, Catal. Lett. **43**, 55 (1997).

J. D. Beckerle, A. D. Johnson, S. T. Ceyer, Phys. Rev. Lett. **62**, 685 (1989).

J. D. Beckerle, A. D. Johnson, S. T. Ceyer, J. Chem. Phys. **93**, 4047 (1990).

F. Boccuzzi, A. Chiorino, J. Phys. Chem. B **104**, 5414 (2000).

F. Boccuzzi, A. Chiorino, M. Manzoli, P. Lu, T. Akita, S. Ichikawa, M. Haruta, J. Catal. **202**, 256 (2001).

M. A. Bollinger, M. A. Vannice, Appl. Catal. B: Environ. **8**, 417 (1996).

G. C. Bond, J. Mol. Catal. A: Chemical **156**, 1 (2000).

G. C. Bond, Gold Bulletin **34**, 117 (2001).

G. C. Bond, P. A. Sermon, Gold Bulletin **6**, 102 (1973).

G. C. Bond, D. T. Thompson, Catal. Rev.-Sci. Eng. **41**, 319 (1999).

G. C. Bond, D. T. Thompson, Gold Bulletin **33**, 41 (2000).

V. A. Bondzie, S. C. Parker, C. T. Campbell, Catal. Lett. **63**, 143 (1999).

W. A. Bone, G. W. Andrew, Proc. R. Soc. A **109**, 459 (1925).

D. Brinkley, M. Dietrich, T. Engel, P. Farral, G. Gantner, A. Schafer, A. Szumacher, Surf. Sci. **395**, 292 (1998).

U. Burghaus, H. Conrad, Surf. Sci. **364**, 109 (1996).

A. J. Capote, T. J. Roberts, R. J. Madix, Surf. Sci. **209**, L151 (1989).

D. Y. Cha, G. Parravano, J. Catal. **18**, 200 (1970).

M. S. Chen, D. W. Goodman, Science **306**, 252 (2004).

T. V. Choudhary, D. W. Goodman, Top. Catal. **21**, 25 (2002).

T. Dellwig, J. Hartmann, J. Libuda, I. Meusel, G. Rupprechter, H. Unterhalt, H.-J. Freund, J. Mol. Catal. A **162**, 51 (2000).

A. Franceschetti, S. J. Pennycook, S. T. Pantelides, Chem. Phys. Lett. **374**, 471 (2003).

S. Galvano, G. Parravano, J. Catal. **55**, 178 (1978).

K. D. Gibson, M. Viste, E. C. Sanchez, S. J. Sibener, J. Chem. Phys. **110**, 2757 (1999).

K. D. Gibson, M. Viste, E. C. Sanchez, S. J. Sibener, J. Chem. Phys. **112**, 2470 (2000).

J. Gland, Surf. Sci. **93**, 487 (1980).

J. M. Gottfried, K. Christmann, Surf. Sci. **566-568**, 1112 (2004).

J. M. Gottfried, N. Elghobashi, S. L. M. Schroeder, K. Christman, Surf. Sci. **523**, 89 (2003).

J. M. Gottfried, K. J. Schmidt, S. L. M. Schroeder, K. Christmann, Surf. Sci. **252**, 197 (2002).

J. M. Gottfried, K. J. Schmidt, S. L. M. Schroeder, K. Christmann, Surf. Sci. **511**, 65 (2002).

J. M. Gottfried, K. J. Schmidt, S. L. M. Schroeder, K. Christmann, Surf. Sci. **525**, 184 (2003).

C. Goyhenex, M. Croci, C. Claeys, C. R. Henry, Surf. Sci. **352-354**, 475 (1996).

J.-D. Grunwaldt, A. Baiker, J. Phys. Chem. B **103**, 1002 (1999).

J. Hagen, L. D. Socaciu, M. Elijazyfer, U. Heiz, T. M. Bernhardt, L. Wöste, Phys. Chem. Chem. Phys. **4**, 1707 (2002).

B. Hammer, J. K. Nørskov, Nature **376**, 238 (1995).

M. Haruta, Catal. Today **36**, 153 (1997).

M. Haruta, CATTECH **6**, 102 (2002).

M. Haruta, T. Kobayashi, H. Sano, N. Yamada, Chem. Lett. **4**, 405 (1987).

M. A. Henderson, W. S. Epling, C. L. Perkins, C. H. F. Peden, U. Diebold, J. Phys. Chem. B **103**, 5328 (1999).

C. H. Henry, Surf. Sci. Rep. **31**, 231 (1998).

C. R. Henry, C. Chapon, C. Duriez, J. Chem. Phys. **95**, 700 (1991).

J. Hoffmann, I. Meusel, J. Hartmann, J. Libuda, H.-J. Freund, J. Catal. **204**, 378 (2001).

H. Huber, D. McIntosh, G. A. Ozin, Inorg. Chem. **16**, 975 (1977).

G. J. Hutchings, Gold Bulletin **37**, 3 (2004).

Y. D. Kim, M. Fischer, G. Ganteför, Chem. Phys. Lett. **377**, 170 (2003).

T. S. Kim, J. D. Stiehl, C. T. Reeves, R. J. Meyer, C. B. Mullins, J. Am. Chem. Soc. **125**, 2018 (2003).

T. S. Kim, J. D. Stiehl, S. M. McClure, P. L. Tanaka, C. B. Mullins, Catal. Lett., Manuscript submitted for publication (2004).

D. A. King, M. G. Wells, Proc. R. Soc. London. A **339**, 245 (1974).

A. Krozer, M. Rodahl, J. Vac. Sci. Technol. A **15**, 1704 (1997).

M. C. Kung, C. K. Costello, H. H. Hung, Catal. **17**, 152 (2004).

X. Lai, T. P. St. Clair, M. Valden, D. W. Goodman, Prog. Surf. Sci. **59**, 25 (1998).

H. Lang, S. Maldonado, K. J. Stevenson, B. D. Chandler, J. Am. Chem. Soc. **126**, 12949 (2004).

M. A. Lazaga, D. T. Wickham, D. H. Parker, G. N. Kastanas, B. E. Koel, ACS Sym. Ser. **523**, 90 (1993).

T. H. Lee, K. M. Ervin, J. Phys. Chem. **98**, 10023 (1994).

S. Lee, C. Fan, T. Wu, S. L. Anderson, J. Am. Chem. Soc. **126**, 5682 (2004).

J. Libuda, I. Meusel, J. Hoffmann, J. Hartmann, H. J. Freund, J. Vac. Sci. Technol. A **19**, 1516 (2000).

Z.-P. Liu, X.-Q. Gong, J. Kohanoff, C. Sanchez, P. Hu, Phys. Rev. Lett. **91**, 266102 (2003).

Z.-P. Liu, P. Hu, A. Alavi, J. Am. Chem. Soc. **124**, 14770 (2002).

H. Liu, A. I. Kozlov, A. P. Kozlova, T. Shido, K. Asakura, Y. Iwasawa, J. Catal. **185**, 252 (1999).

N. Lopez, J. K. Nørskov, J. Am. Chem. Soc. **124**, 11262 (2002).

M. Mavrikakis, P. Stolze, J. K. Norskov, Catal. Lett. **64**, 101 (2000).

S. M. McClure, T. S. Kim, J. D. Stiehl, P. L. Tanaka, C. B. Mullins, J. Phys. Chem. B **108**, 17952 (2004).

I. Meusel, J. Hoffmann, J. Hartmann, M. Heemeier, M. Bäumer, J. Libuda, H.-J. Freund, Catal. Lett. **71**, 5 (2001).

I. Meusel, J. Hoffmann, J. Hartmann, J. Libuda, H.-J. Freund, J. Phys. Chem. B **105**, 3567 (2001).

R. Meyer, C. Lemire, Sh. K. Shaikhutdinov, H. J. Freund, Gold Bulletin **37**, 72 (2004).

G. Mills, M. S. Gordon, H. Metiu, J. Chem. Phys. **118**, 4198 (2003).

B. K. Min, W. T. Wallace, D. W. Goodman, J. Phys. Chem. B **108**, 14609 (2004).

L. M. Molina, M. D. Rasmusen, B. J. Hammer, J. Chem. Phys. **120**, 7673 (2004).

S. M. Newman, A. J. Orr-Ewing, D. A. Newnham, J. Ballard, J. Phys. Chem. A **104**, 9467 (2000).

H. Nienhaus, H. S. Bergh, B. Gergen, A. Majumdar, W. H. Weinberg, E. W. McFarland, Phys. Rev. Lett. **82**, 446 (1999).

M. Okada, M. Nakamura, K. Moritani, T. Kasai, Surf. Sci. **523**, 218 (2003).

D. A. Outka, R. J. Madix, Surf. Sci. **179**, 351 (1987).

D. H. Parker, B. E. Koel, J. Vac. Sci. Technol. A **8**, 2585 (1990).

L. Piccolo, C. Becker, C. R. Henry, Appl. Surf. Sci. **164**, 156 (2000).

K. S. Pitzer, Acc. Chem. Res. **12**, 271 (1979).

J. E. Pollard, Rev. Sci. Instrum. **63**, 1771 (1992).

P. Pyykko, Angew. Chem. Int. Ed. **41**, 3537 (2002).

P. Pyykko, J.-P. Desclaux, Acc. Chem. Res. **12**, 276 (1979).

D. R. Rainer, D. W. Goodman, J. Mol. Catal. A: Chemical **131**, 259 (1998).

D. R. Rainer, C. Xu, D. W. Goodman, J. Mol. Catal. A: Chemical **119**, 307 (1997).

C. T. Rettner, J. J. Lee, J. Chem. Phys. **101**, 10185 (1994).

M. E. Ryskin, B. R. Shub, J. Pavlicek, Z. Knor, Chem. Phys. Lett. **99**, 140 (1983).

N. Saliba, D. H. Parker, B. E. Koel, Surf. Sci. **410**, 270 (1998).

B. E. Salisbury, W. T. Wallace, R. L. Whetten, Chem. Phys. **262**, 131 (2000).

A. Sanchez, S. Abbet, U. Heiz, W.-D. Schneider, H. Häkkinen, R. N. Barnett, U. Landman, J. Phys. Chem. A **103**, 9573 (1999).

A. G. Sault, R. J. Madix, C. T. Campbell, Surf. Sci. **169**, 347 (1986).

M. Selke, C. S. Foote, W. L. Karney, Inorg. Chem. **32**, 5425 (1993).

R. L. Sharpless, L. E. Jusinski, T. G. Slanger, J. Chem. Phys. **91**, 7936 (1989).

R. L. Sharpless, T. G. Slanger, J. Chem. Phys. **91**, 7947 (1989).

M. Shibata, N. Nakano, T. Makabe, J. Appl. Phys. **80**, 6142 (1996).

L. D. Socaciu, J. Hagen, T. M. Bernhardt, L. Wöste, U. Heiz, H. Hakkinen, U. Landman, J. Am. Chem. Soc. **125**, 10437 (2003).

I. Stara, V. Matolin, Surf. Sci. **313**, 99 (1994).

I. Stará, V. Nehasil, V. Matolín, Surf. Sci. **331-333**, 173 (1995).

I. Stará, V. Nehasil, V. Matolín, Surf. Sci. **365**, 69 (1996).

J. D. Stiehl, T. S. Kim, S. M. McClure, C. B. Mullins, J. Am. Chem. Soc. **126**, 1606 (2004).

J. D. Stiehl, T. S. Kim, S. M. McClure, C. B. Mullins, Manuscript in preparation.

J. D. Stiehl, T. S. Kim, C. T. Reeves, R. J. Meyer, C. B. Mullins, J. Phys. Chem. B **108**, 7917 (2004).

D. Stolcic, M. Fischer, G. Ganterför, Y. D. Kim, Q. Sun, P. Jena, J. Am. Chem. Soc. **125**, 2848 (2003).

Q. Sun, P. Jena, Y. D. Kim, M. Fischer, G. Ganteför, J. Chem. Phys. **120**, 6510 (2004).

D. Thompson, Gold Bulletin **31**, 111 (1998).

B. M. W. Trapnell, Proc. R. Soc. A **218**, 566 (1953).

M. Valden, X. Lai, D. W. Goodman, Science **281**, 1647 (1998).

A. V. Walker, B. Klötzer, D. A. King, J. Chem. Phys. **112**, 8631 (2000).

W. T. Wallace, R. L. Whetten, J. Am. Chem. Soc. **124**, 7499 (2002).

D. H. Wells Jr., W. N. Delgass, K. T. Thomson, J. Chem. Phys. **117**, 10597 (2002).

M. C. Wheeler, C. T. Reeves, D. C. Seets, C. B. Mullins, J. Chem. Phys. **108**, 3057 (1997).

M. C. Wheeler, D. C. Seets, C. B. Mullins, J. Chem. Phys. **105**, 1572 (1996).

M. C. Wheeler, D. C. Seets, C. B. Mullins, J. Chem. Phys. **107**, 1672 (1997).

Y. Xu, M. Mavrikakis, J. Phys. Chem. B **107**, 9298 (2003).

B. Yoon, H. Hakkinen, U. Landman, J. Phys. Chem. A **107**, 4066 (2003).

Vita

James Daniel Stiehl was born in Big Spring, Texas on July 8, 1977, the son of Carlota and Freddie Stiehl. In 1995, after graduating from Big Spring High School in Big Spring, Texas, he enrolled in Howard Community College in Big Spring, Texas. While attending Howard Community College, he worked for Avantech Corporation in Big Spring, Texas. After one year of studies at Howard Community College, he enrolled at The University of Texas at Austin. On January 4, 1997, he was married to Ronna Nikole Osborn in Big Spring, Texas. He completed his Bachelor of Science in Chemical Engineering in December 1999. He began his graduate education at the University of Texas at Austin in January 2000.

Permanent address: 3821 Gaines Ct., Austin, Texas 78735

This dissertation was typed by the author.